THE STABILIZATION OF TUNGSTEN(VI) ALKYLS, ALKYLIDENES, AND HYDRIDES USING A BIDENTATE BIS-AMIDE LIGAND

By

DANIEL D. VANDERLENDE

A DISSERTATION PRESENTED TO THE GRADUATE SCHOOL
OF THE UNIVERSITY OF FLORIDA IN PARTIAL FULFILLMENT
OF THE REQUIREMENTS FOR THE DEGREE OF
DOCTOR OF PHILOSOPHY

UNIVERSITY OF FLORIDA

1994

ACKNOWLEDGEMENTS

The people deserving thanks from the author for the completion of this dissertation are innumerable. A great debt is owed to Dr. Jim Boncella, who has guided the author through this adventure. The lessons taught by Jim will have an influence on the rest of the author's life. He not only challenged and motivated the author, he also brought out the best in the author's golf game, teaming with Larry Villanueva and William Vaughan to win the 1993 Analytical Open.

Special thanks goes to Dr. Khalil Abboud. Dr. Abboud solved or helped the author solve all of the crystal structures reported in this dissertation. He taught the author everything the author knows about crystallography. The author is grateful for the patience and enthusiasm Dr. Abboud showed throughout the research which was the basis for this dissertation, exemplified by the eleventh hour structure included in Chapter 4 .

There were many people who passed through the Boncella lab during the author's tenure. Everyone of these people played a role in the completion of this dissertation. Those who have since moved on, Larry, Laura Blosch, Scott Gamble, and Gaines Martin, were positive role models who taught by example how to work hard in a fun group environment. Will Vaughan has been a constant source of fun, excitement, and intellectual stimulation over the past four plus years. The author would also like to remember all the other members of the Boncella group who have made research so stimulating; Percy Doufou, Jerrold Miller, Mary Cajigal, Justine Roth, Jon Penney, Steve Wang and Faisal Shafiq. Who could ever forget Tegan Eve and Melissa Booth?

Special thanks also goes to Mike Cruskie and Chris Marmo who have been great friends and fellow chemists over the years. A special thanks also goes to the Talham group, especially John Pike and Houston Byrd, who both shared their unique perspectives

on life with the author. The author is also indebted to the people who made the research possible on a daily basis; Dr. King, Charlie Cromwell, Rudy and Vern.

None of this would have been possible without my parents who instilled in their son the desire to never be satisfied with past accomplishments. The author would like to acknowledge the love and devotion of the "Coach". He was always there for the author, displaying undying devotion and loyalty. Lastly, the author would like to acknowledge his wife Michelle, who has been the driving force behind the completion of this dissertation. Michelle has always believed that there is nothing her husband cannot accomplish, and that belief has motivated the author to strive to be more than he ever thought he could be, because maybe she is right.

TABLE OF CONTENTS

Abstract of Dissertation Presented to the Graduate School
of the University of Florida in Partial Fulfillment of the
Requirements for the Degree of Doctor of Philosophy

THE STABILIZATION OF TUNGSTEN(VI) ALKYLS, ALKYLIDENES, AND HYDRIDES USING A BIDENTATE BIS-AMIDE LIGAND

By

Daniel D. VanderLende

December, 1994

Chairman: James Boncella
Major Department: Chemistry

The synthesis of a number of W(VI) complexes stabilized by bis-amide chelate ligands was achieved with the goal of preparing new olefin metathesis polymerization catalysts. Addition of $Li_2[(NSiMe_3)_2C_6H_4]$ **2**, to $W(NPh)Cl_4(OEt_2)$ yields $W(NPh)Cl_2[(NSiMe_3)_2C_6H_4]$ **14**. A single crystal diffraction study of **14** reveals that it crystallizes in the space group P $2_1/n$ with a = 10.294(2) Å, b = 17.859(3) Å, c = 12.565Å, β = 104.15(2)°, V = 2384.6(8) $Å^3$, Z = 4. The structure of **14** is unique in that the ligands phenyl ring is in close contact with the metal center, with a fold angle of 53°. Addition of PMe_3 to **14** affords the purple mono-adduct, $W(NPh)Cl_2(PMe_3)[(NSiMe_3)_2C_6H_4]$ **21**. A single crystal diffraction study of **21** reveals that it crystallizes in the space group P-1 with a = 9.562(1) Å, b = 10.277(1) Å, c = 14.920(2) Å, α = 82.15(1)°, β = 80.18(1)°, γ = 80.41(1)°, V = 1415.6(3) $Å^3$, Z = 2. Compound **14** can be alkylated to give the corresponding bis-alkyls, $W(NPh)R_2[[(NSiMe_3)_2C_6H_4]$. The 14 electron bis-alkyl compounds show no evidence of α-agostic W-H-C interactions and have $^1J_{C\alpha\text{-}H}$ values between 120 and 130 Hz.

$W(NPh)(CH_2CMe_3)_2[(NSiMe_3)_2C_6H_4]$ **25** can be heated in the presence of excess PMe_3 to give the new alkylidene complex, $W(NPh)(CHCMe_3)(PMe_3)[(NSiMe_3)_2C_6H_4]$, **36**. Compound **36** crystallizes in the space group P $2_1/c$ with a = 16.116(3) Å, b = 11.340(2) Å, c = 17.960(4) Å, β = 106.28(2)°, V = 3151(1) $Å^3$, Z = 4. The x-ray structure of **36** reveals a unique square pyramidal structure with the alkylidene carbon in the apical position. Compound **36** is an active ROMP catalyst, polymerizing twenty five equivalents of norbornene in ten minutes at room temperature. The reactivity of the catalyst can be altered by the addition of excess PMe_3 to the reaction mixture.

$W(NPh)(CH_2CMe_3)_2[(NSiMe_3)_2C_6H_4]$ **25** reacts with molecular hydrogen in the presence of PMe_3 to give the seven-coordinate dihydride complex, $W(NPh)H_2(PMe_3)_2[(NSiMe_3)_2C_6H_4]$ **39**. The dihydride reacts with two equivalents of ethylene or styrene to give the W(IV) olefin complexes $W(NPh)(\eta^2$-$C_2H_4)(PMe_3)_2[(NSiMe_3)_2C_6H_4]$ **46**, and $W(NPh)(\eta^2$-$CH_2CHPh)(PMe_3)_2[(NSiMe_3)_2C_6H_4]$ **47**. The olefin complexes react with H_2, hydrogenating the olefin and forming the dihydride, **39**.

CHAPTER 1
BACKGROUND AND INTRODUCTION

1.1: High Oxidation State Transition Metal Chemistry Involving Metal Ligand Multiple Bonds.

There has long been an interest in the isolation of high oxidation state transition metal complexes.[1] The term high oxidation state transition metal refers to transition metals which are in their highest or nearly highest oxidation state. Throughout this discussion, high oxidation state transition metals will usually refer to transition metals with zero *d* electrons, or d^0 complexes. The applications of high oxidation state transition metal complexes are innumerable. A plethora of reactions are catalyzed by such compounds[1,2] oxidations, metathesis, polymerizations and many organic transformations. Therefore, the synthesis of novel compounds and investigation of their properties and reactivity are essential in order to expand our understanding of high oxidation state transition metal chemistry.

High oxidation state transition metals were being used in many applications long before the intrinsic characteristics or the structure of discrete molecules were known.[3] In other words, high oxidation state transition metal complexes have been used as heterogeneous catalysts and homogeneous catalysts for decades, but, in order to expand our understanding of the reactions catalyzed by these compounds, the identity of the discreet molecules must be known. Often times, the active species in the reaction is different that the starting compound, and hence the structure of the active species is unknown or unproven.[3] Many high oxidation state transition metal complexes contain multiply bonded atoms; nitrogen, oxygen, and carbon are the most common.[2] Also, the active species in many catalytic processes are postulated to contain metal-ligand multiple

bonds.[3,4] Often, these multiply bonded ligands are the key to the reactivity or stability of the molecules. Therefore, the synthesis and structural elucidation of new multiply bonded ligand-transition metal complexes will always be relevant.

Examples of transition metal oxo[5] $[O]^{2-}$, imido[6] $[NR]^{2-}$ and nitrido[7] $[N]^{3-}$ complexes are numerous. Books and reviews on these types of ligands can be found throughout the literature. The chemistry of high oxidation state transition metal-carbon multiple bonds, alkylidenes $[CHR]^{2-}$ and alkylidynes $[CR]^{3-}$, are rapidly becoming better understood, yet relatively few examples compared to oxo or imido complexes are known.[8] The bonding in oxo, imido, and alkylidene complexes share some common characteristics. They all involve a metal ligand σ-bond and one or more π-bonds between the ligand *p* orbitals and the empty metal *d* orbitals.[1,8,9] In oxo and imido complexes, a lone pair of electrons can also form a second π-bond to the metal center. In imido complexes, this is evident in the fact that for most of the structurally characterized compounds, the M-N-C bond is nearly linear, greater than 160°.[1,8] The bond is considered a six-electron donor and a di-anionic contribution from the ligand, creating a formal bond order of 3, **Figure 1.1**. In alkylidenes, there is not an extra pair of electrons, therefore, the bond is considered as one σ and one π-bond, a four-electron [-2] donor, with a formal a bond order of 2, **Figure 1.2**. This interaction between the ligand π and metal *d*

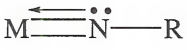

Figure 1.1.
Bonding in imido complexes.

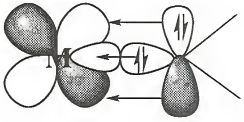

Figure 1.2.
Electronic interactions in alkylidenes.

orbitals leads to a stabilization of the complex due to electron donation to the empty orbitals on the d^0 metal center.[1,9] For this reason, many of the known high oxidation state

compounds contain one of the multiply bonded ligands mentioned. **Figure 1.3** shows how the number of publications in this field of research has grown in just a few decades.[1] It should be recognized that the table does not include oxo complexes, work on which is published at roughly an order of magnitude greater than the others combined.

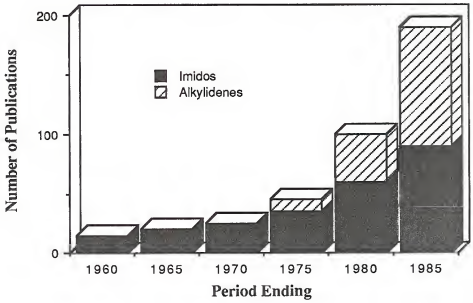

Figure 1.3. Graph of imido and alkylidene publication rates.

It would be difficult and unnecessary to give a complete review of high oxidation state transition metal complexes with multiply bonded ligands in this introduction. Therefore some restraints will be put on the background information. The information relevant to the research that was carried out pertains to W(VI) oxo, imido, and alkylidene compounds. Therefore this discussion will be limited to examples of these and other closely related compounds for direct comparison to the tungsten derivatives. Although numerous new W(VI) imido and a few oxo compounds were isolated as a result of this work, in every instance they behave as spectator ligands. They play an important role in the electronic stabilization of the complexes but do not participate directly in any reactions. This will become more evident in the discussion of the research results.

1.2 Olefin Metathesis and Olefin Metathesis Polymerization

The initial goal of this project was the isolation of thermally stable, coordinatively unsaturated alkylidene complexes. These new complexes were then intended to catalyze specialized metathesis polymerization reactions. And although this goal was attained in part, many novel, unrelated aspects of high oxidation state chemistry were observed along the way.

In just the last two decades, the important role of transition metal alkylidene complexes in olefin metathesis reactions has been thoroughly investigated.[10,11] The olefin metathesis reaction, in general, can be described as the net breaking of carbon-carbon double bonds, and forming two new carbon-carbon double bonds **Figure 1.4**. The

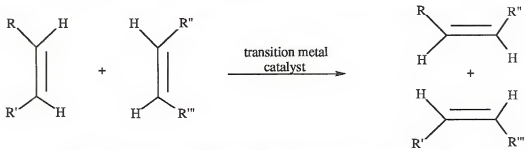

Figure 1.4. Scheme showing the net conversion observed in olefin metathesis reactions.

overall result is the exchange of substituents on the olefins. It was the suggestion by Herrison and Chauvin[12] in 1970 that the mechanism for olefin metathesis involves an alkylidene bond **Figure 1.5**. An olefin can then coordinate to the electrophilic metal center. An intermediate metallacyclobutane is formed which can either cleave to give the original alkylidene/olefin complex or cleave to give a new olefin complex.

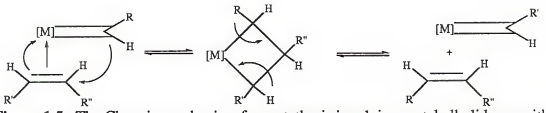

Figure 1.5. The Chauvin mechanism for metathesis involving metal alkylidenes with arrows depicting the direction of electron flow for productive metathesis.

This mechanism gained wide acceptance and seemed quite plausible for systems such as the popular olefin metathesis catalyst, $WOCl_4/EtAlCl_2$, where the formation of an initial tungsten ethylidene complex[3] is easy to rationalize **Figure 1.6**.

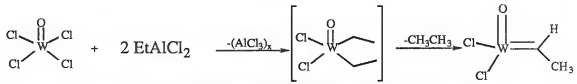

Figure 1.6. The proposed formation of an ethylidene complex in the $WOCl_4/EtAlCl_2$ system.

Postulation and speculation about alkylidene formation officially ended on July 27, 1973, when Schrock[13] at I. E. du Pont Central Research synthesized $Ta(CHCMe_3)(CH_2CMe_3)_3$. Since that time, numerous other alkylidene complexes have been isolated and have been shown to be active catalysts for metathesis and metathesis polymerization reactions. In the early 1980s, tungsten and molybdenum alkylidenes received special attention since they are highly active olefin metathesis catalysts. The fields of olefin metathesis and olefin metathesis polymerization received a boost in 1989 when Schrock published the detailed synthesis[14] of $W(NAr')(CH\text{-}t\text{-}Bu)(OR)_2$ (Ar' = 2,6-^{i}Pr$_2$Ph; OR = O-t-Bu, $OCMe_2(CF_3)$, $OCMe(CF_3)_2$). The $W(NAr')(CH\text{-}t\text{-}Bu)(OCMe(CF_3)_2)_2$ derivative has proven to be the most active alkylidene catalyst to date. Recently, the molybdenum *t*-butoxide derivative has become available commercially from Strem Chemical, through Catalytica, albeit for a hefty price.

Schrock's tungsten and molybdenum catalysts have some unique features which lend to the high reactivity which has been observed. In order to design a new or better catalyst, certain features must be retained. Obviously Schrock's catalyst involves Group (VI) metals in the 6+ oxidation state. That the catalysts are only four coordinate is essential since coordination of the olefin to the metal center is the initial step in metathesis. The imido moiety's role is crucial. There are examples of oxo-alkylidene's where the role of

the oxo is identical to the imido.[15] Of the known tungsten and molybdenum alkylidenes, examples without an imido or oxo ligand are less common.[16]

The imido functionality offers a great electronic stabilization to the metal center. The bonding can be thought of as a σ bond and two π bonds, the second π bond arising from donation of the lone pair of electrons on the imido nitrogen to an empty metal *d* orbital. The imido functionality can also stabilize the complex by adding steric bulk to the metal center. Most of the known alkylidene complexes contain 2,6-disubstituted aryl imido ligands.[8] The other substituents also contribute to the steric bulk around the metal center. All of the alkoxide substituents are rather bulky, and the alkylidene substituent is usually a bulky alkyl group. The steric bulk is necessary since these complexes are known to dimerize forming bridging alkylidenes.[8] The bulky metal center reduces the probability of this transformation. The steric bulk also plays a role in the formation of the alkylidene itself. A large percentage of the known alkylidenes are formed through α-hydrogen abstraction reactions from dialkyl precursors or intermediates.[8] The steric bulk helps promote the α-abstraction, usually of a bulky alkyl substituent. The reactivity of the alkylidene catalysts is observed to increase as the electron withdrawing nature of the alkoxide is increased, O-t-Bu < $OCMe_2(CF_3)$ < $OCMe(CF_3)_2$).[8] This is intuitive since the electron withdrawing nature of the alkoxide would make an already electron deficient molecule more so, thereby increasing the olefin affinity, which, as was mentioned before, is the initial step in olefin metathesis.

As was mentioned earlier, these alkylidene catalysts can facilitate the polymerization of olefins.[10,11] The most common metathesis polymerization reaction is Ring Opening Metathesis Polymerization (ROMP).[10] The ROMP reaction is driven by the relief of ring strain in cyclic olefins. Since olefin metathesis reactions are actually series of equilibria, the opening of a strained ring prohibits the reverse reaction, driving the polymerization.[10] The overall ROMP reaction is shown in **Figure 1.7**. A large volume of work has been done on the ROMP reaction. Norbornene, NBE, is commonly used as the olefin since it is

readily polymerized by a large number of catalysts. Schrock and Grubbs have demonstrated that many ROMP reactions are 'living' polymerizations.[17]

A unique olefin metathesis polymerization reaction which was developed here at the University of Florida involves acyclic dienes.[18] The net reaction for acyclic diene

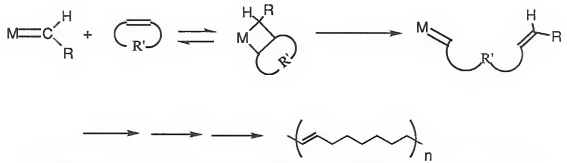

Figure 1.7. The ring opening metathesis polymerization of a cyclic olefin.

metathesis polymerization (ADMET) can be seen in **Figure 1.8.** The equilibrium is driven toward polymer formation by the removal of ethylene, or another small, volatile, olefinic molecule, from the reaction mixture. ADMET polymerization has long been the driving force in the research efforts of the group. ADMET reactions are best carried out in neat monomer in order to maximize the olefin concentration and to prevent side reactions. One of the major hindrances in this chemistry is precipitation of the reaction mixture before the polymerization can be carried to high molecular weight. As an example, when poly(octene) reaches twelve connections in neat 1,9-decadiene, precipitation occurs. Performing the reaction at a temperature above the melting point of the polymer would alleviate this problem. However, at this point, the thermal stability of the catalyst becomes crucial. Schrock's catalyst is thermally unstable, so, although the Schrock catalyst has proven efficient for ADMET, achieving high molecular weight polymer is difficult.

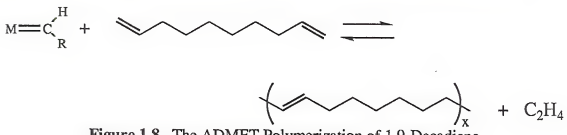

Figure 1.8. The ADMET Polymerization of 1,9-Decadiene

The principles of ADMET have also been applied to depolymerizing unsaturated polymers.[19] Since all the steps of ADMET are reversible, reacting the polymer, another olefin, and catalyst should depolymerize a poly-ene such as polybutadiene. Success has been found when polybutadiene is depolymerized using Schrock's catalyst and end-capped with silylenes. This reaction will be discussed more in Chapter 3.

Although the Schrock catalyst described above represents the ideal at this time, there are shortcomings involved in its preparation and reactivity. From first-hand observations, it has been observed that the preparation of Schrock's catalyst is a lengthy, patience-trying procedure. Not only are there multiple steps involved, but the yields are low and some of the reagents are far from inexpensive. Secondly, once synthesized, the catalysts, especially the fluorinated alkoxides, are particularly air/moisture sensitive. This aspect of its reactivity also translates into an intolerance of certain functional groups. A common phrase heard in polymer laboratories is "The catalyst was poisoned...". Adding to the drawbacks of Schrock type catalysts is their thermal 'instability'. There are polymer systems in which heating the reaction mixture would be advantageous toward achieving maximum yields or molecular weights; however, Schrock's catalysts general decompose over the temperature range of 60-80 °C.[20] So, although the introduction of Schrock's catalysts opened up vast areas in metathesis and polymerization, there is still a great need for new catalysts which are easier and less expensive to prepare.

1.3 Chelate Stabilized Alkylidenes

An intuitive approach to the synthesis of an alkylidene compound with a greater thermal stability would be to use chelating ligands somewhere in the molecule. The use of a chelating ligand may also produce interesting stereochemical properties in the metathesis reactions. This approach has been investigated by Schrock, Grubbs, Boncella, VanKoten

and others. There are a number of options as to where to apply 'chelates' in these complexes. Schrock has made a series of diolate complexes[21] of the type Mo(CHCMe$_2$Ph)(NAr)(diolate) **Figure 1.9**. Although no comment is made about

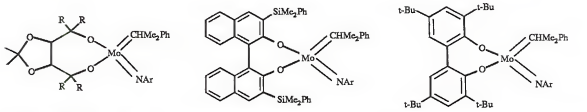

Figure 1.9. Bidentate diolate complexes prepared by Schrock.

the thermal stability, it is assumed that they are more stable than the complexes with monodentate alkoxides. These compounds do, however, allow for stereochemical control of ROMP reactions. Grubbs has taken an interesting approach by synthesizing *o*-substituted aryl alkylidenes[22], where the *o*-substituent has σ-donor properties and can chelate to the metal center, stabilizing the alkylidene **Figure 1.10**.

VanKoten's alkylidenes are stabilized by chelating σ-donors as well.[23] In the tungsten(VI) alkylidene complex, W(NPh)(C$_6$H$_4$-*o*-CH$_2$NMe$_2$)(CHSiMe$_3$)(OSiPh$_3$), the -NMe$_2$ group on the *ortho*-methylene group acts as a σ-donor, adding a chelate effect **Figure 1.11**.

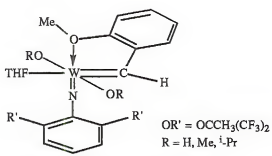

Figure 1.10. Grubbs' Catalyst

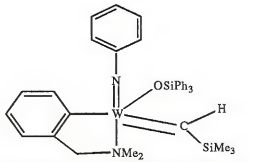

Figure 1.11. VanKoten's Catalyst.

Work done here at Florida by Blosch, Gamble, and Vaughan in the research group of James Boncella[24] has focused on the use of the tris-chelating, mono-anionic ligand hydro(tris)pyrazolylborate, Tp. Six-coordinate alkylidene complexes of the type

TpM(NAr)(CHR)(X) (M = W, Mo; R = CMe_3, CMe_2Ph; X = Cl, Br, OTf, OMe, NHPh) have been isolated **Figure 1.12**. These complexes show remarkable air and thermal stability, although they only show metathesis activity in the presence of a Lewis acid, which generates a vacant coordination site. Once again, the importance of coordinative unsaturation is observed.

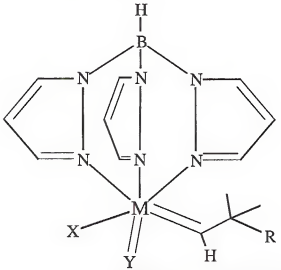

M = W; Mo
Y = NAr; O
X = Cl; Br; OTf; OMe; NHPh
R = Me; Ph

Figure 1.12. Tridentate chelate complexes using the hydro(tris)pyrazolylborate ligand.

The use of chelate ligands has provided two things to the chemistry of alkylidenes. First, it has produced more thermally stable alkylidenes, even air-stable in the case of the Tp alkylidenes. Secondly, the chelates ligands have greatly reduced the reactivity of the alkylidenes towards olefins. The ultimate goal of this work would be to design a ligand which provided stability while maintaining a high olefin affinity at the metal center. Obviously this would mean a coordinatively unsaturated, electron deficient molecule. A look back at the some of the known chelated alkylidene compounds reveals an undesirable trend; the chelate ligand involves a neutral σ-donor interaction. In simple terms, all this does is clog the coordination sphere of the molecule. A more pragmatic approach would eliminate neutral σ-donor ligands to a great extent and concentrate on the use of anionic ligands as chelates. The Tp ligand for example is a tridentate, mono-anionic ligand. Van Koten's chelate could be considered a bidentate, mono-anionic ligand.

1.4 Polydentate, Polyanionic Chelate Ligands

An ideal ligand would be a polyanionic, polydentate ligand. Either a bidentate, di-anionic ligand, or a tridentate, tri-anionic ligand. There are a number of examples in the literature of multidentate, multi-anionic ligands. Schrock and Cummings have used a tetradentate, tri-anionic ligand to prepare some novel high oxidation state titanium,[25] vanadium[25] and tantalum[26] compounds. The ligand, $(Me_3SiNCH_2CH_2)_3N$ was used to stabilize an interesting terminal phosphinidene complex as well as some other high oxidation state early transition metal complexes **Figure 1.13**. Verkade[27] first used methyl derivatives of this ligand, $(MeNCH_2CH_2)_3N$, to stabilize some group (IV) and (V) compounds **Figure 1.14**. Gade[28] has used a similar ligand, $H_3CC(CH_2NHR)_3$ (R = Me, Et, ^iPr, $SiHMe_2$, and $SiMe_3$), to stabilize titanium complexes. This ligand has a carbon in the bridgehead position, avoiding the σ-interaction which the nitrogen had with the electrophilic metal center, creating a tridentate, tri-anionic ligand, thereby decreasing the metal centers coordination number by one.

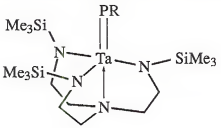

Figure 1.13. Phosphinidene stabilized by Verkade's ligand.

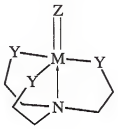

M = V, Ta
Y = O, NMe
Z = O, NR

Figure 1.14. Gade's tetradentate tris-anionic ligands.

Wilkinson[29] has employed the use of *o*-phenylenediamine in the stabilization of tungsten (V) and (VI) compounds. One negative aspect of this particular bidentate, di-anionic ligand is the tendency for rearrangement of the bis-amide to an imido-amine. This problem could be easily overcome by synthesizing N,N'-disubstituted derivatives. This premise is where the present study begins. A number of novel N,N'-disubstituted

derivatives of *o*-phenylenediamine and 1,8-diaminonapthalene were synthesized and their application as bidentate, di-anionic ligands were investigated. All of the work reported here involves tungsten (VI) phenylimido or oxo complexes exclusively. The high-yield synthesis of various tungsten (VI) phenylimido ligand stabilized complexes allows a convenient route into the reaction chemistry of these complexes. This work, involving the preparation of starting materials, will be covered in Chapter 2. Simple alkylation reactions allow the isolation in good yield of a series of mono- or di-alkyl complexes. Isolation of stable *cis*-bisalkyl complexes offers a look into the reaction chemistry of these compounds, and will be the focus of Chapter 3. Heating the bis neopentyl derivative in the presence of PMe_3 induces α-hydrogen abstraction, forming an alkylidene and one equivalent of neopentane. The neopentylidene complex is an active catalyst for the ROMP of norbornene. The activity of the catalyst can be tailored by the addition of excess ligand to the reaction mixture. This will also be covered in Chapter 3. A majority of the chemistry found in Chapters 2 and 3 has previously been published.[30] An interesting feature of the alkyl complexes is that they react at room temperature with molecular hydrogen to form high oxidation state hydride complexes. The addition of a σ-donor ligand accelerates the reaction tremendously as well as aides in the stabilization of the molecule. The seven-coordinate dihydride species formed reacts with ethylene, hydrogenating one equivalent, while the reduced metal species forms a tungsten (IV) ethylene complex. The reactivity of the alkyls towards hydrogen and olefins will be the focus of Chapter 4.

CHAPTER 2
SYNTHESIS OF BIS-AMIDE CHELATE LIGANDS
AND LIGAND-METAL COMPLEXES

2.1: Preparation of Bidentate Ligands.

In order to pursue the use of 1,2-phenylenediamine as a bidentate, di-anionic ligand, an accessible route to the synthesis of bulky N,N'-disubstituted derivatives was desired. A thorough review of the literature reveals surprisingly few examples of such compounds. The only known bisalkyl example is N,N'-dimethyl-1,2-phenylenediamine,[31] which is prepared through a tedious, dangerous, multi-step synthesis. There are examples of other disubstituted derivatives such as -S(O)$_2$tolyl (tosyl)[31] and -C(O)Ph.[32] A slight discrepancy in the literature was discovered for the case of N,N'-bis(trimethylsilyl)-1,2-phenylenediamine, 1,2-(Me$_3$SiNH)$_2$C$_6$H$_4$, **1**. Before this was discovered, however, a nearly quantitative one-step synthesis of **1** was discovered eq **2.1.** *O*-phenylenediamine was dissolved in Et$_2$O on as large a scale as available

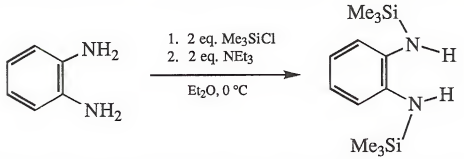

eq 2.1

glassware would allow. A slight excess of two equivalents of Me$_3$SiCl was added, forming a white precipitate, presumably the hydrochloride salt. A slight excess of two equivalents of NEt$_3$ was added to the slurry. The solution became yellow amidst the solid. Filtering and removing solvent gave a bright yellow solid in greater than 95% yield. It is

important to note that the slightest impurity causes formation of a yellow oil, partly due to the low melting point (29 °C) of **1**.

The preparation of **1** described above differs greatly from the literature methods. Compound **1** was first reported in the literature in 1960 by Birkofer.[33] Birkofer refluxed *o*-phenylenediamine, two equivalents of Me_3SiCl and NEt_3 in toluene followed by a fractional distillation to give a moderate yield of **1**. In 1970, West[34] reported refluxing *o*-phenylenediamine, hexamethyldisilazane, and a catalytic amount of Me_3SiCl in THF for 24 hours. Fractional distillation using a spinning band column gave an 80% yield of **1**. West also reported that addition of MeLi to **1** in THF solvent caused rapid 1,4 anionic rearrangements to occur.[34] This finding was an important consideration when solvents for the ligation chemistry were chosen. In 1985, Lappert reported heating *o*-phenylenediamine, Me_3SiCl, and NEt_3 in toluene (with no mention of Birkofer).[35] Lappert then treated **1** with $MgBu_2$ to give the deprotonated dimer, $[Mg\{\mu\text{-}N(SiMe_3)C_6H_4N(SiMe_3)\text{-}o\}(OEt_2)]_2$. Maatta[36] reports another preparation in 1992. Here, *o*-phenylenediamine is deprotonated with two equivalents n-BuLi, followed by addition of two equivalents of Me_3SiCl. The product, **1**, is isolated as a yellow oil by vacuum distillation in 80% yield. One concern that this report brought out was that when $(Me_3SiNH)_2C_6H_4$, **1**, was allowed to react with WCl_6, two equivalents of HCl and two equivalents of Me_3SiCl were lost, forming a bridging di-imide **eq 2.2**.

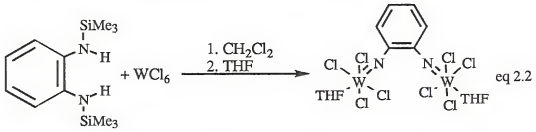

eq 2.2

From Lappert's account, **1** should be susceptible to deprotonation. Addition of two equivalents of n-BuLi to **1** afforded the white salt $Li_2(Me_3SiN)_2C_6H_4$, **2**. Interestingly, the salt was soluble in C_6D_6 and the ^1H NMR of **2** verifies that there were no N-H

protons. The salt, however, was extremely moisture sensitive and spontaneously ignited upon exposure to air, hence prolonged storage was difficult. Before the application of **1** and/or **2** as a ligand will be addressed, the synthesis of other potential ligands will be discussed.

Although the high yield synthesis discussed for **1** might seem applicable for a series of silyl chlorides, it did not prove to be. However, when refluxing hexanes were used as the solvent instead of Et_2O, a series of silylated compounds were isolated in high yield. This general route applies to making the -$SiMe_2Ph$, **3**; -$SiMePh_2$, **4**; or -$SiMe_2$-*t*-Bu, **5**, derivatives of *o*-phenylenediamine. Another derivative of *o*-phenylenediamine was prepared in this manner, 4,5-dimethyl-1,2-$(Me_3SiNH)_2C_6H_2$, **6**. This route was also utilized to prepare 1,8-$(Me_3SiNH)_2C_{10}H_4$, **7**, in high yield and on a large scale from 1,8-diaminonaphthalene and two equivalents of both Me_3SiCl and NEt_3. An asymmetric disubstituted *o*-phenylenediamine derivative, 1-(PhNH)-2-$(Me_3SiNH)C_6H_4$, **8**, was synthesized similarly from N-phenyl-*o*-phenylenediamine, Me_3SiCl and NEt_3.

Attempts to synthesize dialkyl derivatives of *o*-phenylenediamine proved less successful. In an attempt to synthesize 1,2-$(^iPrNH)_2C_6H_4$, *o*-phenylenediamine was slurried with excess sodium acetate in a cold acetic acid/acetone/water mixture. Excess $NaBH_4$ was added slowly. After neutralizing the solution with NaOH and isolation of products, a 1:1 mixture of products was formed. They were separated by flash chromatography and analyzed. 1,2-$(^iPrNH)_2C_6H_4$, **9**, was isolated as a colorless oil. The other product was a heterocyclic compound, **10**, which is shown in **eq 2.3**. The heterocycle most likely forms by an attack of one imine nitrogen on the other imine carbon, followed by a 1,3 proton shift. Altering the reaction conditions did not change the relative yields of **9** and **10**. The ^1H NMR of **10** is shown in **Figure 2.1**. Since formation of the 7-membered heterocylce seemed unavoidable in this system, the same reaction was attempted using 1,8-diaminonaphthalene. Here, the formation of a 6-membered heterocycle might be less likely due to the strain involved in one imine attacking

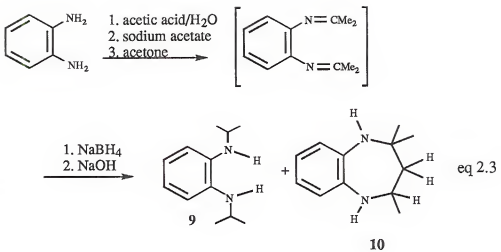

eq 2.3

the other. A mixture was not observed. A 90% yield of a 6-member heterocycle, **11**, was the only compound isolated **eq 2.4**. This compound probably arises from attack of the imine carbon on the lone pair of electrons from the nitrogen, followed by a 1,3 proton shift. Changes in the reaction conditions did not afford any of the desired diamine.

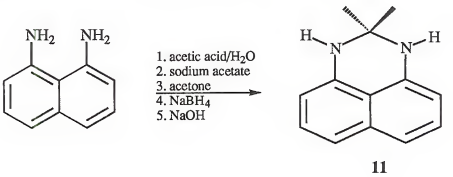

eq 2.4

2.2: Synthesis of New Ligand Metal Complexes.

Addition of these new ligands to metals was the next step in the project. Two starting materials were initially chosen as trial compounds, $WOCl_4$, which was readily available, and $W(NPh)Cl_4(OEt_2)$. $W(NPh)Cl_4(OEt_2)$ can be prepared in high yield from the addition of PhNCO to $WOCl_4$, resulting in the loss of CO_2. The ligand chosen for the majority of the work reported was $1,2\text{-}(Me_3SiNH)_2C_6H_4$, **1**. There are two simple routes available for the addition of the ligand to the metal center. First, the ligand could be doubly

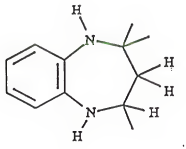

10

Figure 2.1. The ^1H NMR spectrum of the 7-membered heterocycle, 10.

deprotonated and then added to the metal center in a simple metathesis reaction, forming the ligand complex and two equivalents of a chloride salt. The other route would be to add the diamine ligand directly to the metal, losing HCl either spontaneously or through addition of a base such as NEt_3. The first route proved the more successful, and the second route was attempted with minimal success.

An Et_2O solution of $WOCl_4$ was added to **2** at -78 °C. Work-up afforded a moderate yield of $WOCl_2(Me_3SiN)_2C_6H_4$, **13, eq 2.5**. Studies of the reaction chemistry of this compound were not undertaken since isolating pure **13** is extremely

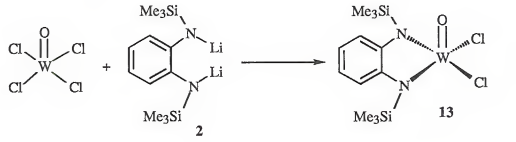

eq 2.5

difficult. Altering the reaction conditions did not alleviate this problem. Attempts are currently underway to alter the starting W=O complex and allow cleaner isolation of products, thereby allowing a thorough study of the reactivity of **13**[a] .

In a similar reaction, $W(NPh)Cl_4(OEt_2)$ was allowed to react with **2** at -78 °C, which afforded $W(NPh)Cl_2(Me_3SiN)_2C_6H_4$, **14**, as an orange-red powder. The bis-amido complex, **14**, was also prepared on a large scale by deprotonating the diamine *in situ*. This method proved the most successful in preparing **14** in high yield **eq 2.6**. With an easy, large scale, high yield synthesis, **14** was an excellent starting point to investigate the reactivity of these chelated complexes. The electron count of the tungsten is formally considered to be 14 electrons, considering the imido as a 6 electron donor with the amide bonds contributing 1 electron each to the total electron count. The electronic donation of

[a] William Vaughan has undertaken the synthesis of other W=O complexes to be used as precursors for the addition of the ligand, **1**. These W=O complexes have 'softer' substituents and would presumably be more tolerant to metathesis.

the bidentate ligand is unclear, the nature of which could make the molecule a 14e-, 16e- or 18e- complex.

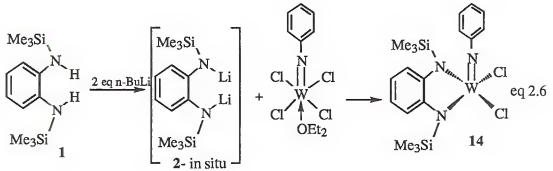

X-ray quality crystals were obtained by dissolving **14** in toluene and cooling to -10 °C. The thermal ellipsoid plot of **14** is shown in **Figure 2.2**, while selected bond lengths and angles are found in **Table 2.1**. The geometry of the molecule is square pyramidal with the imido nitrogen in the axial position. The W atom lies .58 Å above the plane defined by the two amido nitrogens and the two chlorides. This is similar to the crystal structure of $W(NPh)Cl_4(OEt_2)$, which is octahedral with the imido *cis* to all four chlorides. The imido nitrogen bond length is 1.730(10) Å, which is well within the range of other imido complexes where the imido group is considered to be a six electron donor because of donation of the lone pair of electrons on the nitrogen to an empty *d* orbital on the metal center. One feature of the structure of the molecule that is quite surprising is the 'orientation' of the ligand. The phenyl group of the bis-amide ligand is distorted and bent toward the metal center. The dihedral angle between the plane of the C1-C6 ring and W, N1, N2 is only 130°, as if there were a metal-olefin type interaction between the W and the phenyl ring of the ligand. The complement of this angle is referred to as the 'fold angle', 50 °, and is quite diagnostic when compared to other compounds. The interaction appears quite significant; the distances between W and C1 and W and C2 are only 2.58(1) Å. Although this is greater than the W-C bond length in high oxidation state tungsten alkyl complexes, it is still within the vanderWaal's radii. In the few compounds that are known with this type of ligand, the distances are much greater (>2.80 Å).[29,37] There are only a

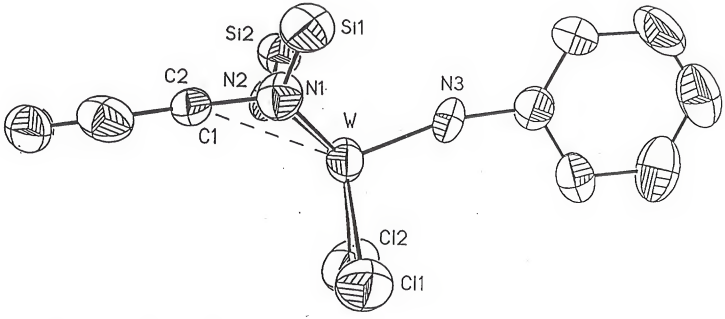

Figure 2.2. Thermal ellipsoid plot $W(NPh)Cl_2[(Me_3SiN)_2C_6H_4]$, 14. The protons and silyl methyl groups have been omitted for clearity.

few examples of structures of *o*-phenylenediamido-type ligands.[29,37,38] None of these structures appear to have an interaction between the ring carbons and the metal center. If the ring is in fact acting as a two electron donor, the electron count on the metal would now be 16e-.

Table 2.1: Selected Bond Lengths (Å) and Angles (°) for compound **14**.

1	2	3	1-2	1-2-3
Cl1	W	Cl2	2.383(4)	82.9(2)
Cl2	W	N1	2.387(4)	150.5(3)
N1	W	N2	1.951(11)	83.9(4)
N2	W	N3	1.952(11)	110.2(5)
N3	W	C1	1.730(10)	137.4(4)
C1	W	C2	2.582(13)	31.9(4)
C2	W	Cl1	2.582(13)	117.2(3)
N1	Si1	C13	1.768(10)	108.4(7)
N2	Si2	C16	1.781(12)	106.0(7)
C1	N1	W	1.42(2)	98.8(7)
C2	N2	W	1.40(2)	99.4(8)
C7	N3	W	1.39(2)	166.2(9)

Analogies can be made to some other types of compounds where similar bonding exists. Peterson[39] solved the crystal structure of a Cp_2Zr chelated bis-amido complex in which the distances between the β-carbons and the zirconium are 2.612(3) Å and 2.603(3) Å. Peterson claims that this close interaction is due to donation from the filled π-orbital of the C=C bond to the empty d_z^2 orbital on the zirconium as shown in **Figure 2.3**. Rothwell[40] observed similar results with quite similar bond lengths, in the 2.40-2.60 Å range, for other enediamido and enamidolate chelate compounds of zirconium, titanium and tantalum as shown in **Figure 2.4**. These compounds, including **14**, not only have close contact distances, but also have abnormally large 'fold angles'. The compounds prepared by Rothwell and Peterson have fold angles between 35 and 50 °. Rothwell also measured the $\Delta G^{\ddagger}$'s for the barrier to 'flip' these enediamido metallacycle rings. The $\Delta G^{\ddagger}$'s were in the 13-16 kcal/mol range.[40] This type of 'flip' would not be observed in a molecule such

as **14** since the molecule does not have a mirror plane through the metal center. Both Rothwell and Peterson also point out the fact that although the M-Cβ bond lengths are longer than normal for similar M-R complexes, they are within the range of M-C bond lengths in M-Cp complexes. Typically, W-Cp metal-carbon bond lengths are between

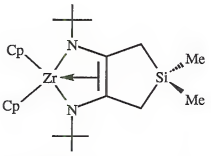

Figure 2.3:
A zirconacene enediamido complex.

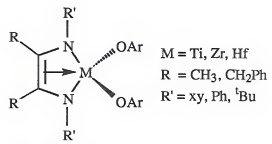

Figure 2.4:
Enediamido complexes of group 4 metals.

2.3 and 2.45 Å. This is shorter than the 2.58 Å observed for **14**, and does not fit as well with the comparisons suggested by Rothwell and Peterson. Lappert has observed similar behavior for some bidentate, di-anionic *o*-xylidene complexes of some bis-cyclopentadienyl group 4 and 5 metals.[41] The metallacycles in these compounds also displayed a significant interaction with the metal center, having fold angles between 41° and 53 °.

Continued investigation of the use of these chelating bis-amide ligands led to the synthesis of other new compounds. There were two goals for preparing new derivatives of these bis-amide derivatives, less solubility and more crystallizability. To this end, 1,2-$(Me_2PhSiNH)_2C_6H_4$, **3**, was deprotonated *in situ* and reacted with $W(NPh)Cl_4(OEt_2)$ to yield $W(NPh)Cl_2(Me_2PhSiN)_2C_6H_4$, **15**. This compound was somewhat less soluble but recrystallization proved unfruitful. Yellow crystals of 1,8-$K_2(Me_3SiN)_2C_{10}H_4$, **16** or 1,8-$Li_2(Me_3SiN)_2C_{10}H_4$, **17** were isolated when 1,8-$(Me_3SiNH)_2C_{10}H_4$, **7**, was deprotonated with two equivalents of KH or n-BuLi. These salts react readily with $W(NPh)Cl_4(OEt_2)$ to give $W(NPh)Cl_2(Me_3SiN)C_{10}H_4$, **18**, as a dark powder which was markedly less soluble than **13**, **14**, or **15** **eq 2.7**. Nonetheless, a suitable solvent could

not be found for recrystallization. The same reaction using 4,5-dimethyl-1,2-$(Me_3SiNH)_2C_6H_2$, **6**, yielded $W(NPh)Cl_2[4,5\text{-}Me_2\text{-}1,2\text{-}(Me_3SiN)_2C_6H_2]$, **19**. This

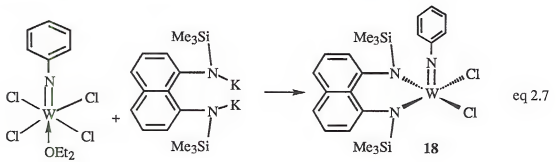

eq 2.7

complex certainly simplified the ^1H NMR spectrum, but did not show any greater ease in isolation or crystallization. Attempts were made at synthesizing tungsten phenyl imido derivatives using the other ligands mentioned; however, although results were encouraging, full characterization of these derivatives was not obtained.

It was also possible to substitute the chloride atoms in **14** with a more labile substituent. This was desirable if alkylation of the dichloride proved unsuccessful. When **14** was allowed to react with two equivalents of AgOTf, the bistriflate complex, $W(NPh)(OTf)_2[(Me_3SiN)_2C_6H_4](OEt_2)$, **20**, was isolated as a bright orange powder. This complex must be more electron deficient than **14** since it forms an etherate complex, whereas **14** does not.

Since all these compounds are five-coordinate, electron deficient molecules, they would be expected to form adducts with σ-donor ligands. When PMe_3 was added to a red Et_2O solution of **14**, the solution immediately turned purple. Addition of pentane followed by slowly cooling the sample to -10 °C yielded dark purple crystals of $W(NPh)Cl_2(PMe_3)[1,2\text{-}(Me_3SiN)_2C_6H_4]$, **21**. Integration of the ^1H NMR and combustion analysis confirmed the stoichiometry of **21**. Although **21** appears as a discreet mono-adduct, the ^{31}P NMR spectrum shows a very broad singlet for the PMe_3 ligand, nearly 250 Hz wide, and suggests that at room temperature an equilibrium between **21** and free PMe_3 was established. More evidence will be given for this ligand exchange later.

Purple, crystalline σ-adduct complexes were also formed when **14** was exposed to THF, **22**; 3-picoline, **23**; or CH_3CN, **24**, **eq 2.9**. Addition of these σ-donors increases the

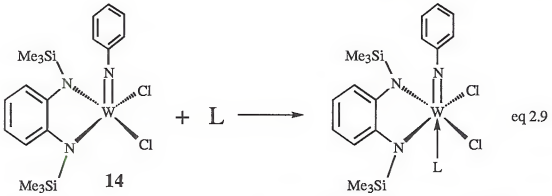

eq 2.9

L = PMe_3, **21**; THF, **22**; 3-picoline, **23**; CH_3CN, 24

formal electron count of the molecules to 16e- with no π-donation from the folding of the ligand at this point. The donation of this electron density, as well as now having a 6-coordinate complex, would clearly have an impact on the ligand 'folding' which was observed in the structure of **14**. Recrystallization of the PMe_3 adduct, **21**, by slowly cooling a pentane solution to -10 °C gave purple, x-ray quality crystals.

The structure of **21**, shown in **Figure 2.9**, has some unique features. Selected bond lengths and angles for the structure of **21** can be found in **Table 2.2**. The PMe_3 adds to the molecule *trans* to imido nitrogen, creating an octahedral geometry, with the amido nitrogens and the chlorides mutually *cis* in the basal plane. In a comparison between the structures of **14** and **21**, one very general thing that stands out. Because of the added electron density and steric bulk of the PMe_3, all the bonds to the metal center are longer in **21**. For instance, even the chlorides are 0.06 Å or more further away. Most significantly, the fold angle has increased from 50 ° to only 28 °. The W-C_{ring} distances have increased from 2.58 Å each in **14** to 2.79 and 2.78 Å in **21**. It is interesting to note that the geometry around the nitrogen atoms in the bis-amide ligands in both **14** and **21** is virtually planar. The amide bond lengths in **21** are only slightly longer, 2.010(5) Å and 1.990(5) Å than in **14**, 1.951(11) Å and 1.952(11) Å. One feature of this structure which is quite

Table 2.2: Selected Bond Lengths (Å) and Angles (°) for compound **21**.

1	2	3	1-2	1-2-3
Cl1	W	Cl2	2.449(2)	92.43(7)
Cl1	W	P		75.86(7)
Cl2	W	P	2.443(2)	75.70(7)
P	W	N1	2.720(2)	87.2(2)
P	W	N2		89.2(2)
P	W	N3		160.3(2)
N1	W	N2	2.010(5)	80.8(2)
N2	W	N3	1.990(5)	105.8(3)
N3	W	C1	1.747(6)	124.6(2)
C1	W	C2	2.797(6)	29.7(2)
C2	W	Cl1	2.785(6)	137.4(2)
N1	Si1		1.781(6)	
C1	N1	W	1.402(8)	108.8(4)
C2	N2	W	1.387(9)	109.8(5)
C7	N3	W	1.388(9)	164.3(5)

unusual is the extremely long W-P bond length, 2.720(2) Å. This bond appears to be at least 0.2 Å longer than most W-P bond lengths in W(VI) complexes. This weak interaction is supported by the afore mentioned broad singlet observed in the ^{31}P NMR spectrum. This long bond length may be due to *trans* influence of the imido nitrogen, which is a strong *trans* influencing ligand.

A number of interesting new W(VI) imido and oxo complexes have now been prepared. These new complexes have interesting structural characteristics which will play an important role in influencing the chemistry associated with them.

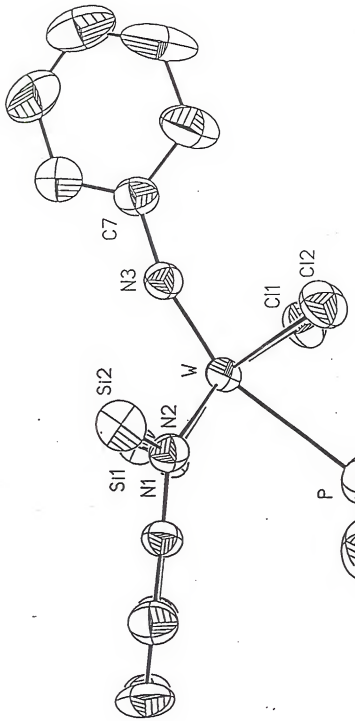

Figure 2.9. Thermal ellipsoid plot W(NPh)Cl$_2$(PMe$_3$)[(Me$_3$SiN)$_2$C$_6$H$_4$], 21. The protons and silyl methyl groups have been omitted for clearity.

CHAPTER 3
SYNTHESIS AND REACTIVITY OF W(VI) ALKYLS AND ALKYLIDENES

3.1: Background Information on W(VI) Alkyls and Alkylidenes.

In order to pursue the project goal of creating a new olefin metathesis catalyst, alkylation of the W(VI) dichloride was investigated. There are surprisingly few examples of group(VI) d^0 alkyl complexes in the literature.[1,2,42,43] There are numerous examples of d^0 group (IV) alkyl and dialkyl complexes, most of which are used as Ziegler-Naatta type catalysts. Homoleptic alkyls, such as WMe_6 are well-known.[42] Other alkyls are less prevalent. Schrock has isolated a number of W(VI) imido alkyl complexes.[44] Many of these were isolated in attempts to find precursors for alkylidene complexes. It was observed that $W(NPh)Cl_2(CH_2CMe_3)_2$ was not isolable. However, if one or two of the chlorides are substituted with t-butoxide ligands, dialkyls can be isolated, W(NPh)Cl(O-*t*-Bu)$(CH_2CMe_3)_2$ and W(NPh)(O-t-Bu)$_2(CH_2CMe_3)_2$. In these compounds, the alkyl groups are oriented *cis* to one another in a trigonal bipyramidal geometry. There are also examples in which the alkyl groups are *trans* to one another. Schrauzer prepared a variety of W(VI) dioxo complexes[45] of the type $W(O)_2R_2$(bipy), where R = Me, Et, n-Pr, and CH_2CMe_3. These compounds are quite stable due to the chelate effect of the bipyridine ligand, which also serves to 'lock' the alkyls trans to one another, limiting reductive elimination or α-hydrogen abstraction reactions. The bonding in d^0 alkyl complexes is rather straight-forward. The alkyl ligand acts as a 2e- donor ligand forming a σ-bond with the metal center. The most common means of preparing alkyl compounds is by simple metathetical exchange reactions.[42] Grignard reagents and lithium, zinc, or aluminum alkyls are commonly used as alkylating agents.

There are many possible reactions that can take place when a d^0 metal is alkylated, prohibiting isolation of a transition metal alkyl complex. If the alkyl group has β-protons, the metal can undergo a β-hydrogen elimination reaction.[2,42] Another reaction that takes place, especially with bulky alkyl groups, is α-hydrogen abstraction.[2] An alkylidene is formed as a result. There are two mechanisms proposed for this reaction, neither of which has been proven. One is initial α-elimination to form an alkylidene-hydride complex. Evidence for this mechanism comes from the chemistry of later transition metals. This addition is not possible for a d^0 metal center because the reaction involves oxidation of the metal center. The other mechanism proposes a three-center, two-electron transition state which eliminates alkane, forming the alkylidene. Both α-abstraction mechanisms can be seen in **Figure 3.1**. Since the discovery of the first alkylidene complex, other routes have been discovered for preparing alkylidenes.[46]

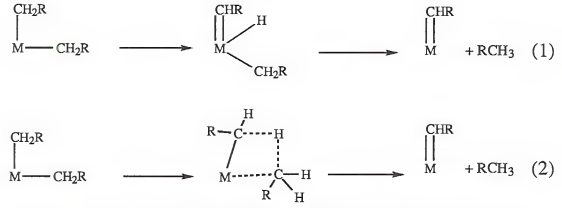

Figure 3.1. The two α-abstraction mechanisms for alkylidene formation.

Despite these developments, α-abstraction reactions are still the most common method for preparing alkylidene complexes. Neopentylidene (=CHCMe$_3$) and neophylidene (=CHCMe$_2$Ph) complexes are the most prevalent, due to their steric bulk and lack of β-protons. Reactions that proceed through α-abstraction can be divided into two general categories, proximal α-abstraction and ligand induced α-abstraction[a]. Proximal α-

[a] Proximal α-abstraction and ligand induced α-abstraction are not commonly used in the literature, however coining these terms is useful for the discussion.

abstraction refers to reactions in which an alkylidene is formed by α-abstraction immediately upon alkylation. This type of reaction was observed for the addition of excess neopentyl grignard to $TaCl_5$, forming $Ta(CHCMe_3)(CH_2CMe_3)_3$.[13] The mere steric bulk of the neopentyl groups induces α-abstraction, eliminating neopentane. The second type of reaction, ligand induced α-abstraction, is characterized by the addition of a σ-donor ligand, most commonly PMe_3, to a *cis* bis-alkyl complex, inducing α-abstraction and elimination of an alkane. A classical example is the addition of PMe_3 to $W(NPh)(CH_2CMe_3)_2(PMe_3)Cl_2$, which results in the formation of the alkylidene complex $W(NPh)(CHCMe_3)(PMe_3)_2Cl_2$ and neopentane.[44] These principles will be discussed as they apply to the synthesis of the new alkylidene complexes that were synthesized during this study.

3.2: Synthesis of W(VI) Bis-Alkyl Complexes.

Most of the reaction chemistry was performed on compound **14**, since it was the first compound isolated and was available in large quantities. When **14** was allowed to react with two equivalents of $ClMgCH_2CMe_3$ in Et_20 at -78 °C, the bis-alkyl complex $W(NPh)(CH_2CMe_3)_2[(Me_3SiN)_2C_6H_4]$, **25**, was isolated as a dark red crystalline solid **eq 3.1**. The yield for this reaction was usually about 75-80%, and seems only to be

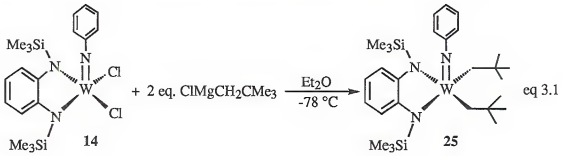

eq 3.1

limited by the extreme solubility of **25** in hydrocarbon solvents. There are many interesting characteristics of this compound. The ^1H NMR, shown in **Figure 3.2**,

showed that there was a plane of symmetry in the molecule. The neopentyl methyl groups were equivalent as were the -$SiMe_3$ methyls. The methylene protons were observed as diastereotopic protons at 2.13 ppm and 2.29 ppm. The $^2J_{H-H}$ was 10 Hz, while there were ^{183}W satellites observed at 11 Hz from $^2J_{W-H}$. The aromatic region also shows the ligands protons resonating in an AA'BB' spin system, stemming from the symmetry plane in the molecule. These observations are consistent with the square pyramidal structure drawn in **eq 3.1** for **25**. Since **25** is only a 14e- complex (the degree of interaction of the metal center with the phenyl ring of the bis-amide ligand is not known, so an electron count of 16e- might also be possible), and coordinatively unsaturated, an agostic interaction of one of the neopentyl methylene protons and the metal center is conceivable. It has been established that the magnitude of the coupling of the methylene proton with the methylene carbon is diagnostic of an agostic interaction. If the coupling constant is less than 120 Hz, then an agostic interaction is likely.[47] The $^1J_{C-H}$ for **25** was 123 Hz, and is consistent with a "normal" metal alkyl σ-bond. An interesting point is that **25** was isolable as a *cis* (bis)-neopentyl complex. Recalling the structure of **14**, the steric crowding around the metal center is overwhelming. It would seem likely that the bis-neopentyl complex would undergo a proximal α-hydrogen abstraction upon alkylation. The chelation of the bis-amido ligand may hinder the α-abstraction since rearrangement to a tetrahedral, four-coordinate alkylidene is necessary.

Other bis alkyl complexes can be prepared in an analogous manner. The neophyl derivative $W(NPh)(CH_2CMe_2Ph)_2[(Me_3SiN)_2C_6H_4]$, **26**, was isolated in 85% yield as a brownish powder which is less soluble in hydrocarbons than compound **25**. For the case of the dimethyl derivative, $W(NPh)(CH_3)_2[(Me_3SiN)_2C_6H_4]$, **27**, isolation was more difficult. The compound was extremely soluble in pentane, and could only be isolated by cooling a concentrated solution of **27** in Et_2O (1.2 grams in 2 ml) to -78° C, which gave a red solid after several days. The ^1H NMR spectrum of **27** is shown in **Figure 3.3** and clearly shows the 3:1 ratio of -$SiMe_3$ to W-Me_2 peaks. Coupling of ^{183}W to the methyl

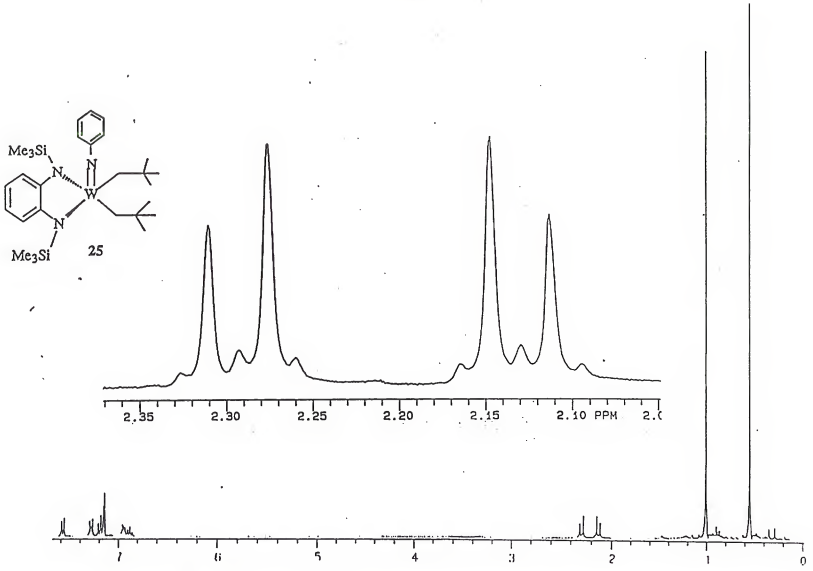

Figure 3.2. The ^{1}H NMR of W(NPh)(CH_2CMe_3)$_2$[$(Me_3SiN)_2C_6H_4$], 25.

protons was also observed and gives rise to the satellites of the methyl peak with $^2J_{W-H} = 6$ Hz. The $^1J_{C-H}$ for **27** was 123 Hz as well, indicating that an agostic interaction is unlikely. When **14** was treated with two equivalents of ClMgEt, a red oil was isolated. The red oil appeared by NMR to be pure $W(NPh)(CH_2CH_3)_2[(Me_3SiN)_2C_6H_4]$, **28**. The ^1H NMR spectrum revealed methylene resonances as multiplets at 1.91 and 2.31 ppm, while the ethyl-CH_3 protons resonated as a singlet at 1.86 ppm. The $^1J_{C-H}$ for **28** was 120 Hz, consistent with the other bis-alkyls isolated. It was interesting that an electron deficient bis-alkyl complex with β-protons was isolated. Often times these types of alkyls decompose by β-hydrogen elimination making them difficult to isolate. The dibenzyl complex, $W(NPh)(CH_2Ph)_2[(Me_3SiN)_2C_6H_4]$, **29**, was prepared using benzyl grignard as the alkylating agent. The ^1H NMR was interesting because the benzyl methylene protons did not appear to be diastereotopic, as were the methylene protons in **25**, **26** and **28**. The methylene protons resonated as a singlet at 2.78 ppm and integrate 2:9 to the -$SiMe_3$ peak. However, when **29** was heated to 80 °C in C_7D_8, the resonance becomes what appeared to be a triplet. Cooling the sample only broadened the singlet. The methylene protons are considered diastereotopic, yet coincidentally have identical chemical shifts, obscuring any coupling.

The synthesis of other bis-alkyl complexes has been investigated and show promise, although most of the products have not been completely characterized. Reacting two equivalents of allyl magnesium chloride with **14** gave a mixture of compounds. It appeared as though the major product was a bis-allyl complex where one allyl group was bound in an η^1 manner while the other was η^3. More characterization is necessary to determine the identity of the compounds. The substitution of the chlorides on **14** with aryl groups was also investigated. A bright red powder was isolated when **14** is allowed to react with two equivalents of PhLi. The ^1H NMR confirmed the identity of the compound as $W(NPh)Ph_2[(Me_3SiN)_2C_6H_4]$, **30**. This chemistry is currently being investigated by other members of the Boncella research group. Since the reactivity of **14** has shown so

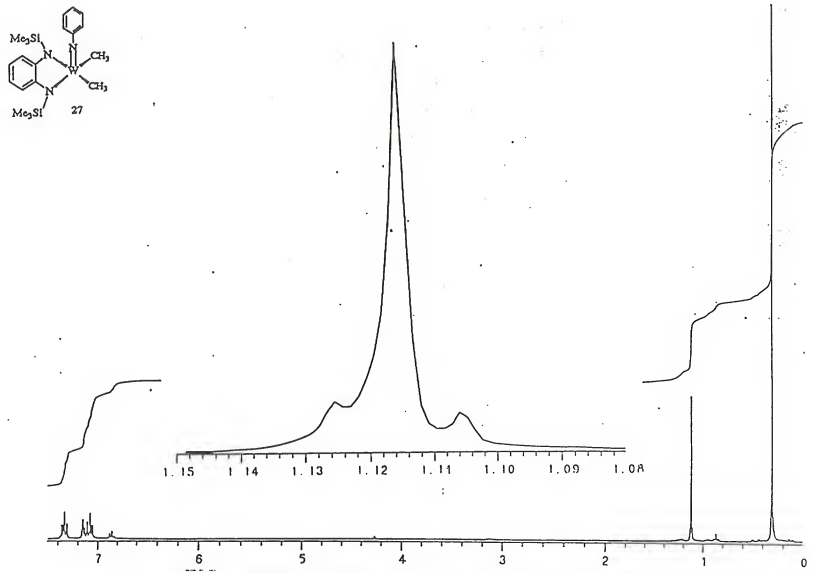

Figure 3.3. The ^1H NMR of $W(NPh)(CH_3)_2[(Me_3SiN)_2C_6H_4]$, 27.

much promise, alkylation of other dichloride derivatives was investigated. Allowing $W(O)Cl_2[(Me_3SiN)_2C_6H_4]$, **13**, to react with two equivalents of neopentyl grignard does not afford isolation of the bis-neopentyl complex as expected. However, the ^1H NMR spectrum of the brown solid shows resonances similar to the diastereotopic methylene protons of **25**. This result was not unexpected since the chemistry of the oxo complex was consistently less clean than the imido compounds. A similar result was observed when $W(NPh)Cl_2(Me_3SiN)_2C_{10}H_4$, **18**, was allowed to react with neopentyl grignard. Full characterization was not achieved but the spectral data were consistent with a bis-neopentyl complex. Better results were achieved when $W(NPh)Cl_2(Me_2PhSiN)_2C_6H_4$, **15**, and $W(NPh)Cl_2[4,5\text{-}Me_2\text{-}1,2\text{-}(Me_3SiN)_2C_6H_2]$, **19**, were allowed to react with neopentyl grignard. The two new bis-neopentyl complexes, $W(NPh)(CH_2CMe_3)_2(Me_2PhSiN)_2C_6H_4$, **31** and $W(NPh)(CH_2CMe_3)_2[4,5\text{-}Me_2\text{-}1,2\text{-}(Me_3SiN)_2C_6H_2]$, **32**, were isolated as dark red solids and have spectral properties that are similar to **25**.

Heretofore, only bis-alkyl or bis-aryl compounds were isolated. However, adding only one equivalent of alkyl to the metal center should also be possible. When one equivalent of neopentyl grignard was allowed to react with **14**, the mono-neopentyl chloride complex $W(NPh)Cl(CH_2CMe_3)(Me_3SiN)_2C_6H_4$, **33** was isolated as a red powder eq 3.2. The methylene protons of the neopentyl groups were observed as

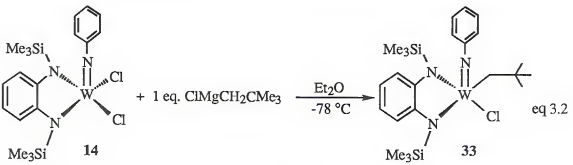

eq 3.2

diastereotopic doublets at 1.93 and 2.08 ppm respectively ($^2J_{H\text{-}H}$ = 10 Hz). The ^1H NMR spectrum of the mono-neopentyl complex, **33**, differs from the bis-alkyls due to the

absence of a plane of symmetry. The -$SiMe_3$ resonances were observed as inequivalent singlets, whereas they were equivalent in the bis alkyl complexes. In the aryl region, an AA'BB' spin system was no longer observed for the bis-amide ligand, each ligand aryl proton was inequivalent (two doublets and two triplets).

There are few examples of mixed alkyl complexes, so **33** would be a prime candidate to allow asymmetric substitution. When **33** was allowed to react with one equivalent of MeLi in an NMR tube, $W(NPh)(CH_3)(CH_2CMe_3)(Me_3SiN)_2C_6H_4$ was generated. The ^1H NMR showed four singlets in the alkyl region, in a 3:3:3:1 ratio, corresponding to the two-$SiMe_3$ groups, the neopentyl group, and the methyl group. Diastereotopic methylene protons are also observed. This compound was not isolated on a preparatory scale. Another asymmetric compound was isolated when **33** was allowed to react with one equivalent of $LiNMe_2$, forming $W(NPh)(CH_2CMe_3)(NMe_2)(Me_3SiN)_2C_6H_4$, **34**, **eq 3.3**.

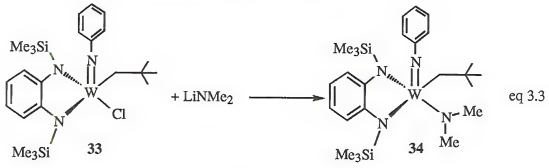

The ^1H NMR spectrum of **34** reveals diastereotopic methylene protons as doublets at 1.33 and 2.60 ppm respectively. There is lack of rotation about the W-NMe_2 bond, since two singlets were observed at 3.19 and 3.68 ppm. This lack of rotation is due to the π-donation of the lone pair of electrons on the amide nitrogen to the metal center. This type of interaction is quite common in electron deficient molecules such as **34**. Taking into account the electronic donation from the bis-amide ligand, this molecule should be considered as being electronically saturated.

3.3: Alkylidene Formation From Bis-Alkyl Complexes.

In Section 3.1, the two mechanisms of alkylidene formation from bis-alkyl complexes were discussed. The fact that bis-alkyl complexes were isolated does not eliminate proximal α-abstraction as a route to alkylidene formation. Without adding a σ-donor ligand, α-abstraction could be thermally induced. Although there are no examples of thermally induced α-abstraction reactions, this route should be viable. Many proximal α-abstraction reactions are performed at reduced temperatures, and warmed to room temperatures where α-abstraction takes place. Since the bis-alkyl complexes are thought to exist at low temperatures in these reactions, α-abstraction occurs at or near room temperature. Heating a C_6D_6 solution of **25** in a sealed NMR tube gave a very interesting result. Neopentane formation was observed in the ^1H NMR, however, it was not a result of α-hydrogen abstraction. The ^1H NMR spectrum reveals what appears to be a metallacyclobutane complex formed from the γ-abstraction of a proton from a neopentyl methyl group **eq. 3.4**. The ^1H NMR spectrum of the β,β'-dimethylmetallacyclobutane complex, $W(NPh)(CH_2CMe_2CH_2)(Me_3SiN)_2C_6H_4$, **35**, is consistent with other

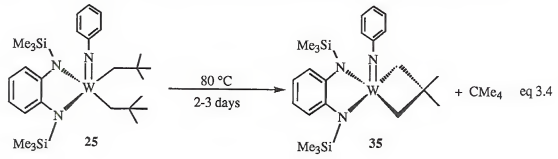

eq 3.4

metallacyclobutane complexes in the literature.[48] There are two doublets, at -1.7 and 2.1 ppm respectively ($^2J_{H-H}$ = 9 Hz), corresponding to the methylene protons of the metallacycle. The large difference in chemical shift of the protons is consistent with other metallacycles.[48] The methyl protons of the metallacycle resonated at 0.54 and 0.57 ppm respectively. They were inequivalent since they lie above and below the plane of the

metallacycle. This compound has not been fully characterized since it was difficult to isolate and purify. The difficulty in isolating the metallacycle results from the 2-3 days of heating which were required for the complete thermolysis of **25** to **35**. During this time, metallacycle formed earlier in the reaction started to decompose to unidentifiable products. However, **35** is formed by other routes and will be discussed at length later in Chapter Four. It seems unusual that **25** would undergo a γ-abstraction, however there are examples of this type of reaction in the literature. For example, Marks[49] thermally decomposes $Cp^*_2Th(CH_2CMe_3)_2$ and observes the loss of neopentane, giving the β,β'-dimethylcyclobutane thorium complex, $Cp^*_2Th(CH_2C(Me)_2CH_2)$.

Further investigation into this reaction using other bis-alkyls proved to be unfruitful. The bis-neophyl complex, **26**, was interesting since it possesses at least three thermal decomposition routes that involve proton abstraction reactions. These include: α-hydrogen abstraction, forming a neophylidene; γ-abstraction similar to **25** to give a β-methyl, β'-phenyl metallacyclobutane; or *ortho*-metallation, forming a five-membered metallacycle. Examples of each of these types of reactions have been reported in the literature. The α-abstraction and γ-abstraction reactions have already been discussed. Orthometallation reactions are observed for compounds in which the abstraction of a proton from the ortho position of an aryl group forms a five-membered ring.[2,50] A good example is the thermolysis of $CH_3Rh(PPh_3)_3$, shown in **Figure 3.4**, in which the ortho proton of

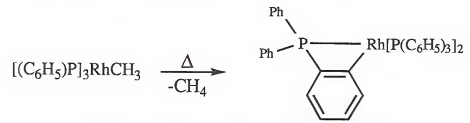

Figure 3.4. Orthometallation of $(Ph_3P)_3RhMe$

one of the phenyl groups is abstracted, releasing methane and forming a metallacycle.[51] However, when **26** was thermally decomposed at 90 °C for 3 days, no discernible products were observed. Interestingly, the β-methyl, β'-phenyl-metallacyclobutane

complex will be isolated and discussed by an alternate route in Chapter 4. Similarly, only complete decomposition to indiscernible products was observed when the dibenzyl and diethyl compounds were heated. The dimethyl complex was unique in that it was thermally stable over a period of 10 days at 90 °C.

Since no thermal pathways seemed to lead to alkylidene formation, ligand-induced α-abstraction was attempted. In a sealable NMR tube, one equivalent of PMe_3 was added to a C_6D_6 solution of the bis-neopentyl complex, **25**. Over a period of ten days at room temperature, no reaction was observed by ^1H NMR. Interestingly enough, no peak shifts were observed corresponding to coordination of PMe_3. Even upon cooling a C_7D_8 solution of **25** and PMe_3 gives no evidence of ligand coordination by observation of the ^1H NMR. This behavior was contradictory to the behavior of the dichloride precursor, **14**, which forms adducts with σ-donors quite readily. The bis-neopentyl complex, **25**, is isoelectronic with **14**, but the steric environment at the metal center in **25** would obviously be much more hindered. The tube was then warmed to 70 °C in an oil bath. After only three hours, neopentane formation was observed by ^1H NMR. Additionally, a doublet began to grow in at 9.62 ppm, indicative of an alkylidene proton coupled to a bound phosphine. The reaction proceeded nearly to completion at this temperature in 3 days; however, it was found that the reaction proceeds faster and much cleaner with two or three equivalents of phosphine present and a temperature of *ca.* 90 °C, **eq 3.5**.

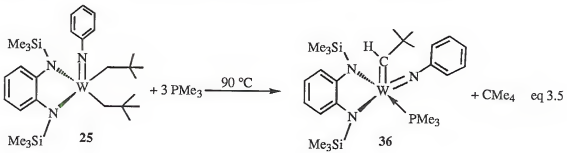

eq 3.5

In order to prepare and characterize this new alkylidene on a preparatory scale, a problem had to be overcome. In an open system, PMe_3, which has a high vapor pressure and boils

at 39 °C, would be lost when the reaction was heated to 90 °C. Additionally, heating a solution in a closed system using conventional Schlenkware would be dangerous due to a possible buildup of pressure. This problem was overcome by dissolving **25** in toluene in a tube fitted with a Young's joint with a Teflon seal. Three equivalents of PMe_3 were added and the reaction was heated to 90 °C for 12 hours. The color of the solution changed from dark green to bright orange over the time of the reaction. After cooling to room temperature, the solution was transferred to a Schlenk flask where the solvent was removed. Extracting with pentane and cooling to -10 ° C gave orange crystals of the new alkylidene complex, $W(NPh)(CHCMe_3)(PMe_3)[(Me_3SiN)_2C_6H_4]$, **36**.

In the ^1H NMR of **36**, a doublet was observed at 9.62 ppm ($^3J_{P\text{-}H}$ = 4 Hz) corresponding to the alkylidene proton. Tungsten satellites were also observed for this resonance ($^2J_{W\text{-}H}$ = 11 Hz). The alkylidene carbon was observed at 277.4 ppm ($^1J_{C\text{-}H\alpha}$ = 110 Hz). This coupling is consistent with an agostic interaction between the alkylidene proton and the metal center. The PMe_3 resonance was observed as a doublet at 0.98 ppm ($^1J_{P\text{-}H}$ = 9 Hz) in the ^1H NMR spectrum. There are three other singlets in the alkyl region of the ^1H NMR spectrum of **36**, all in a 1:1:1 ratio. One is the neopentyl methyl group, 1.39 ppm, while the other two are the silyl methyl groups, 0.38 and 0.41 ppm. The aromatic region also confirms that the molecule no longer has a plane of symmetry which would make the silyl methyls equivalent.

The geometry of the five-coordinate alkylidene complex, **36**, cannot be deduced merely from the spectroscopic data. Since this was a five-coordinate complex, there were numerous square pyramidal and trigonal bipyramidal complexes which would have fit the spectral data. Therefore determination of the crystallographic structure was essential, not only to determine the geometry of the molecule, but also to gain insight into the catalytic activity of the molecule which will be discussed later in this chapter. Slowly cooling a pentane solution of **36** to -10 °C afforded single orange crystals which were suitable for diffraction.

The thermal ellipsoid plot of **36** is shown in **Figure 3.5**. Selected bond lengths and angles can be found in **Table 3.1**. Upon examining other group (VI) alkylidene complexes,[8] it was found that the structure of **36** was very unique. The geometry was square planar with the alkylidene in the apical position. The tungsten atom lies 0.61 Å above the square plane defined by the imido nitrogen, the PMe_3 phosphorous atom, and the two amide nitrogens. The average deviation of N1, N2, N3, and P1 from the square plane was only 0.03 Å. Re-examining the issue of the interaction between metal center and the π-system of the bis-amide ligand gives an expected result. Since the electron count of the molecule has been increased by two by the addition of the ligand, a decrease in the fold-angle would be expected. The fold angle was 40 °, a 10 ° increase from the dichloride structure, **14**, yet 12 ° less than the fold angle in the six-coordinate PMe_3 adduct of the dichloride, **21**. The 40 ° fold angle suggests a weak interaction between the aryl ring of the bis-amide ligand and the metal center. The angle may be due, in part, to the great steric bulk around the metal center. Thus, the folding of the bis-amide ligand may be necessary to relieve steric interactions.

It was apparent that the chelating nature of the ligand has dictated the observed geometry of the molecule. The literature reveals that five-coordinate imido-alkylidene complexes of tungsten and molybdenum prefer to adopt trigonal bipyramidal, rather than square pyramidal structures. The compounds, *anti*-W(*trans*--CHCH=CHMe)[N-2,6-$C_6H_3(^iPr)_2$](OCMe$(CF_3)_2]_2$(quinuclidine)[52] and W(CHCH=CHPh_2)[N-2,6-$C_6H_3(^iPr)_2$](OCMe$(CF_3)_2]_2$[P$(OMe)_3$][53] are good examples of the preferred trigonal bipyramidal structure of these types of compounds **Figure 3.6**. Although **36** and these two alkylidenes have similar substituents, the geometry's are much different. The geometric constraints of the chelating bis-amide ligand must be responsible for the

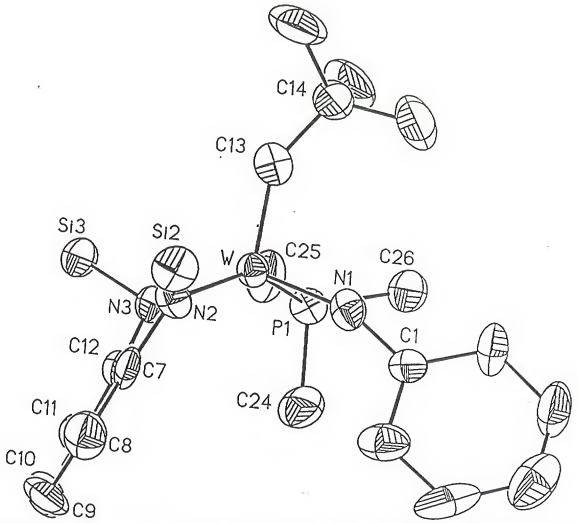

Figure 3.5. The thermal ellipsoid plot of W(NPh)(CHCMe$_3$)(PMe$_3$)[(Me$_3$SiN)$_2$C$_6$H$_4$], 36. The protons and the silyl methyls have been omitted for clarity.

Table 3.1: Bond Lengths (Å) and Angles (°) for the non-H atoms of compound **36**.

1	2	3	1-2	1-2-3
P1	W	N1	2.502(4)	82.8(4)
P1	W	N2		148.1(3)
P1	W	N3		81.2(3)
N1	W	N2	1.789(9)	98.4(4)
N1	W	N3		140.1(4)
N1	W	C13		103.6(5)
N2	W	N3	2.095(10)	77.8(4)
N2	W	C13		113.0(5)
N3	W	C13	2.067(10)	114.6(4)
N2	Si2	C18	1.736(11)	108.6(6)
N3	Si3	C21	1.761(9)	111.8(6)
C1	N1	W	1.387(14)	160.8(9)
C7	N2	W	1.39(2)	106.6(8)
W	N2	Si2		129.8(5)
C12	N3	W	1.40(2)	105.6(7)
C8	C7	N2		128.6(13)
C12	C7	N2	1.43(2)	114.6(11)
C14	C13	W	1.50(2)	148.4(9)
C13	W	P1	1.884(13)	97.5(4)

unique geometry of **36**. The bis-amide ligand of **36** should be able to coordinate in a axial-equatorial ligation, allowing the molecule to adopt a trigonal bipyramidal geometry, but it is not observed.

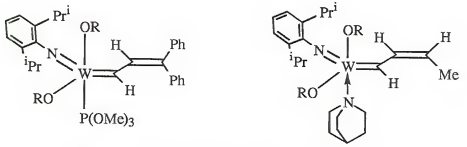

Figure 3.6. Examples of trigonal bipyramidal alkylidenes.

Although the solid state structure of the compound has been solved, the structure in solution was actually the key to the reactivity of the molecule. When the alkylidene proton was irradiated in an nOe experiment, a 6% enhancement was observed for both the silyl

methyl groups. No significant enhancement was observed for the imido aryl protons, or the PMe_3 methyls. When the neopentyl methyls were irradiated, the *ortho*-arylimido protons and the PMe_3 protons where enhanced by 2.5% and 3.7% respectively, while no significant enhancement was observed for the silyl methyl groups. This geometry will be referred to as *syn*, where the neopentylidene *t*-butyl group is *syn* to the imido group.

There are two reactions which should be considered at this time to better understand the role of the PMe_3 in the formation of the alkylidene. First when Cu(I)Cl was added to a C_6D_6 solution of the alkylidene, **36**, formation of the metallacyclobutane complex, **35**, was observed by ^1H NMR **eq 3.6**. Cu(I)Cl forms an insoluble adduct with PMe_3 and effectively removes it from the solution. The four-coordinate alkylidene then undergoes a rearrangement to the metallacycle. The rearrangement is effectively a 1,3 shift of a proton

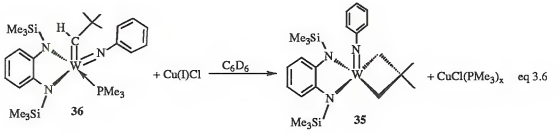

from a γ-methyl to the alkylidene carbon, as well as forming the new W-C bond. Although the nature of this rearrangement is not known, the result is undeniable and will be discussed further in Chapter 4. Secondly, when PMe_3 was added to a C_6D_6 solution of the metallacycle, **35**, complete conversion to the alkylidene, **36**, was observed by ^1H NMR **eq 3.7**. These two reactions show the relationship between the alkylidene, **36**, and the metallacycle, **35**.

Insight into the mechanism by which the alkylidene, **36**, is formed from the bis-neopentyl complex, **25**, **eq 3.5**, is gained by these reactions. The thermolysis of **25** in the absence of PMe_3 might initially give a four-coordinate alkylidene, which quickly rearranges to give the five-coordinate metallacycle, **35**. In the presence of PMe_3, the four-coordinate alkylidene is 'trapped' by the phosphine, forming **36**. The intermediate four-

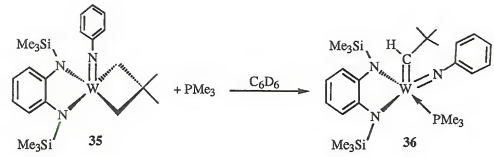

eq 3.7

coordinate alkylidene could be tetrahedral, and coordination of the PMe_3 would result in rearrangement to the observed geometry of **36**, with the alkylidene in the apical position. This mechanism can be seen in **Figure 3.7**. Regardless of the actual mechanism, the observed net result was still α-abstraction induced by PMe_3.

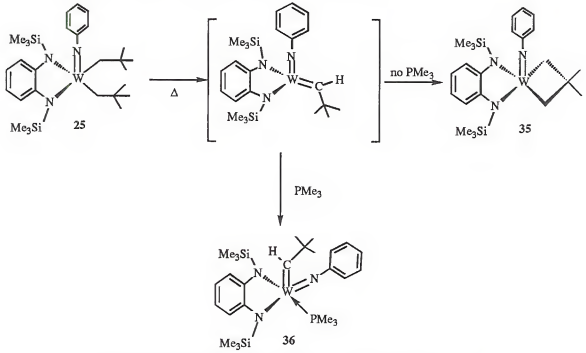

Figure 3.7. Scheme for alkylidene and metallacycle formation showing an intermediate tetrahedral alkylidene.

Although the application of the PMe_3 ligand to induce an α-abstraction reaction might be widely applied to the other bis-alkyl compounds isolated, the bis-neopentyl appears to be a unique case. The neophylidene compound can be isolated, however, a

longer reaction time is necessary. When the dimethyl complex, **27**, was heated to 90 °C in the presence of excess PMe_3, no reaction was observed over 10 days, not even decompostion of the dimethyl complex. Once again, it was astonishing that no PMe_3 adduct formation was observed. Adduct formation would be expected since the methyl substituents are not much bigger than the chlorides in **14**. When the diethyl complex, 28, was heated to 90 ° C with PMe_3, decomposition to indistinguishable products was observed. Surprisingly, when the dibenzyl complex, **29**, was heated with excess PMe_3 the compound appeared quite stable. No benzylidene formation was observed over time in the ^1H NMR, although after a week at 90 °C, decomposition occurred. Though disheartening, it is not uncommon to see a unique behavior when dealing with neopentyl and neophyl compounds. The first as well as the most common examples of alkylidenes are either neopentyl or neophyl.

The nature of the σ-donor ligand necessary to induce α-abstraction was also investigated. It would be advantageous to be able to prepare alkylidenes from the bis-neopentyl compound using the weakest σ-donors available. This would facilitate easy removal of them either to isolate a four-coordinate alkylidene or the *in situ* dissociation of the ligand forming a transient four-coordinate intermediate. When the bis-neopentyl complex, **25**, was heated in the presence of PEt_3 in a sealable NMR tube, the alkylidene complex $W(NPh)(CHCMe_3)(PEt_3)[(Me_3SiN)_2C_6H_4]$, **37**, was observed. However, when trying to isolate **37** on a preparatory scale, a mixture of the alkylidene and the metallacyclobutane complex was isolated. The lack of phosphorous coupling to the alkylidene proton in the ^1H NMR of **37**, which was observed as a broad singlet at 9.82 ppm, was evidence of the weak coordination of the PEt_3 ligand. Weak coordination was also evident from the ^{31}P NMR spectrum. The PEt_3 was observed as a broad singlet at -11.42 ppm; no ^{183}W satellites were observed as was the case with the PMe_3 adduct of the alkylidene. As expected, when PMe_3 was added to a C_6D_6 solution of **37**, immediate formation of the PMe_3 adduct, **36**, was observed by ^1H NMR. Using other phosphines

did not lead to the isolation of new alkylidenes, only decomposition or formation of the metallacyclobutane complex was observed by ^{1}H NMR. These reactions were attempted using $PMePh_2$, PCy_3, and PPh_3. When quinuclidine, $N(CH_2CH_2)_3CH$, was heated in a C_6D_6 solution of the bis-neopentyl product, the metallacycle was the only product observed. This was curious since quinuclidine serves as a σ-donor for other electron deficient organometallic compounds, including a number of alkylidenes.[52] Only decomposition was observed when THF or DME were utilized as the σ-donor ligands.

One property of the new alkylidene which was promising was the thermal stability of the molecule. A NMR tube containing a C_7D_8 solution of the PMe_3 adduct, **36**, can be heated to 90 °C over days with no observed decomposition in the ^{1}H NMR spectrum. Even though more alkylidenes could not be prepared, the isolation of this new alkylidene offers a starting point for a study into the metathesis activity of this chelated alkylidene. Although it would have been desirable to be able to prepare more derivatives of alkylidenes using this new *o*-phenylenediamine ligand system it is not unusual to see this type of reactivity. The formation of alkylidenes by means of α-abstraction of an alkyl proton is a delicate reaction. There are many factors which influence the reaction products. The sterics of the ancillary ligands and bis alkyl groups play important roles, as well as the electronics of the ancillary ligands. These factors play important roles not only in the α-abstraction reaction, but also in the stability of the alkylidene itself. There are many decomposition pathways available for alkylidenes, and the balance of steric and electronic factors of all the substituents must be carefully controlled for isolation of a stable alkylidene.[54]

3.4. Metathesis activity of W(NPh)(CHCMe$_3$)(PMe$_3$)[(Me$_3$SiN)$_2$C$_6$H$_4$], **36**.

Before examining the metathesis reactivity of the alkylidene, the mechanism of this reaction should be considered as well as how it applies to the known structure of **36**.

Schrock has done extensive studies[8] which have concluded that in olefin metathesis reactions the olefin prefers to attack the C-N-O face in the alkoxide alkylidenes. This would translate to the C-N_{imido}-N_{amido} face in the chelated alkylidene. The open coordination site in **36** is *trans* to the alkylidene carbon, where, if the olefin coordinated, rearrangement of a six-coordinate complex would be necessary. The most likely mechanism for olefin metathesis with this new alkylidene involves prior dissociation of the PMe_3 ligand, followed by attack of the olefin on the vacant coordination site at the C-N_{imido}-N_{amido} face of the molecule. Support for this mechanism will be offered throughout the discussion.

When a pentane solution of W(NPh)(CHCMe$_3$)(PMe$_3$)[(Me$_3$SiN)$_2$C$_6$H$_4$], **36**, was refluxed with one equivalent of diphenylacetylene, a metallacyclobutene complex, W(NPh)[C(H)(*t*-Bu)C(Ph)C(Ph)][(Me$_3$SiN)$_2$C$_6$H$_4$], **38**, was isolated as a red oil **eq 3.8**. In the ^{1}H NMR spectrum a singlet was observed at 2.82 ppm ($J^2_{W\text{-}H}$ = 8 Hz)

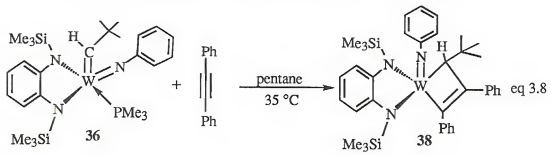

eq 3.8

corresponding to the α-proton of the metallacyclobutene complex. Metallacyclobutene complexes of tungsten are quite common, arising from the metathesis of alkylidenes with diphenylacetylene.[55] Although the reaction took place under relatively mild conditions by heating to 35 °C, it is important to note that the reaction must be carried out in an open system. A different result is observed if the phosphine is not liberated from the reaction mixture. In a sealable NMR tube, a C_6D_6 solution of **36** and diphenylacetylene was warmed to 50 °C for 3 days. The ^{1}H NMR reveals the formation of **38** within 10 hours, however, after 3 days, a singlet was apparent at 5.50 ppm, as well as a much smaller

singlet at 5.45 ppm. A broad singlet was observed at 0.90 ppm, presumably a new PMe_3 resonance. The new product was apparently a vinyl alkylidene, arising from the PMe_3 induced ring opening of the metallacycle, **eq 3.9**.

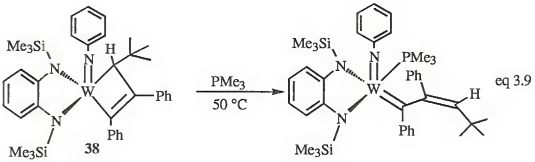

eq 3.9

The observation of two new olefinic resonances was most likely due to formation of both *cis* and *trans* isomers of the vinyl alkylidene. This reaction has been observed for other metallacyclobutene complexes when σ-donor ligands are added.[55]

The ring opening metathesis polymerization (ROMP) of norbornene, NBE, was chosen in order to investigate the olefin metathesis activity of **36**. The alkylidene, **36**, polymerized 25 equivalents of NBE in 10 minutes. Analysis of the polymer using GPC techniques reveals a very high molecular weight for the polynorbornene. The molecular weight was determined to be 61,000 g/mol versus a polystyrene standard. However, Schrock and Grubbs have determined that a conversion factor of 2.2 is appropriate for polynorbornene versus polystyrene.[17] This would make the corrected M_n = 27,000 g/mol. This was still enormous compared to the molecular weight which would be expected if all the catalyst was active. If 100% of the catalyst was initiated and propagating, the molecular weight should be near 2500 g/mol. This result showed that less than 10% of the catalyst was active. This result was consistent with the prediction that phosphine must be lost in order for the olefin to coordinate to the metal center. Also, in order to observe such a high molecular weight, the rate of the propagation step must be much faster than the rate of the initiation step. **Figure 3.8** demonstrates this as well as the dependence the reaction would have on the presence of PMe_3 in the reaction mixture.

Grubbs studied the effect PMe_3 had on the ROMP of cyclobutene[56] by Schrock's catalyst, W(NAr)(CH-t-Bu)(O-t-Bu)$_2$, Ar = 2,6-diisopropylphenyl. The observations made by Grubbs were consistent with the ROMP of NBE by the catalyst, **36**. In order to observe the effect of added PMe_3, **36** was dissolved in toluene in the presence of ten equivalents of PMe_3. A toluene solution of 150 equivalents of NBE was then added and the mixture was stirred for one hour. Precipitation with methanol gave a 80% yield of polynorbornene. The lack of consumption of the monomer, even over the longer reaction time, demonstrates the effect of PMe_3 on the rate of the reaction. Analysis of the polymer using GPC techniques versus a polystyrene standard gave a corrected M_n = 35,000 g/mol. The theoretical M_n, 14,124 g/mol, was roughly 50% of the observed M_n, compared to less

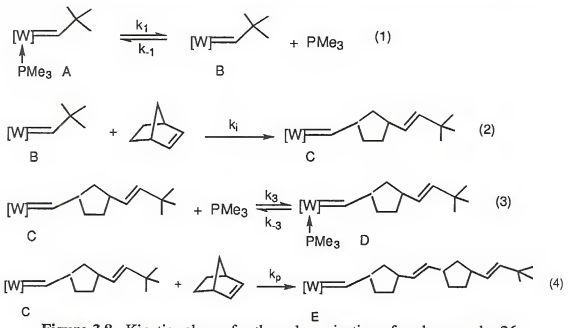

Figure 3.8. Kinetic scheme for the polymerization of norbornene by **36**.

than 10% for the uninhibited polymerization reactions. All of the GPC data for the NBE polymerization reactions can be found in **Table 3.2**. The percentage of active catalyst has been increased dramatically by the addition of PMe_3. It is important to note how the phosphine is affecting the polymerization. The added PMe_3 must be hindering propagation to a much greater extent than it is hindering initiation. Grubbs measured the K_{eq} of PMe_3

binding to both the uninitiated catalyst, A, and the propagating alkylidene, D.[56] It was observed that the PMe_3 binds much more strongly to the propagating alkylidene than the uninitiated catalyst. This large difference in binding energy virtually stalls the propagation of the polynorbornene, allowing much more alkylidene to initiate. For the polymerization of NBE using **36** as the catalyst in the presence of PMe_3, the reaction was slowed to such an extent that after an hour, the reaction only reached 80% completion. But, judging from the M_n of the polynorbene polymers formed, the percentage of active catalyst was still well below 100%.

The percentage of active catalyst was normally observed to be between 40% and 60% when ten equivalents of PMe_3 were used. So, in the inhibited polymerization of NBE using **36**, although the added phosphine makes $k_3 >> k_{-1}$, k_{-1} was still much larger than k_1. If $k_{-1} > k_1$, then the observed percentage of active catalyst was understandable. At room temperature, an equilibrium was observed between A and B for Grubbs' system, with the equilibrium favoring B.[56] At room temperature, no equilibrium was observed for **36**, the PMe_3 was tightly bound with distinctive ^{183}W satellites ($^1J_{W\text{-}P}$ = 128 Hz).

The nature of the propagating alkylidene was also observed in an NMR tube reaction. Five equivalents of PMe_3 and five equivalents of NBE were allowed to react with **36** in C_6D_6. After one hour the ^1H NMR spectrum of the reaction revealed that only 80% of the NBE was consumed. Also, *ca.* 40% of **36** was converted into propagating alkylidene. Two broad resonances were observed at 9.09 and 9.31 ppm. These peaks correspond to the syn and anti isomers of the propagating alkylidene species.[17,56]

One property that was not mentioned about the poly(norbornene) polymers catalyzed by **36** was the molecular weight distribution. The polydispersity index, PDI, is a measure of distribution of the molecular weight of the polymer chains and is calculated by M_w/M_n where M_w is the weight-averaged molecular weight and M_n is the number-average molecular weight. All of the polymers which were prepared displayed very narrow polydispersities, regardless of whether or not the polymerizations were inhibited by PMe_3.

A comprehensive theoretical study was done by Gold[57] in order to understand the relationship between the observed PDI values and the relative rates of propagation and initiation, k_p/k_i. This study, simplified by others,[58] allows a determination of the theoretical M_w/M_n based on k_p/k_i. The formula takes into account the initial concentrations of catalyst and monomer, and the concentrations of catalyst and monomer at any given time.

From NMR experiments, after 30 minutes the uninhibited NBE polymerization has 10% active catalyst with 40% of the monomer consumed. This gives a relative k_p/k_i of 115. This was extremely fast although the high molecular weights observed agree with this calculation. In a similar experiment inhibited by 5 equivalents of PMe_3, the relative k_p/k_i was observed to be 30. The effect of the PMe_3 can be seen on the relative rate, however, a k_p/k_i of less than 1 would serve to initiate all the catalyst and give better control of the molecular weight of the polymerization. From Gold's calculations,[57] relative k_p/k_i's of this magnitude should give PDI values between 1.005 and 1.12.

Table 3.2. Polymerization of NBE using **36**, inhibited vs. uninhibited.

eq's of NBE	time	Mn/ corrected[a]	PDI	Mn/ theoretical	% yield
		Inhibited with 10 equivalents of PMe_3			
150	1 hr	35,000 g/mol	1.01	14,124 g/mol	80
1000	1 hr	104,000 g/mol	1.00	94,217 g/mol	65
163	3 hrs	94,000 g/mol	1.07	15,357 g/mol	85
70	4 hrs	126,000 g/mol	1.07	6,592 g/mol	88
		Uninhibited			
25	5 min	28,000 g/mol	1.12	2,354 g/mol	90
100[b]	5 min	37,000 g/mol	1.07	9,517 g/mol	90
342	10 min	120,000 g/mol	1.03	32,202 g/mol	90
52	1 hr	115,000 g/mol	1.04	4,888 g/mol	95

a. A correction factor of 2.2 was applied for polynorbornene vs. polystyrene.
b. The polymer was end-capped with benzaldehyde after 5 minutes.

The catalytic reactivity of **36** has been examined for other systems as well. The alkylidene, **36**, catalyzes the polymerization of cyclooctene, however, only at elevated temperatures. This supports the mechanism of dissociation of PMe_3 before the olefin can attack. The ROMP of cyclooctene has a higher activation barrier than NBE since there was much less ring strain to be relieved and the NBE is much smaller, allowing NBE monomer to coordinate more readily to an open coordination site of the catalyst. The ADMET polymerization of 1,9 decadiene has also been investigated. It was already discussed that **36** is stable to thermal decomposition in refluxing toluene, therefore, it should be a candidate for a thermally stable ADMET catalyst. Observations did not agree with this assertion. The alkylidene does catalyze the ADMET oligomerization of 1,9-decadiene, however, the reaction never proceeded past dimers and trimers. It has been suggested that **36** has a preference for internal olefins, causing unproductive metathesis, however this or any other explanation has not been substantiated.

One aspect of the ADMET reaction which was observed was the poisoning of the catalyst by the ethylene produced in the reaction. When ethylene was bubbled into a C_6D_6 solution of **36**, the ^1H NMR initially reveals what appears to be a metallacyclobutane complex with an α-t-butyl group. There were multiplets at 2.40 ppm, 2.62 ppm, and 3.76 ppm in a 1:1:1 ratio. A new singlet at 1.20 was also observed in a 9:1 ratio with the singlets. Over time these resonances diminished as resonances grew in which correspond to a unsubstituted metallacyclobutane complex. The ^1H NMR reveals multiplets at 1.80 ppm, 1.91 ppm, 2.20 ppm, 2.58 ppm and 2.75 ppm in a 1:1:1:2:1 ratio. **Figure 3.9** shows the scheme by which the α-t-butyl metallacyclobutane is formed and then further reacts to give the unsubstituted metallacyclobutane complex. Although there was no other spectral data to support this mechanism, this appears analogous to the behavior displayed by Schrock's catalyst.[48,59] The peak positions of both metallacycles correspond to observations made for the alkylidene, $W(NAr)(CH\text{-}t\text{-}Bu)(OR)_2$ and ethylene.[59] Examination of the room temperature ^1H NMR over the course of the reaction did not

reveal the intermediate methylidene complex, which must be formed before the unsubstituted metallacycle can be formed.

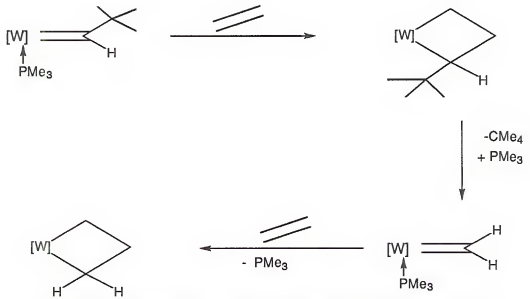

Figure 3.9. Proposed mechanism for formation of an unsubstituted metallacycle from the reaction of **36** and excess ethylene.

Recently, the applications of ADMET have been expanded to the depolymerization of unsaturated polymers. Wagener has utilized Schrock's catalyst in order to depolymerize 1,4-polybutadiene, end-capped with a silylene.[60] Although **36** proved unsuccessful for the polymerization of 1,9-decadiene, possibly because of a preference for internal olefins, its activity as a depolymerization catalyst was investigated. 500 equivalents of 1,4-polybutadiene was dissolved in minimal toluene in the presence of **36**. After 24 hours, 500 equivalents of the end-capping group were added. GPC analysis revealed that the depolymerization was successful. Only monomer and dimer were present. Currently, further work is being done on this reaction.

In this chapter, the substitution of the chlorides in **14** led to the isolation of numerous new alkyl complexes. The chemistry of the bis-neopentyl derivative, **25**, led to the isolation of a new metallacycle and new alkylidene complex. The metathesis reactivity of the alkylidene, **36**, was investigated and shown to be inhibited by the addition of PMe_3.

The reactivity of the bis-neopentyl derivative, **25**, involving molecular hydrogen will be the focus of Chapter 4, and will draw on many of the same principles discussed in this chapter.

CHAPTER 4
FORMATION OF W(VI) HYDRIDES FROM THE BIS-ALKYL COMPLEXES

4.1. High Oxidation State Transition Metal Hydride Complexes

The synthesis of high oxidation state transition metal hydride and polyhydride complexes is a highly active area of chemical research.[61,62] Complexes containing M-H bonds have long been known to be important intermediates in a plethora of catalytic processes.[62,63] The hydrogenation of olefins, both catalytic and stoichiometric, is one of the most important functions of transition metal hydride complexes.[61,64] Recently, Rothwell even demonstrated the catalytic hydrogenation of benzene using a tantalum(V) hydride complex. There are a number of methods that have been utilized in the preparation of these hydride complexes. One common preparative method is the high pressure hydrogenation of metal-alkyl bonds.[61,62] Another means of preparing hydride complexes is the oxidative addition of hydrogen to lower oxidation state compounds such as W(IV) and Ta(III).[61,62,66] Transition metal hydride complexes have also been prepared by utilizing hydride reagents such as n-Bu_3SnH or $LiBEt_3H$.[67] Because of its small size, many hydrides have coordination numbers greater than six. Also, most monomeric hydrides are stabilized by strong σ-donors ligands, such as phosphines.

4.2. Preparation of W(VI) Hydride Complexes.

There have been many reports of the hydrogenation of high oxidation state alkyl complexes to give hydrides, however, frequently these reactions are performed under forcing conditions (extremely high pressures of hydrogen in the presence of phosphine ligands at elevated temperatures).[61,62] Rothwell observed the reaction of hydrogen and

$Ta(R)_2(OAr)_3$ to give $Ta(H)_2(OAr)_3(PR_3)$ in the presence of phosphine.[68] This reaction was carried out at 90 °C under 8300 kPa of hydrogen for 24 hours **eq 4.1**. These

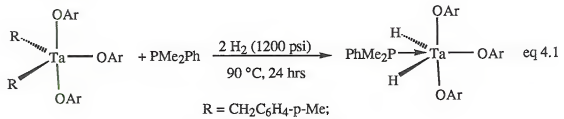

$R = CH_2C_6H_4$-p-Me;
$OAr = OC_6H_3$-2,6-Pr^i_2

conditions are typical for the hydrogenation of alkyl compounds and are quite harsh. Similar conditions were not necessary for the hydrogenation of some of the bis-alkyl complexes discussed in Chapter 3. When $W(NPh)(CH_2CMe_3)_2[(Me_3SiN)_2C_6H_4]$, **25**, was placed under two atmospheres of hydrogen in the presence of two equivalents of PMe_3 at room temperature, the conversion of the bis-neopentyl to a new dihydride complex was complete in less than two hours. The dark brown solution turned magenta, and small red crystals precipitated from solution **eq 4.2**. The new complex was the seven coordinate dihydride, $W(NPh)(H)_2(PMe_3)_2[(Me_3SiN)_2C_6H_4]$, **39**.

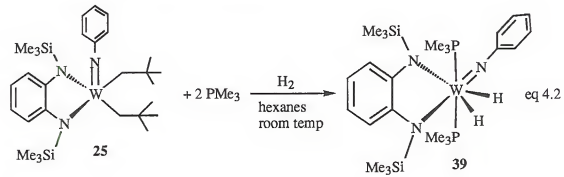

Compound **39** was characterized by multinuclear NMR and X-Ray crystallography. At room temperature, the ^1H NMR spectrum reveals the hydride resonances as a broad triplet at 9.28 ppm with a peak separation of 38 Hz. The two PMe_3 groups appeared as a singlet at 1.04 ppm, while the silyl methyls were inequivalent singlets at 0.79 and 0.81 ppm, respectively. The two phosphines were observed as a singlet at

-24.46 ppm ($^1J_{W\text{-}H}$ = 188 Hz) in the ^{31}P NMR spectrum. When the ^1H NMR spectrum was taken at -50 °C, numerous changes were observed. First of all, the PMe_3 resonance resolved into a triplet with a peak separation of 3 Hz at 0.84 ppm. Secondly, the silyl methyls separated further, resonating at 0.69 and 0.75 ppm. The hydrides appeared as a doublet of doublets at 8.92 ppm and 9.06 ppm respectively. The apparent coupling was 37 Hz.

Unfortunately, high quality single crystals of **39** have not yet been obtained. Numerous attempts were made to acquire crystallographic data on **39**. Some data was collected although an accurate structure could not be determined. The data suggest the presence of *trans*-phosphines with the amido and imido nitrogens in the equatorial plane. In order to have equivalent phosphines and inequivalent hydrides, the hydrides probably lie *cis* to each other, in the plane of the imido and amido nitrogens. This geometry, shown in **eq 4.2**, should give an ABX_2 resonance for the hydrides, which would be a doublet of triplets. The doublet of doublets observed at low temperature are very broad and may be due to a second order effect. A concerted effort is currently underway to obtain an X-ray structure of **39**. The PMe_2Ph derivative, $W(NPh)(H)_2(PMe_2Ph)_2[(Me_3SiN)_2C_6H_4]$, **40**, was prepared in an analogous reaction. The hydride ligands were observed as a broad singlet at 9.80 ppm in the ^1H NMR spectrum at room temperature. At -50 °C, a triplet at 9.56 ppm was observed with 39 Hz coupling, analogous to **39**. The ^{31}P NMR spectrum revealed a singlet at -22.48 ppm with 183 Hz ^{183}W satellites. The PMe_2Ph derivative was prepared in the hopes growing better crystals, since most of the structurally characterized hydrides are the PMe_2Ph derivative.[61,62,67]

The seven-coordinate dihydride, **39**, should serve as an excellent model to study the reactivity of dihydride complexes. Therefore, a more convenient route to the synthesis of this compound would be useful. Avoiding the alkylation step and adding hydride to the dichloride, **14** would be a viable route. Two equivalents of superhydride, $LiBEt_3H$, were allowed to react with **14** in cold Et_2O. Work-up afforded **39** as a brown-red powder.

There was residual BEt_3 which could not be removed from the compound. Although this reaction was important in showing the ability of **14** to add hydride, it was not employed to make the hydrides for the reactivity studies.

When two equivalents of PCy_3 were utilized as the phosphine ligands, the steric bulk of the ligand prevented isolation of the analogous bis-phosphine complex. Although combustion analysis has not been performed because of the excess phosphine present, the spectral data are consistent with the isolation of the monophosphine complex $W(NPh)(H)_2(PCy_3)[(Me_3SiN)_2C_6H_4]$, **41**, **eq 4.3**. The ^1H NMR spectrum of **41** reveals a doublet at 11.35 ppm ($^2J_{P\text{-}H}$ = 83 Hz).

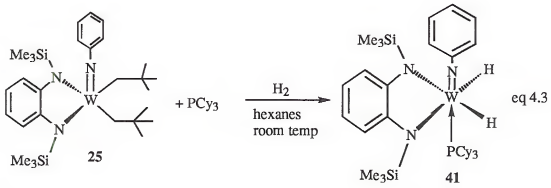

Satellites due to the ^{183}W $^1J_{W\text{-}H}$ coupling were observed at 64 Hz. The silyl methyl groups were observed as a singlet at 0.83 ppm. The ^{31}P NMR spectrum of **41** reveals a singlet at 66.53 ppm ($^1J_{P\text{-}H}$ = 83 Hz).

The chelating nature of the bis-amide ligand again dictates the geometry of the molecule. Rothwell prepared $Ta(OAr)_2Cl(H)_2(L)_2$ derivatives using PMe_3, PMe_2Ph, $PMePh_2$.[68] The structures of these compounds reveal that the phosphines are always *trans* to one another. In these compounds, the aryloxides are always *trans* to one another as well. This differed from **39** and **40** in which the amide nitrogens must be *cis* to one another because of the chelating nature of the ligand. In order to investigate the role of the *trans* phosphines, and to fine out whether or not cis phosphine complexes were stable, a chelating phosphine was selected. Diphenylphosphinoethane, DPPE, was utilized in a

reaction similar to eq **4.2**. The new hydride was found to be $W(NPh)(H)_2(DPPE)[(Me_3SiN)_2C_6H_4]$, **42**, **eq 4.4**.

The ^1H NMR spectrum of **42** reveals a very symmetrical molecule. The silyl methyls were observed as a singlet at 0.49 ppm. The methylene protons of the DPPE ligand were observed as multiplets at 2.23 and 2.42 ppm. The hydrides were equivalent at all temperatures observed. At room temperature the hydrides appeared as a complex multiplet which can be viewed as the X part of an ABX_2 spin system where the phosphines are A and B. Satellites due to ^{183}W coupling were observed at 58 Hz for each of the peaks in the spectrum. The ^1H NMR spectrum of the hydride region can be seen in **Figure 4.1**.

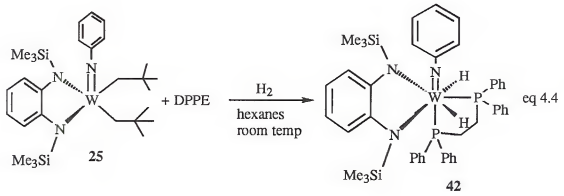

The phosphines were inequivalent in the ^{31}P NMR spectrum, and appear as doublets, at -12.70 and 30.43 ppm, respectively ($^2J_{P\text{-}P}$ = 83 Hz). The geometry of this seven-coordinate dihydride can be inferred from the NMR data. Having one leg of the DPPE bisect the two hydrides is the only possible geometry giving both equivalent silyl methyls and hydrides as well as inequivalent phosphines.

There are few examples of high oxidation state hydride complexes where strong σ-donor ligands are not coordinated to the metal center. Coincident with this is that there are few coordinatively unsaturated high oxidation state hydride complexes. One of the few examples resulted when Rothwell hydrogenated $Ta(OAr)_3(CH_2C_6H_4\text{-}4\text{-}Me)_2$ under 1200 psi of hydrogen at 90 °C for 24 hrs to give $Ta(H)(OAr)_4$ in low yield.[68] The monohydride

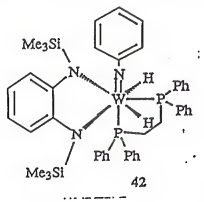

42

Figure 4.1. The ^1H NMR spectrum of the hydride region of $W(NPh)(H)_2(DPPE)[(Me_3SiN)_2C_6H_4]$, 42

is presumably formed in a ligand exchange reaction. There are also metallocene derivatives of the type Cp_2MH_2, but these will not prove insightful to this discussion.[69]

When phosphine was present upon hydrogenating the bis-neopentyl complex, **25**, the reaction was complete in a matter of hours. When no phosphine was added to the reaction, the hydrogenation proceeded much more slowly, and allows an examination of the mechanism of the reaction. When H_2 gas was sealed in an NMR tube containing a C_6D_6 solution of **25**, hydrogenation of the metal carbon bonds took place in a matter of days. The rate was dependent on the pressure of H_2 gas. When a very low pressure of gas, < 20 psi was sealed in the tube, the reaction took nearly a week to reach completion. However, when 30 psi of H_2 was used, the reaction was complete in about 36 hours. The product is only observable under an atmosphere of H_2 gas. The product of the hydrogenation was presumably a dimer due to interpretation of the NMR data. The silyl methyl groups were observed as a singlet at 0.33 ppm in the ^1H NMR spectrum. Two equivalents of neopentane were observed at 0.93 ppm. The spectrum also reveals a singlet at 15.68 ppm with 168 Hz ^{183}W satellites corresponding to the two hydrides. The tungsten satellites were actually observed as doublets, J = 4 Hz. The observation of the tungsten satellites as doublets was the key evidence in proposing a dimeric structure. Cotton observed a similar coupling effect in the $W_2Cl_4(NHCMe_3)(PR_3)_2$ system.[69] The only observable satellites will be from a dimer with only one ^{183}W, due to only 14% abundance. This would constitute an ABX spin system, resulting in a doublet of doublets. The hydride resonance is shown in **Figure 4.2**. The shift of the hydrides was in the normal range for high oxidation state group 5 and 6 complexes in the literature.[61-68] Evidence for proposing bridging imido groups will be given later in the chapter. The reaction is shown in **eq 4.5**. When the sample was evaporated to dryness, the dihydride isomerized or rearranged, forming what appeared to be a bridging hydride. When the sample was redissolved in C_6D_6, the ^1H NMR spectrum changed dramatically. At room temperature, the hydrides did not appear in the spectrum, although a broad increase in the integral was observed between

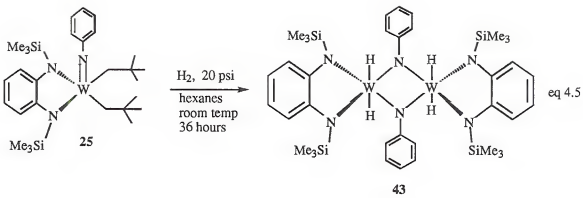

eq 4.5

11 and 13 ppm. When the sample was cooled to -25 °C, a sharp singlet at 12.58 ppm and a broad singlet at 15.80 ppm were observed in a 1:1 ratio. When the sample was cooled further, to -50 °C, the sharp singlet remained unchanged while the broad singlet split into two broad singlets at 15.28 ppm and 15.98 ppm respectively. The ratio of the three peaks was observed to be 2:1:1. The broad singlets are consistent with being bridging hydrides, while the sharp singlet appears to be the terminal hydrides. The sharp singlet actually had satellites at 53 Hz and 100 Hz. Although the true identity of the molecule cannot be confirmed, it is assuredly still a dihydride complex of sorts. When two equivalents of PMe_3 were added to the sample, the bis-phosphine dihydride, **39**, was formed by observation of the ^1H NMR. There is not enough known at this time to make more substantial conclusions, but work is continuing in this area.

As was mentioned earlier, since the hydrogenation, at very low pressures of H_2, takes a number of days, an opportunity to observe intermediates and deduce a mechanism was presented. In an NMR tube reaction, **25** was dissolved in C_6D_6 and sealed under an atmosphere of less than 20 psi H_2. After twelve hours, the ^1H NMR revealed four compounds in the reaction mixture. There was 25% starting material, neopentane, and two new compounds, the metallacyclobutane, **35**, and a monohydride complex, **44 eq 4.6**. The spectrum reveals the two doublets, at -1.7 and 2.1 ppm, which correspond to the metallacyclobutane complex discussed in Chapter Three.

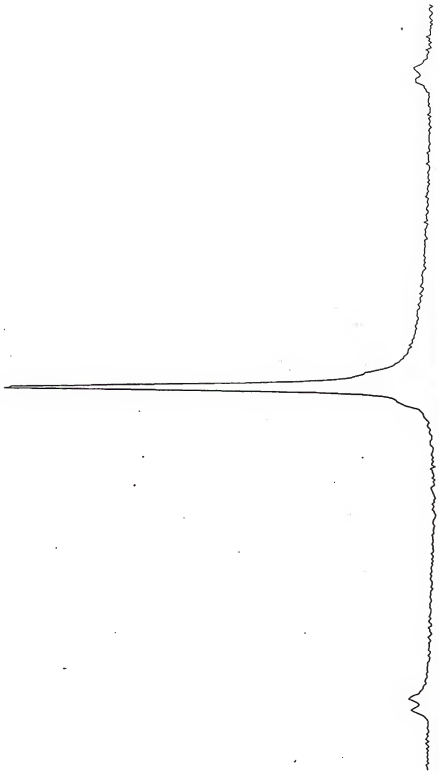

Figure 4.2. The ^{1}H NMR spectrum of the hydride resonance of 43.

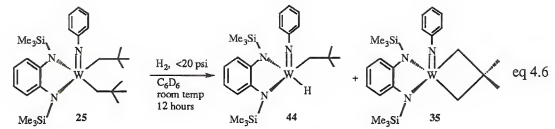

eq 4.6

The monohydride, W(NPh)(CH_2CMe_3)(H)[$(Me_3SiN)_2C_6H_4$], **44**, was characterized by a singlet at 18.43 ppm ($^1J_{W-H}$ = 151 Hz). The methylene protons of the monohydride-neopentyl complex appeared diastereotopic with a doublet at 2.60 ppm and a broad singlet at 3.28 ppm. As the reaction was observed over the course of the following 3 days, the bis-neopentyl complex, **25**, disappeared completely and the dihydride complex, **43**, grew in. Over the course of a number of trials of this NMR tube reaction, it was observed that the bis-neopentyl reached at least 90% completion before dihydride formation initiated.

The metallacyclobutane complex was thought to be in an equilibrium with the monohydride complex under an H_2 atmosphere. The metallacycle was formed when H_2 was lost from the monohydride by a net γ-hydrogen elimination mechanism. The reverse reaction takes place when H_2 was added across one of the W-C bonds of the metallacycle **eq 4.7**. This equilibrium was

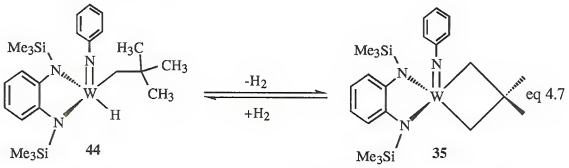

eq 4.7

demonstrated by adding H_2 to an NMR tube containing a C_6D_6 solution of **25**, then degassing the reaction after eight hours. The ^1H NMR spectrum, which was taken immediately after degassing, revealed the three compounds expected, **25**, **35**, and **44** in roughly a 1:1:3 ratio. Over the course of two weeks, the reaction was degassed

periodically. During this time, the bis-neopentyl complex was completely consumed. Also, as the reaction proceeded, the monohydride decreased and was only observable in trace amounts. **Figure 4.3** demonstrates how only a catalytic amount of hydrogen was necessary for complete conversion of the bis-neopentyl complex to the metallacycle.

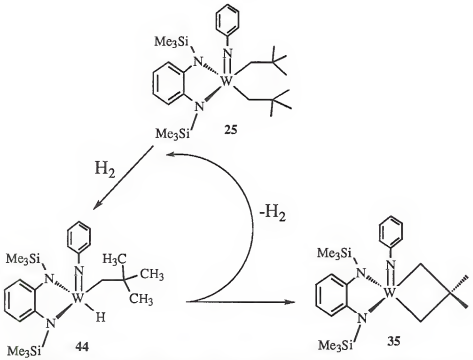

Figure 4.3. Formation of the metallacycle, **35**, by the addition of a catalytic amount of H_2 to the bis-neopentyl complex, **25**.

All of the observations which have been made pertaining to the hydrogenation of **25** in the absence of PMe_3 were from NMR tube experiments. When complete hydrogenation of **25** was carried out on a preparatory scale only the bridging hydride was isolated. It appears to be the same bridging hydride which was observed when **43** was evaporated to dryness and redissolved in C_6D_6. When a pentane solution of **25** was stirred under two atmospheres of H_2 for 36 hours and cooled to -10 °C, dark crystals were formed which were suitable for X-ray diffraction.

The X-ray structure revealed a unique dimeric structure. The thermal ellipsiod plot of **45** is shown in **Figure 4.4**. The structure was interesting since there is a neopentyl

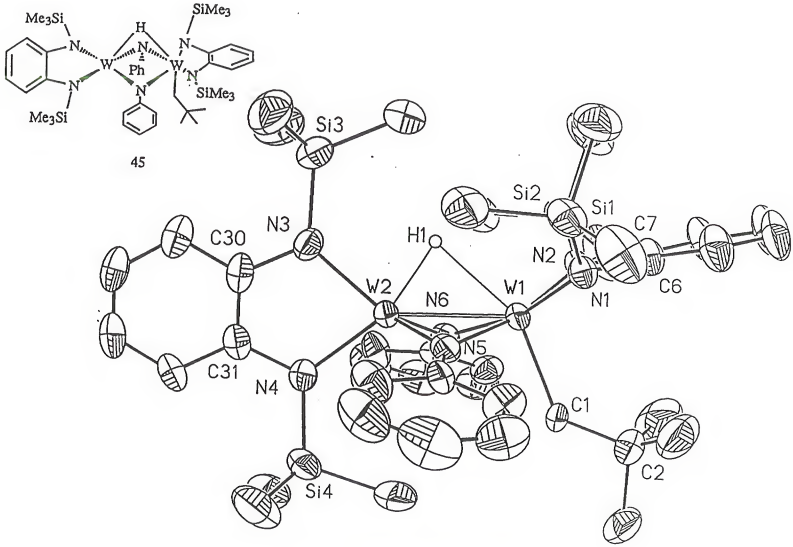

Figure 4.4. Thermal Ellipsoid Plot of 45.

group on one of the tungsten atoms and not on the other. Both of the imido groups were bridging and both the nitrogen's lie slightly closer to the tungsten without the neopentyl group, probably in order to relieve steric congestion. The bridging hydride was located and refined. It was found to be 2.07(10)Å from W1 and 1.87(11)Å from W2. Although the terminal hydrides were not found in the difference Fourier map, there appears to be open coordination sites which could accommodate the terminal hydrides, both on the unsubstituted tungsten. The open coordination sites are in the axial positions. The fold angle of the bis-amide ligand on the neopentyl substituted tungsten was 54 °. The fold angle of the bis-amide ligand on the unsubstituted tungsten was 0 °. The planarity of the bis-amide ligand would be due to the seven-coordinate nature of the tungsten atom. The ^{1}H NMR of **45** reveals that the molecule is quite fluxional, with all of the hydrides appearing as a very broad singlet at 12.9 ppm.

Hydrogenation of the bis-neophyl complex, **26**, gave results similar to **25**. However, the metallacycle was always observed in a much lower ratio than in the bis-neopentyl hydrogenation. This was probably because the β-methyl, β'-phenyl-metallacyclobutane complex was much less stable than the β,β'-dimethyl-metallacyclobutane complex. Therefore, it loses H_2 and reverts to the monohydride much more readily.

Another means of investigating this equilibrium was to examine the effect of added phosphine to the reaction mixture. Once the equilibrium was established and the reaction degassed, one equivalent of PMe_3 was added to the reaction mixture. Surprisingly, the alkylidene, **36**, was formed almost immediately. This reaction proceeds by an α-hydrogen abstraction from the monohydride complex, eliminating H_2, or possibly rearrangement of the metallacycle. The H_2 released then adds to the metallacyclobutane, forming more monohydride to react with the phosphine. The mechanism for this reaction can be seen in **Figure 4.5**. This would be the first example of an α-abstraction involving the loss of hydrogen to form an alkylidene. Undoubtedly, reductive elimination of neopentane would

be a more expected than α-abstraction. The implications of such a mechanism contradict many of the criterion which dictate α-abstraction reactions in high-oxidation state transition

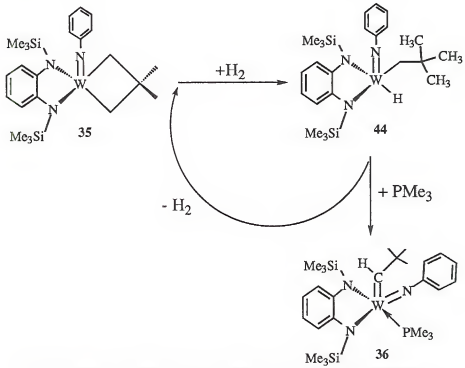

Figure 4.5. Mechanism for the formation of the alkylidene by α-abstraction from the equilibrium mixture of **35** and **44**.

metals. Certainly no steric relief was gained by the elimination of H_2. The W-C_α-C_β angle decreases from an alkyl to an alkylidene but that is overshadowed by the addition of PMe_3 to the metal center.

This brings up the question of the hydrogenation of the alkylidene. When a C_6D_6 sample of **36** and one equivalent of PMe_3 was placed under two atmospheres of H_2, the dihydride, bis-phosphine complex, **39**, was formed in a matter of hours **eq 4.8.** A different observation was made when the alkylidene was hydrogenated under an extremely low pressure of H_2 in the absence of 'added' phosphine. Over the course of ten days, the alkylidene was completely consumed to give a one to one mixture of two products and one equivalent of neopentane. The two products were the dihydride, bis-phosphine complex, **39**, and the metallacyclobutane complex, **35**. The two products were most likely formed

by the disproportionation of the intermediates since there were less than two equivalents of H_2 added.

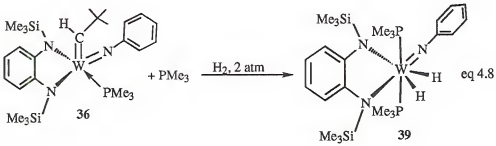

It cannot be denied that there appears to be a number of loose ends in the chemistry of these new hydride complexes, especially in the absence of phosphines. However, it is also undeniable that there was a wealth of information that lead to the conclusions which were made. Although isolation of a number of these compounds is unlikely due to their instability, crystallographic data on one or more of these compounds would be quite insightful. The discovery of an example α-hydrogen abstraction involving the monohydride-neopentyl has enormous implications and will be investigated further.

4.3. Reactivity of the Dihydrides.

High oxidation state transition metal hydrides complexes are known to hydrogenate olefins both stoichiometrically and catalytically.[62,63] Rothwell even demonstrated the hydrogenation of arenes using Ta(V) dihydrides.[65] Coordination of the olefin was an essential step in the reaction. Olefins are π-acceptor ligands and require filled metal *d*-orbitals to facilitate back-bonding. Therefore d^0 olefin complexes are unlikely. Nonetheless d^1 and d^2 complexes should have sufficient orbitals to overlap with an olefin acceptor orbital, stabilizing a π-olefin complex. Ligands with a strong electronic donation to the metal center should aid in the isolation of coordinated π-olefin complexes. Imido ligands $(\equiv NR)^{2-}$ are strong π-donors because of the lone electron pair and should aid in the

isolation of π-olefin complexes. Strong σ-donors, such as phosphines should also aid in creating a suitable electronic environment for π-olefin complexes. Currently, there are very few examples of d^1 or d^2 π-olefin complexes which have been thoroughly characterized.[71] Therefore, the isolation of π-olefin complexes is essential to the advancement of this chemistry.

Initial investigation into the reactivity of some of the phosphine stabilized hydride complexes, **39** and **42**, has begun. When a C_6D_6 sample of $W(NPh)(H)_2(PMe_3)_2[(Me_3SiN)_2C_6H_4]$, **39**, in a sealable NMR tube was placed under an atmosphere of ethylene, ethane formation was observed by the observation of a singlet at 1.1 ppm in the ^1H NMR spectrum. A second equivalent of ethylene was bound to the reduced metal center, forming the W(IV) ethylene complex, $W(NPh)(\eta^2\text{-}C_2H_4)(PMe_3)_2[(Me_3SiN)_2C_6H_4]$, **46**, **eq 4.9**. The ^1H NMR spectrum of the ethylene complex reveals that the compound is quite fluxional at room temperature.

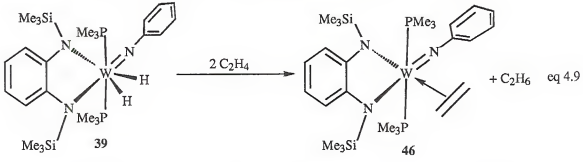

eq 4.9

The room temperature ^1H NMR spectrum is shown in **Figure 4.6**. The ethylene protons were observed as two multiplets at 1.96 and 2.19 ppm respectively. The coupled ^{13}C NMR spectrum revealed a triplet at 36 ppm corresponding to the ethylene carbons. The $^1J_{C\text{-}H}$ coupling of the carbons was 156 Hz, typical for an ethylene complex, indicating that little 'metallacyclopropane' character was evident[71]. The PMe_3 ligands were equivalent and were observed at 1.05 ppm in the ^1H NMR spectrum. At room temperature, the ^{31}P NMR spectrum revealed a broad singlet at -23.2 ppm while at -25 °C, a sharp singlet at -21.77 ppm with 238 Hz ^{183}W satellites was observed. The silyl methyls appeared as a

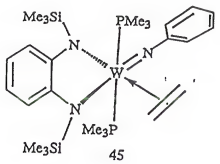

45

Figure 4.6. The ^{1}H NMR spectrum of W(NPh)(η^2-C_2H_4)(PMe_3)$_2$[$(Me_3SiN)_2C_6H_4$], 46, at 23 °C

broad singlet, nearly 120 Hz wide, at 0.50 ppm in the ^1H NMR spectrum at room temperature. When the sample was cooled to -25 °C, two sharp singlets were observed at 0.39 ppm and 0.42 ppm. A tantalum ethylene complex prepared by Schrock[72] and tungsten olefin complexes prepared by Nielson[73] show that the ethylene prefers to coordinate *cis* to the imido. The ethylene also preferred to coordinate *cis* to phosphine ligands. In every case, the ethylene coordinated *trans* to an 'X' ligand. Nielson obtained crystallographic data on $W(NPh)Cl_2(Me_2C{=}CH_2)(PMe_3)_2$ which clearly demonstrated this geometry.[73] The spectral data for **46** were consistent with these compounds and support a *trans* phosphine structure. Difference nOe experiments on **46** showed that upon irradiation of the *ortho*-protons of the imido group, a 4.8% enhancement was observed for the coordinated ethylene. This substantiates the *cis* orientation of the imido and the ethylene.

A W(IV) olefin complex was also formed when two equivalents of styrene was allowed to react with the dihydride, **39**. In an NMR tube experiment, formation of ethylbenzene was observed along with formation of the styrene complex, $W(NPh)(\eta^2\text{-}CH_2CHPh)(PMe_3)_2[(Me_3SiN)_2C_6H_4]$, **47**. The olefinic peaks were observed as sharp multiplets at 2.62 and 2.80 ppm and a triplet at 3.87 ppm in a 1:1:1 ratio. The orientation of the coordinated styrene is not known, although it appears by NMR that only one orientation is adapted.

When the catalytic hydrogenation of ethylene and cyclooctene was attempted using the dihydride, **39**, mixed results were observed. Cyclooctene and H_2 were added to an NMR sample of **39**. Over time, even with mild heating, it did not appear as though any cyclooctene was hydrogenated by observation of the NMR. It was already known that one equivalent of ethylene is stoichiometrically hydrogenated by **39**, so detection of catalysis by NMR proved difficult. It appeared as though, over days, that the ratio between the ethylene and the ethane appeared to decrease. Further work will be focused on this reaction.

The reaction of ethylene and the DPPE dihydride, **41**, did not yield an ethylene complex. Instead, no reaction was observed at room temperature over three days. However, when a purple C_6D_6 solution of **41** and ethylene was heated to 90 °C for 12 hours, the color changed to yellow. The ^1H NMR revealed that DPPE had been lost from the metal center. The resonances corresponding to the hydrides and free ethylene were also no longer present. The product formed appears to be a metallacyclopentane complex formed by the addition of two equivalents of ethylene to the metal center.[74] The overall reaction can be seen in **eq 4.10**. The complex appeared to have

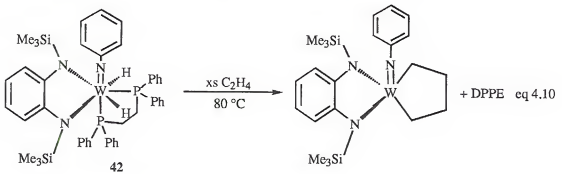

42 eq 4.10

a plane of symmetry due to the observation of a singlet at 0.31 ppm in the ^1H NMR spectrum and two AA'BB' multiplets at 7.11 ppm and 7.41 ppm. The metallacyclopentane protons were observed as three multiplets, at 1.58 ppm, 2.41 ppm, and 2.89 ppm in a 2:2:4 ratio.

A reaction that is important to mention at this point is the reaction of excess ethylene with the bis-neopentyl complex, **25**. When ethylene was allowed to react with a C_6D_6 solution of **25**, the ^1H NMR revealed that 1-butene was released. The formation of 1-butene was very slow but very clean, a 60:40 mixture of ethylene and 1-butene was observed after 14 days at room temperature. Throughout the reaction, the concentration of **25** remained virtually unchanged while formation of other organometallic products was not observed. After 14 days, the sample was heated to 80 °C for 8 hours. The ^1H NMR spectrum revealed that all of the ethylene had been consumed. There was no bis-neopentyl complex observable in the NMR, although the large amount of 1-butene obscured much of

the spectrum. The sample was degassed thoroughly. The ^1H NMR revealed that the organometallic product was identical to the proposed metallacyclopentane complex from the reaction of **42** and ethylene.

The fact that 1-butene formation was observed without observation of a new organometallic compound suggests that a very small amount of an active catalyst was being produced at room temperature. At higher temperature, all of the bis-neopentyl must be converted to the active catalyst. The formation of 1-butene from the metallacyclopentane complex would go by a simple β-hydrogen elimination reaction. Therefore, the formation of the metallacyclopentane is the key step of the reaction. The formation of metallacyclopentane compounds from addition of two equivalents of ethylene to a low oxidation state metal center is well known.[2,74,75] These metallacyclopentane complexes are also known to undergo β-hydrogen elimination reactions, forming 1-butene. The formation of a reduced metal species, W(IV), in this case, would be formed by the reductive coupling of the two neopentyl groups. The mechanism for this reaction can be seen in **Figure 4.7**.

Most of the work reported in this chapter involves very recent results, and has brought up many new questions as well as areas for future work. Other members of the research group will continue this work, and hopefully continue to make great strides in this area.

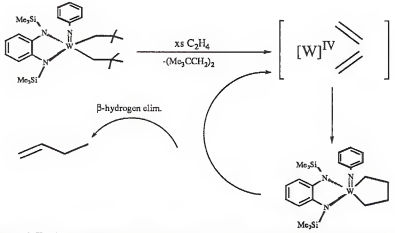

Figure 4.7. The catalytic formation of 1-butene from the addition of ethylene to the bis-neopentyl complex, **25**.

CHAPTER 5
EXPERIMENTAL

Unless otherwise noted, all procedures were performed under dry argon atmosphere using standard Schlenk techniques or in a nitrogen atmosphere dry box. All solvents were dried according to established literature procedures.

^{1}H, ^{13}C and ^{31}P NMR spectra were recorded on a Varian VXR-300 (300 MHz), a General Electric QE-300 (300 MHz), or a Varian Gemini-300 (300 MHz) spectrometer. Chemical shifts were referenced to the residual protons of the dueterated solvents and are reported in ppm downfield of TMS for ^{1}H and ^{13}C NMR spectra. ^{31}P NMR were referenced to an external H_3PO_4 standard. Elemental analysis were performed by Atlantic Microlabs, Inc., Norcross, GA.

Preparation of N,N'-bis(trimethylsilyl)-o-phenylenediamine, **1**:

Trimethylsilylchloride (12.7 mL, 0.10 mol) was added slowly to a solution of o-phenylenediamine (5.00 g, 0.047 mol) in 50 mL of Et_2O. A white precipitate formed upon addition. Triethylamine (13.9 mL, 0.10 mol) was then added slowly, ensuring that stirring continued throughout the addition. After stirring for 3 hours at room temperature, the mixture was filtered and the solid was washed twice with 15 mL of Et_2O. The filtrate was stripped of solvent under reduced pressure to give 10.2 grams of a yellow solid; yield, 86.8%. M.P.; 29.5 °C.

Preparation of $Li_2[1,2\text{-}(NSiMe_3)_2C_6H_4]$, **2**:

A solution of N,N'-bis(trimethylsilyl)-o-phenylenediamine (5.26 g, 20.9 mmol) in 75 mL of pentane was cooled to -78 °C. To this solution, 2 equivalents of n-BuLi (16.8 mL, 41.9 mmol, 2.5 M sol. in hexanes) was added slowly. A white precipitate formed as gas was evolved. Upon addition, a bubbler was attached and the reaction was stirred at room temperature for 2 hours under a flow of argon. The mixture was filtered and the solid dried under reduced pressure. The volume of the filtrate was reduced to 25 mL under reduced pressure and cooled to -15 °C to give colorless crystals. Yield; 4.93 g (combined), 89.5%.

Preparation of N,N'-bis(dimethylphenylsilyl)-o-phenylenediamine, **3**:

O-phenylenediamine (1.58g, 14.64 mmol) was slurried in 50 mL of hexanes. Two equivalents of both dimethylphenylsilylchloride (4.90 mL, 29.29 mmol) and triethylamine (4.08 mL, 29.29 mmol) were added via syringe. The mixture was then refluxed for 12 hours. Upon cooling, a white salt precipitated from solution. The mixture was filtered. The yellow solution was stripped of solvent under reduced pressure to give 4.86 grams of a yellow/red solid; yield, 87.0%. Anal. Calc'd for $C_{22}H_{28}N_2Si_2$: C, 70.15; H, 7.49; N, 7.44. Found: C, 69.89; H, 7.28; N, 7.21.

Preparation of N,N'-bis(methyldiphenylsilyl)-o-phenylenediamine, **4**:

O-phenylenediamine (0.64 g, 5.94 mmol), methyldiphenylsilylchloride (2.50 mL, 11.81 mmol) and triethylamine (1.82 mL, 13.00 mmol) were reacted as described above for **3** to give 2.09 grams of a reddish solid; yield 70.3%. Anal. Calc'd for $C_{32}H_{32}N_2Si_2$: C, 76.75; H, 6.44; N, 5.60. Found: C, 76.39; H, 6.23; N, 5.27.

Preparation of N,N'-bis(trimethylsilyl)-4,5-dimethyl-1,2-diaminobenzene, **6**:

4,5-dimethyl-1,2-diaminobenzene (5.11 g, 37.52 mmol), trimethylsilylchloride (9.52 g, 75.05 mmol), and triethylamine (10.53 mL, 75.05 mmol) were reacted as described above for **3** to give 9.12 grams of a yellow solid; yield, 88.53%. Anal. Calc'd for $C_{14}H_{28}N_2Si_2$: C, 59.93; H, 10.06; N, 9.99. Found: C, 60.13; H, 10.29; N, 10.21.

Preparation of N,N'-(trimethylsilyl)-1,8-diaminonapthalene, **7**:

1,8-diaminonapthalene (10.61 g, 67.07 mmol), trimethylsilylchloride (17.87 mL, 140.84 mmol), and triethylamine (19.63 mL, 140.84 mmol) were reacted as described for **3** above to give 18.15 grams of a red solid; yield, 89.4%. Anal. Calc'd for $C_{16}H_{26}N_2Si_2$: C, 63.49; H, 8.67; N, 9.27. Found: C, 63.17; H, 8.39; N, 9.08.

Preparation of N-phenyl, N'-trimethylsilyl-o-phenylenediamine, **8**:

N-phenyl-o-phenylenediamine (1.53 g, 8.28 mmol), trimethylsilylchloride (1.18 mL, 8.50 mmol), and triethylamine (1.08 mL, 8.50 mol) were reacted as described above for **3** to give 1.64 grams of a reddish solid; yield; 77.2%. Anal. Calc'd for $C_{15}H_{20}N_2Si$: C, 70.24; H, 7.87; N, 10.93. Found: C, 69.91; H, 7.68; N, 10.73.

Preparation of 1,2-(^{i}PrNH)$_2$C$_6$H$_4$ **9** and 1,2-[N(H)C(Me)$_2$CH$_2$CH(Me)N(H)]-C$_6$H$_4$ **10**

O-phenylenediamine (2.5 g, 23.12 mmol) and sodium acetate (7.21 g, 87.9 mmol) were slurried in 15 mL of acetic acid, 20 mL of acetone, and 40 mL of H_2O. The mixture was stirred for 30 minutes in an ice bath. $NaBH_4$ (14.97 g, 277.4 mmol) was added slowly. Upon addition, the reaction was allowed to warm to room temperature and was stirred for one hour. NaOH (6 M solution) was added until slightly basic by litmus test. The mixture was then extracted with Et_2O (2 x 20 mL). The Et_2O was removed in vacuo to

yield a red oil. The oil was separated by flash chromatography on a Silica column using hexanes. The heterocyclic compound 1,2-[N(H)C(Me)$_2$CH$_2$CH(Me)N(H)]-C$_6$H$_4$ **10**, was eluted first, solvent was striped in vacuo to give a white powder (1.31 g, 41.1%). Anal. Calc'd for $C_{12}H_{20}N_2$: C, 75.80; H, 9.47; N, 14.74. Found: C, 75.71; H, 9.64; N, 14.75. The diamine, 1,2-(^{i}PrNH)$_2$C$_6$H$_4$ **9**, was eluted last and was isolated by cooling the hexanes solution to -78 °C to yield a white powder, which melted to a colorless oil upon warming (0.87 g, 29.3 %).

Preparation of 1,8-[N(H)C(Me)$_2$N(H)]C$_{10}$H$_4$ **11**

1,8-Diaminonapthalene (2.57 g, 16.25 mmol) and sodium acetate (5.06 g, 61.75 mmol) were slurried in 10 mL of acetic acid, 20 mL of acetone, and 40 mL of H_2O. After stirring in an ice bath for 30 minutes, $NaBH_4$ (15.95 g, 285.9 mmol) was added slowly. Upon addition, the reaction was allowed to warm to room temperature and was stirred for one hour. NaOH (6 M solution) was added until slightly basic by litmus test. The mixture was then extracted with Et_2O (2 x 20 mL). The Et_2O was removed in vacuo to yield red powder (2.96 g, 91.9%). Anal. Calc'd for $C_{13}H_{14}N_2$: C, 78.76; H, 7.12; N, 14.13. Found: C, 78.22; H, 7.09; N, 14.49.

Preparation of WOCl$_2$[(NSiMe$_3$)$_2$C$_6$H$_4$], **13**:

$WOCl_4$ (1.00 g, 2.93 mmol) and 1.1 equivalents of Li$_2$[1,2-(NSiMe$_3$)$_2$C$_6$H$_4$] **2** (0.85 g, 3.20 mmol) were combined in a Schlenk tube and cooled to -78 °C. 50 mL of Et_2O which had been cooled to -78 °C was added. The reaction was warmed to room temperature and stirred for 8 hours. Solvent was removed under reduced pressure. The solid was extracted with 50 mL of pentane and filtered through a Celite pad. The dark solution was cooled to -78 °C to afford a dark red powder (0.39 g, 25.6% yield). Anal. Calc'd for $C_{12}H_{22}N_2OCl_2Si_2W$: C, 27.65; H, 4.26; N, 5.37. Found: C, 27.61; H, 4.29; N, 5.41.

Preparation of $W(NPh)Cl_2[(NSiMe_3)_2C_6H_4]$, **14**:

N,N'-bis(trimethylsilyl)-o-phenylenediamine **1** (3.83 g, 15.16 mmol) was dissolved in 30 mL of Et_2O and cooled to -78 °C. Two equivalents of n-BuLi (12.13 mL, 30.32 mmol, 2.5 M soln in hexanes) were then added. The reaction was warmed to room temperature and stirred for one hour. The reaction was recooled and .95 equivalents of $W(NPh)Cl_4(OEt_2)$ (7.10 g, 14.4 mmol) in 20 mL of Et_2O was added. The reaction was stirred for three hours, then filtered through a celite pad, which, in turn, was rinsed with more Et_2O. Solvent was removed under reduced pressure. The dark red solid was washed with pentane until an orange powder remained. The powder was dried to yield 7.31 g of **14**; 85.1%. Anal. Calc'd for $C_{18}H_{27}N_3Cl_2Si_2W$: C, 36.25; H, 4.56; N, 7.05. Found: C, 35.91; H, 4.78; N, 6.78.

Preparation of 1,8-$K_2(Me_3SiN)C_{10}H_4$ **16** and 1,8-$Li_2(Me_3SiN)C_{10}H_4$, **17**

1,8-Diaminonapthalene was dissolved in pentane and cooled to 0 °C. Two equivalents of either KH or n-BuLi were then added. The reactions were allowed to warm and stirred for one hour. Yellow precipitate formed during the reaction. Cooling the reaction mixtures to -10 °C afforded nearly quantitative yields of the corresponding salts as yellow crystals.

Preparation of $W(NPh)Cl_2[1,8\text{-}(NSiMe_3)_2C_{10}H_6]$, **18**:

1,8-$(NHSiMe_3)_2C_{10}H_6$ **7** (1.28 g, 4.23 mmol) was dissolved in 25 mL of Et_2O and cooled to 78 °C. Two equivalents n-BuLi (3.38 mL, 8.46 mmol, 2.5 M in Et_2O) were added via syringe. The reaction was allowed to warm to room temperature and stirred for one hour. Over this time the color of the solution changed from red to yellow. The solution was recooled and .95 equivalents of $W(NPh)Cl_4(OEt_2)$ (2.02 g, 4.10 mmol) in a 25 mL Et_2O solution were added. The reaction was allowed to warm to room temperature

and was stirred for 6 hours. The mixture, which had turned dark red, was filtered through a celite pad and was washed with Et_2O until colorless. The solvent was removed under reduced pressure and dried for 4 hours. The solid was then washed 3 times with 20 mL of pentane and dried under reduced pressure overnight. 2.13 grams of a dark red solid were isolated; yield, 80.4%. Anal. Calc'd for $C_{22}H_{29}N_3Cl_2Si_2W$: C, 40.88; H, 4.52; N, 6.50. Found: C, 40.59; H, 4.21; N, 6.19.

Preparation of $W(NPh)Cl_2[4,5\text{-}(CH_3)_2\text{-}1,2\text{-}(NSiMe_3)_2C_6H_2]$, **19**:

N,N'-bis(trimethylsilyl)-4,5-dimethyl-1,2-diaminobenzene **6** (1.29 g, 4.70 mmol), $W(NPh)Cl4(OEt2)$ (2.29 g, 4.65 mmol), and n-BuLi (3.76 mL, 9.40 mmol, 2.5 M in in Et_20)were reacted as described above for **14**. 1.89 g of a red solid were isolated; 64% yield. Anal. Calc'd for $C_{20}H_{31}N_3Cl_2Si_2W$: C, 38.47; H, 5.00; N, 6.73. Found: C, 38.29; H, 4.78; N, 6.48.

Preparation of $W(NPh)(OSO_2CF_3)_2[(Me_3SiN)_2C_6H_4](OEt_2)$ **20**:

$W(NPh)Cl_2[(NSiMe_3)_2C_6H_4]$ **14** (0.50 g, 0.84 mmol) and two equivalents of $Ag(OSO_2CF_3)_2$ (0.43 g, 1.68 mmol) were combined in a Schelnk tube and dissolved in 25 mL of 0 °C Et_2O. After stirring at room temperature for 8 hours, the Et_2O was removed under reduced pressure. The solid was extracted with Et_2O and filtered through Celite until colorless. The reddish solution was concentrated to 10 mL and cooled to -10 °C to give 0.59 grams of **20** as an orange solid, yield: 85.0%.

Preparation of $W(NPh)Cl_2(PMe_3)[(NSiMe_3)_2C_6H_4]$, **21**:

$W(NPh)Cl_2[(NSiMe_3)_2C_6H_4]$ **14** (0.68 g, 1.14 mmol) was slurried in 30 mL of pentane. Excess PMe_3 (4.55 mL, 2.00 mmol, .44 M in toluene) was added to the reaction. The reaction immediately turned from redish to deep purple. The reaction was cooled to -78 °C to give **21** as 0.71 grams of purple crystals, yield; 90.5%.

Preparation of $W(NPh)Cl_2(L)[(NSiMe_3)_2C_6H_4]$, L = THF, **22**; 3-Picoline, **23**; CH_3CN, **24**:

$W(NPh)Cl_2[(NSiMe_3)_2C_6H_4]$ **14** was dissolved in a minimum amount of the solvent, L. The deep purple solution was then added slowly to a stirring pentane solution, which immediately turned purple. The solutions were then cooled to -78 °C to give purple crystals of the mono-adduct.

Preparation of $W(NPh)(CH_2C(CH_3)_3)_2[(NSiMe_3)_2C_6H_4]$, **25**:

$W(NPh)Cl_2[(NSiMe_3)_2C_6H_4]$ (2.78g, 4.66 mmol) was dissolved in 30 mL of Et_2O and cooled to -78 °C. Two equivalents of $ClMgCH_2C(CH_3)_3$ (7.37 mL, 9.32 mmol, 1.27 M soln in Et_2O) were then added. The reaction was allowed to warm to room temperature after 30 minutes. After one hour, solvent was removed under reduced pressure. The solid was extracted with pentane until clear and filtered through a Celite pad. The solution was concentrated to a total volume of about 10 mL and cooled in an -78 °C cold bath to yield dark crystals of **25**; 2.19 g (yield 70.1%). Anal. Calc'd for $C_{28}H_{47}N_3Si_2W$: C, 50.52; H, 7.12; N, 6.31. Found: C, 50.36; H, 7.04; N, 6.14.

Preparation of $W(NPh)(CH_2C(CH_3)_2Ph)_2[(NSiMe_3)_2C_6H_4]$, **26**:

$W(NPh)Cl_2[(NSiMe_3)_2C_6H_4]$ (2.04 g, 3.42 mmol) was dissolved in 30 mL of Et_2O and cooled to -78 °C. Two equivalents of $ClMgCH_2C(CH_3)_2Ph$ (6.55 mL, 6.84 mmol, 1.045 M soln in Et_2O) were then added. The reaction was allowed to warm to room temperature after 30 minutes. After one hour, solvent was removed under reduced pressure. The solid was extracted with pentane until clear and filtered through a Celite pad. The solution was concentrated to a total volume of about 15 mL and cooled in an -78 °C cold bath to yield 2.21 g of **26** as a light brown solid. Yield: 82.4%. Anal. Calc'd for $C_{38}H_{45}N_3Si_2W$: C, 58.23; H, 5.79; N, 5.36. Found: C, 57.95; H, 5.58; N, 5.29.

Preparation of W(NPh)$(CH_3)_2$[$(NSiMe_3)_2C_6H_4$], **27**:

W(NPh)Cl_2[$(NSiMe_3)_2C_6H_4$] (1.03 g, 1.73 mmol) was dissolved in 20 mL of Et_2O and cooled to -78 °C. Two equivalents of MeLi (2.47 mL, 3.46 mmol, 1.4 M soln in Et_2O) were then added. The reaction was allowed to warm to room temperature after 15 minutes. After 30 minutes, solvent was removed under reduced pressure. The solid was extracted with pentane until clear and filtered through a Celite pad. The solution was concentrated to a total volume of about 5 mL and cooled in an -78 °C cold bath to yield 680 mg of **27** as a gold-brown solid. Yield: 70.8%. Anal. Calc'd for $C_{20}H_{33}N_3Si_2W$: C, 43.24; H, 5.99; N, 7.56. Found: C, 42.89; H, 5.94; N, 7.29.

Preparation of W(NPh)$(CH_2CH_3)_2$[$(NSiMe_3)_2C_6H_4$], **28**:

W(NPh)Cl_2[$(NSiMe_3)_2C_6H_4$] (1.12 g, 1.88 mmol) was dissolved in 25 mL of Et_2O and cooled to -78 °C. Two equivalents of EtMgCl (1.88 mL, 3.76 mmol, 2.0 M soln in Et_2O) were then added. The reaction was allowed to warm to room temperature after 15 minutes. After 30 minutes, solvent was removed under reduced pressure. The solid was extracted with pentane until clear and filtered through a Celite pad. The solvent was removed under reduced pressure to yield 0.98 g of **28** as a thick red oil.. Yield: 89.3%.

Preparation of W(NPh)$(CH_2Ph)_2$[$(NSiMe_3)_2C_6H_4$], **29**:

W(NPh)Cl_2[$(NSiMe_3)_2C_6H_4$] **14** (2.02 g, 3.39 mmol) was dissolved in 25 mL of Et_2O and cooled to -78 °C. Two equivalents of $ClMgCH_2Ph$ (6.77 mL, 6.77 mmol, 1.0 M soln. in Et_2O) were then added. The reaction was allowed to warm to room temperature after 15 minutes. After 30 minutes, solvent was removed under reduced pressure. The solid was extracted with pentane until clear and filtered through a Celite pad. The solution was concentrated to 10 mL and cooled to -78 °C to give 1.47 grams of **29** as a dark solid.

Yield: 61.3%. Anal. Calc'd for $C_{32}H_{41}N_3Si_2W$: C, 54.31; H, 5.84; N, 5.94. Found: C, 53.98; H, 5.61; N, 5.69.

Preparation of W(NPh)(Cl)(CH_2CMe_3)[$(NSiMe_3)_2C_6H_4$], **33:**

W(NPh)Cl_2[$(NSiMe_3)_2C_6H_4$] **14** (1.65 g, 2.77 mmol) was dissolved in 25 mL of Et_2O and cooled to -78 °C. One equivalent of $ClMgCH_2CMe_3$ (2.31 mL, 2.77 mmol, 1.2 M soln in Et_2O) was then added. The reaction was allowed to warm to room temperature after 15 minutes. After 45 minutes, solvent was removed under reduced pressure. The solid was extracted with pentane until clear and filtered through a Celite pad. The solution was concentrated to 5 mL and cooled to -78 °C to give 1.09 grams of **33** as a red solid. Yield: 62.3%. Anal. Calc'd for $C_{23}H_{38}N_3ClSi_2W$: C, 43.71; H, 6.06; N, 6.65. Found: C, 43.38; H, 5.81; N, 6.09.

Preparation of W(NPh)($CHCMe_3$)(PMe_3)[$(NSiMe_3)_2C_6H_4$], **36:**

In a 200 mL glass tube fitted with a teflon Young's joint, W(NPh)(CH_2CMe_3)$_2$[$(NSiMe_3)_2C_6H_4$] (1.25 g, 1.87 mmol) was dissolved in 25 mL of toluene. Five equivalents of PMe_3 (.968 mL, 9.35 mmol) were then added and the tube was sealed. The reaction was then heated to 70 °C for 24 hours. The solution was transferred to a round-bottom Schlenk were solvent was removed under reduced pressure. The brown oil was extracted with pentane and the volume of the filtrate was concentrated to about 15 mL. The solution was cooled to -10 °C to yield 0.83 g of **36** as orange crystals; yield 66.0%. Anal. Calc'd for $C_{26}H_{46}N_3PSi_2W$: C, 46.49; H, 6.90; N, 6.26. Found: C, 46.23; H, 6.81; N, 6.05.

Preparation of W(NPh)[CH(*t*-Bu)C(Ph)C(Ph)][$(Me_3SiN)_2C_6H_4$] **38**

W(NPh)($CHCMe_3$)(PMe_3)[$(NSiMe_3)_2C_6H_4$] **36** (0.21 g, 0.31 mmol) and diphenylacetylene (0.06 g, 0.34 mmol) were dissolved in 25 mL of pentane. The reaction

was then refluxed for 20 hours. Upon cooling, solvent was stripped in vacuo to give a red oil which appeared pure by ^1H NMR.

Preparation of $W(NPh)(H)_2(PMe_3)_2(TMS_2pda)$, **39**:

Method 1:

In a glass tube with a Teflon Young's joint, $W(NPh)(CH_2CMe_3)_2(TMS_2pda)$ (1.66 g, 2.48 mmol), **25** was dissolved in 25 mL of hexanes. PMe_3 (0.64 mL, 6.20 mmol) was added via syringe. The solution was then placed in liquid nitrogen while a vacuum was applied. Once the solution was frozen solid under vacuum, the flask was sealed. Hydrogen gas was then purged through the neck of the flask. Once the neck was purged, the H_2 hose was wired securely to the flask. The flask was opened until the H_2 reached a pressure of 10 PSI. The flask was then resealed and the H_2 line removed. The reaction was then allowed to warm to room temperature. After four hours of stirring, the color of the solution changed from brown to magenta. Magenta crystals had also precipitated from solution. The solution was transferred to a Schlenk tube and cooled to -10 °C to give magenta crystals. The mother liquors were concentrated and cooled to give more of the same. Total Yield of **39**: 1.48 g (87.8%). Anal Calcd for $C_{24}H_{47}N_3P_2Si_2W$: C, 42.41; H, 6.97; N, 6.18. Found: C, 42.18; H, 6.79; N, 6.03.

Method 2:

$W(NPh)Cl_2(TMS_2pda)$ (1.08 g, 1.81 mmol), **14** was dissolved in 20 mL of Et_2O and cooled to -78 °C in an isopropanol/dry ice bath. Two equivalents of PMe_3 (0.38 mL, 3.62 mmol) were added via syringe. Two equivalents of $LiBEt_3H$ (3.62 mL, 3.62 mmol, 1.0 M solution in THF) were added slowly. After warming to room temperature and stirring for four hours, the solvent was removed under reduced pressure. The solid was extracted twice with 10 mL of pentane. The brown solution was concentrated to 5 mL and

cooled to -10 °C. 0.87 g of a brown-red solid precipitated from solution. ^1H NMR confirmed the formation of **39** with about 15% BEt_3 impurity present.

Method 3:

$W(NPh)(CHCMe_3)(PMe_3)(TMS_2pda)$ **36** (50 mg, 0.07 mmol) was dissolved in C_6D_6 in a NMR tube fitted with a teflon Young's joint. One equivalent of PMe_3 (7 μL, 0.07 mmol) was added via microliter syringe. The NMR tube was then fitted with a Schlenk adapter. The NMR tube was frozen in liquid nitrogen and placed under vacuum. The tube was then sealed frozen, under vacuum. Hydrogen gas was then purged through the Schlenk adapter for five minutes. The teflon seal was opened to allow the H_2 to fill the vacuum in the NMR tube. The NMR tube was charged with about 15 PSI of H_2. Over a period of less than 2 hours, complete conversion of **36** to **39** was observed in the ^1H NMR.

Preparation of $W(NPh)(H)_2(DPPE)(TMS_2pda)$, **42**:

In a glass tube with a Teflon Young's joint, $W(NPh)(CH_2CMe_3)_2(TMS_2pda)$ (0.65 g, 0.98 mmol) and DPPE (0.39 g, 0.98 mmol) were dissolved in 30 mL of hexanes. The solution was then placed in liquid nitrogen while a vacuum was applied. H_2 gas was introduced as described for **39**. The reaction was then allowed to warm to room temperature. After eight hours of stirring, the color of the solution had changed from brown to purple. Purple solid had also precipitated from solution. The solution was transferred to a Schlenk tube, concentrated to 10 mL, and cooled to -10 °C to give a purple solid. Total Yield: 0.71 g (78.2%). Anal. Calcd. for $C_{44}H_{53}N_3Si_2P_2W$: C, 57.08; H, 5.77; N, 4.54. Found: C, 57.33; H, 5.84; N, 4.54.

Preparation of W(NPh)(η^2-C_2H_4)(PMe_3)$_2$(TMS_2pda), **46**:

In a glass tube with a Teflon Young's joint, W(NPh)$(H)_2(PMe_3)_2(TMS_2pda)$, **39**, (0.64 g, 0.94 mmol) was dissolved in 20 mL of pentane. The solution was then placed in liquid nitrogen under vacuum. Once the solution was frozen solid under vacuum, the flask was sealed. Ethylene was purged through the neck of the flask and then the hose was wired on. The flask was opened to a low pressure of ethylene (2 PSI) for about ten seconds. Then flask was then resealed and allowed to warm to room temperature. After 12 hours, the color of the solution had lightened. The solution was transferred to a Schlenk tube and cooled to -10 °C. Purple-brown solid formed and was isolated. The mother liquors were reduced in volume under reduced pressure to about 5 mL and recooled to yield more solid. Total yield; 0.59 grams, 89.1%. Anal. Calcd. for $C_{26}H_{49}N_3Si_2P_2W$: C, 44.25; H, 7.00; N, 5.95. Found: C, 43.91; H, 6.79; N, 5.78.

Polymerization Experiments:

All of the ROMP experiments were carried out under an inert atmosphere in deolifinated toluene solutions. The reactions were terminated by transfering the mixtures to stirring methanol with a trace of BHT added to insure against radical reations upon precipitation. The precipitated polymers were dried in vacuo and analyzed by GPC.

APPENDIX A
TABLES OF SPECTROSCOPIC DATA

Spectroscopic Data

Table A-1. ^{1}H NMR Data

compound	δ, ppm	mult	J, Hz	int	assignt
1,2-[$(CH_3)_3SiNH]_2C_6H_4$ **1**	0.18	s		18	-SiMe_3
	3.00	br s		2	-NH
	6.83	m		2	aromatic
	6.89	m		2	
1,2-$Li_2[(CH_3)_3SiN]_2C_6H_4$ **2**	0.22	s		18	-SiMe_3
	6.59	m		2	aromatic
	6.87	m		2	aromatic
1,2-[$(CH_3)_2PhSiNH]_2C_6H_4$ **3**	0.33	s		12	-SiMe_2Ph
	3.28	br s		2	-NH
	6.69	m		2	aromatic
	6.88	m		2	aromatic
	7.20	m		6	aromatic
	7.57	m		4	aromatic
1,2-[$(CH_3)Ph_2SiNH]_2C_6H_4$ **4**	0.61	s		6	-SiMePh_2
	3.57	br s		2	-NH
	6.58	m		2	aromatic
	6.92	m		2	aromatic
	7.18	m		12	aromatic
	7.58	m		8	aromatic
4,5-Me_2-1,2-$(Me_3SiNH)_2C_6H_4$ **6**	0.19	s		18	-SiMe_3
	2.12	s		6	4,5-Me_2
	2.95	br s		2	-NH
	6.80	s		2	aromatic
1,8-$(Me_3SiNH)_2C_{10}H_6$ **7**	0.17	s		18	-SiMe_3
	5.38	br s		2	-NH
	6.70	d	7	2	p-$C_{10}H_6$
	7.19	t	8	2	m-$C_{10}H_6$
	7.33	d	7	2	o-$C_{10}H_6$
1,2-Ph[$(CH_3)_3SiNH]C_6H_4$ **8**	0.11	s		9	-SiMe_3
	4.09	br s		1	-NH
	4.43	br s		1	-NH
	6.49	d	8	2	aroamtic
	6.73	t	8	2	aromatic
	6.96	t	8	2	aromatic
	7.07	m		3	aromatic
1,2-(^{i}PrNH)$_2C_6H_4$ **9**	0.98	d	6	12	-CHMe_2
	3.08	br s		2	-NH
	3.32	quin	6	2	-C$H$$Me_2$
	6.69	m		2	aromatic
	6.93	m		2	aromatic

1,2-[N(H)C(Me)$_2$CH$_2$CH(Me)N(H)]-C$_6$H$_4$ **10**	0.83	d	6	3	-CHMe
	0.89	s		3	-CMe(Me)
	1.07	s		3	-CMe(Me)
	1.25	dd	6	1	-CHH
	1.62	t	6	1	-CHH
	2.90	br s		2	-NH
	3.17	qd	4	1	-CHMe
	6.45	m		2	aromatic
	6.80	m		2	aromatic
1,8-[N(H)C(Me)$_2$N(H)]C$_{10}$H$_4$ **11**	0.98	s		6	-CMe$_2$
	3.42	br s		2	-NH
	6.26	d	7	2	aromatic
	7.23	d	7	2	aromatic
	7.35	t	7	2	aromatic
W(O)Cl$_2$[(Me$_3$SiN)$_2$C$_6$H$_4$] **13**	0.39	s		18	-SiMe$_3$
	6.80	m		2	aromatic
	6.95	m		2	
W(NPh)Cl$_2$[(Me$_3$SiN)$_2$C$_6$H$_4$] **14**	0.35	s		18	-SiMe$_3$
	6.71	t	8	1	p-NPh-H
	6.94	m		2	aromatic
	7.01	t	8	2	m-NPh-H
	7.14	m		2	aromatic
	7.31	d	8	2	o-NPh-H
W(NPh)Cl$_2$[(Me$_2$PhSiN)$_2$C$_6$H$_4$] **15**	0.62	s		6	-SiMe$_2$Ph
	0.68	s		6	-SiMe$_2$Ph
	6.62	m		2	aromatic
	6.65	t	8	1	p-NPh-H
	6.92	t	8	2	m-NPh-H
	7.02 to 7.47				aromatic
W(NPh)Cl$_2$[1,8-(Me$_3$SiN)$_2$C$_{10}$H$_6$] **18**	0.41	s		18	-SiMe$_3$
	6.39	d	7	2	p-C$_{10}$H$_6$
	6.72	t	8	1	p-NPh-H
	6.93	d	7	2	o-C$_{10}$H$_6$
	6.98	t	8	2	m-NPh-H
	7.13	t	7	2	m-C$_{10}$H$_6$
	7.48	d	8	2	o-NPh-H
W(NPh)Cl$_2$[4,5-Me$_2$-1,2-(Me$_3$SiN)$_2$C$_6$H$_4$] **19**	0.41	s		18	-SiMe$_3$
	1.99	s		6	4,5-Me$_2$Ph
	6.73	t	8	1	p-NPh-H
	7.02	t	8	2	m-NPh-H
	7.07	s		2	aromatic
	7.35	d	8	2	o-NPh-H

$W(NPh)(OSO_2CF_3)_2[(Me_3SiN)_2C_6H_4]$-$(OEt_2)$ **20**	0.32	s		18	-Si<u>Me</u>$_3$
	1.09	t	7	6	-O<u>Et</u>$_2$
	3.25	q	7	4	-O<u>Et</u>$_2$
	6.55	t	8	1	p-NPh-<u>H</u>
	7.02	t	8	2	m-NPh-<u>H</u>
	7.09	m		2	aromatic
	7.30	m		2	aromatic
	7.38	d	8	2	o-NPh-<u>H</u>
$W(NPh)Cl_2(PMe_3)[(Me_3SiN)_2C_6H_4]$ **21**	0.42	s		18	-Si<u>Me</u>$_3$
	0.79	d	J^2_{P-H}=9	9	-P<u>Me</u>$_3$
	6.63	t	8	1	p-NPh-<u>H</u>
	6.83	m		2	aromatic
	7.01	m		2	aromatic
	7.17	t	8	2	m-NPh-<u>H</u>
	7.49	d	8	2	o-NPh-<u>H</u>
$W(NPh)Cl_2(THF)[(Me_3SiN)_2C_6H_4]$ **22**	0.41	s		18	-Si<u>Me</u>$_3$
	0.92	qnt	3	4	-THF
	3.63	t	6	4	-THF
	6.62	t	8	1	p-NPh-<u>H</u>
	6.85	m		2	aromatic
	7.03	m		2	aromatic
	7.10	t	8	2	m-NPh-<u>H</u>
	7.47	d	8	2	o-NPh-<u>H</u>
$W(NPh)Cl_2$(3-Me-py)$[(Me_3SiN)_2C_6H_4]$ **23**	0.42	s		18	-Si<u>Me</u>$_3$
	2.17	s		3	py-<u>Me</u>
	6.21	t	2	1	py-5-<u>H</u>
	6.33	d	8	1	py-4-<u>H</u>
	6.54	m		2	aromatic
	6.65	t	11	1	p-NPh-<u>H</u>
	6.76	m		2	aromatic
	7.18	t	9	2	m-NPh-<u>H</u>
	7.61	d	7	2	o-NPh-<u>H</u>
	8.72	s		1	py-1-<u>H</u>
	8.75	d	6	1	py-6-<u>H</u>
$W(NPh)Cl_2(NCCH_3)[(Me_3SiN)_2C_6H_4]$ **24**	0.38	s		18	-Si<u>Me</u>$_3$
	0.49	s		3	-NCC<u>Me</u>
	6.67	t	7	1	p-NPh-<u>H</u>
	6.93	m		2	aromatic
	7.04	t	7		m-NPh-<u>H</u>
	7.14	m		2	aromatic
	7.34	d	7	2	o-NPh-<u>H</u>
$W(NPh)(CH_2CMe_3)_2[(Me_3SiN)_2$-$C_6H_4]$ **25**	0.54	s		18	-Si<u>Me</u>$_3$
	1.00	s		18	-C<u>Me</u>$_3$

	2.13	d	10 J^2_{WH}=11	2	-CH_2CMe$_3$
	2.29	d	10 J^2_{WH}=11	2	-CH_2CMe$_3$
	6.83	t	7	1	p-NPh-H
	6.86	m		2	aromatic
	7.19	t	7	2	m-NPh-H
	7.25	m		2	aromatic
	7.59	d	7	2	o-NPh-H
W(NPh)(CH_2CMe$_2$Ph)$_2$[(Me$_3$SiN)$_2$-C$_6$H$_4$] **26**	0.42	s		18	-SiMe$_3$
	1.37	s		9	-CMe$_2$Ph
	1.38	s		9	-CMe$_2$Ph
	1.95	d	11 J^2_{WH}=11	2	-CH_2C
	2.94	d	11 J^2_{WH}=11	2	-CH_2C
	6.83	t	7	1	aromatic
	6.94	t	7	2	
	6.97	m		2	
	7.01	t	7	4	
	7.06	t	7	2	
	7.18	d	7	4	
	7.19	d	7	2	
	7.30	m		2	
W(NPh)(CH$_3$)$_2$[(Me$_3$SiN)$_2$C$_6$H$_4$] **27**	0.31	s		18	-SiMe$_3$
	1.12	s	$J^2_{W\text{-}H}$=6	6	W-Me
	6.86	t	8	1	p-NPh-H
	7.06	m		2	aromatic
	7.11	t	8	2	m-NPh-H
	7.32	d	8	2	o-NPh-H
	7.35	m		2	aromatic
W(NPh)(CH_2CH$_3$)$_2$[(Me$_3$SiN)$_2$C$_6$H$_4$] **28**	0.29	s		18	-SiMe$_3$
	1.86	s		6	-CH$_2$CH_3
	1.91	m		2	-CH_2CH$_3$
	2.31	m		2	-CH_2CH$_3$
	6.86	t	8	1	p-NPh-H
	7.04	m		2	aromatic
	7.11	t	8	2	m-NPh-H
	7.31	d	8	2	o-NPh-H
	7.37	m		2	aromatic
W(NPh)(CH_2Ph)$_2$[(Me$_3$SiN)$_2$C$_6$H$_4$] **29**	0.09	s		18	-SiMe$_3$
	2.78	s		4	-CH_2Ph
	6.81	t	8	2	p-CH$_2$Ph-H
	6.88	t	8	1	p-NPh-H
	7.04 to 7.19				aromatic
	7.30	d	8	2	o-NPh-H

	7.37	m		2	aromatic
spectrum taken at +80 °C in C_7D_8					
	2.71	m	7	4	-$C\underline{H}_2$Ph
$W(NPh)Ph_2[(Me_3SiN)_2C_6H_4]$ **30**	0.11	s		18	-SiMe_3
	6.82	t	7	2	aromatic
	6.86	t	7	1	
	7.04	t	7	4	
	7.18	t	7	2	
	7.21	m		2	
	7.39	m		2	
	7.52	d	7	2	
	7.62	d	7	4	
$W(NPh)(CH_2CMe_3)_2$-$[(Me_2PhSiN)_2C_6H_4]$ **31**	0.81	s		12	-SiMe_2Ph
	1.03	s		18	-$CH_2C\underline{Me}_3$
	2.04	d	10 J^2_{WH}=11	2	-$C\underline{H}_2CMe_3$
	2.78	d	10 J^2_{WH}=11	2	-$C\underline{H}_2CMe_3$
	6.59 to 7.68				aromatic
$W(NPh)Cl(CH_2CMe_3)[(Me_3SiN)_2$-$C_6H_4]$ **33**	0.24	s		9	-SiMe_3
	0.42	s		9	-SiMe_3
	1.23	s		9	-$CH_2C\underline{Me}_3$
	1.93	d	10	1	-$C\underline{H}_2CMe_3$
	2.08	d	10	1	-$C\underline{H}_2CMe_3$
	6.76	t	7	1	p-NPh-H
	6.94 to 7.24				aromatic
	7.41	d	8	2	o-NPh-H
$W(NPh)(CH_2CMe_3)(NMe_2)[(Me_3SiN)_2$ $C_6H_4]$ **34**	0.31	s		9	-SiMe_3
	0.46	s		9	-SiMe_3
	1.03	s		9	-$CH_2C\underline{Me}_3$
	1.33	d	10	1	-$C\underline{H}_2CMe_3$
	2.60	d	10	1	-$C\underline{H}_2CMe_3$
	3.19	s		3	-$N\underline{Me}_2$
	3.68	s		3	-$N\underline{Me}_2$
	6.72 to 7.28				aromatic
$W(NPh)(CH_2C(Me)_2CH_2)$-$[(Me_3SiN)_2C_6H_4]$ **35**	-1.70	d	9	2	-$C\underline{H}_2$
	0.39	s		9	-SiMe_3
	0.54	s		3	-$CH_2C\underline{Me}_2$-
	0.57	s		3	-$CH_2C\underline{Me}_2$-

	1.24	s		9	-SiMe$_3$
	2.11	d	9	2	-CH$_2$
	6.75 to 7.59				aromatic
W(NPh)(CHCMe$_3$)(PMe$_3$)-[(Me$_3$SiN)$_2$C$_6$H$_4$] **36**	0.38	s		9	-SiMe$_3$
	0.41	s		9	-SiMe$_3$
	0.98	d	$^2J_{P-H}$=9	9	-PMe$_3$
	1.39	s		9	-CMe$_3$
	6.68 to 7.13			9	aromatic
W(NPh)[CH(*t*-Bu)C(Ph)C(Ph)]-[(Me$_3$SiN)$_2$C$_6$H$_4$] **38**	-0.08	s		9	-SiMe$_3$
	0.43	s		9	-SiMe$_3$
	1.38	s		9	-*t*-Bu
	2.81	s	$^2J_{W-H}$ = 8	1	-C-H
	6.62 to 7.64				aromatic
W(NPh)(H)$_2$(PMe$_3$)$_2$[(Me$_3$SiN)$_2$C$_6$H$_4$] **39**	0.79	s		9	-SiMe$_3$
	0.81	s		9	-SiMe$_3$
	1.04	s		18	-PMe$_3$
	6.80 to 7.45				aromatic
	9.28	t	J = 38	2	W-H
Spectrum in C_7D_8 at -50 °C	0.69	s		9	-SiMe$_3$
	0.75	s		9	-SiMe$_3$
	0.84	t	J^2_{P-H}= 3	18	-PMe$_3$
	6.74 to 7.38				aromatic
	9.00	m			W-H
W(NPh)(H)$_2$(PMe$_2$Ph)$_2$-[(Me$_3$SiN)$_2$C$_6$H$_4$] **40**	0.53	s		18	-SiMe$_3$
	1.22	s		6	-PMe$_2$Ph
	6.72 to 7.29				aromatic
	9.63	br s		2	W-H
Spectrum in C_7D_8 at -50 °C	0.53	s		9	-SiMe$_3$
	0.59	s		9	-SiMe$_3$
	1.19	t	J_{P-H} = 4	12	-PMe$_2$Ph
	9.56	t	J = 40	2	W-H

$W(NPh)(H)_2(PCy_3)[(Me_3SiN)_2C_6H_4]$ **41**	0.81	s		18	-SiMe$_3$
	1.04 to 1.93	m's		11	PCy$_3$
	6.81	t	7	1	p-Ph-H
	6.95	m		2	aromatic
	6.99	t	7	2	m-Ph-H
	7.18	d	7	2	o-Ph-H
	7.47	m		2	aromatic
$W(NPh)(H)_2DPPE[(Me_3SiN)_2C_6H_4]$ **42**	0.49	s		18	-SiMe$_3$
	2.23	m		2	PCH_2CH_2P
	2.42	m		2	PCH_2CH_2P
	6.72	m		2	aromatic
	6.76	m	8	4	aromatic
	6.94	m		2	
	6.98 to 7.18	m			
	7.69	t	8	4	aromatic
	10.33	d	J = 23	1	W-H
	10.62	d	J = 23	1	W-H
$W(NPh)(H)(CH_2CMe_3)$-$[(Me_3SiN)_2C_6H_4]$ **44**	0.34	s		9	-SiMe$_3$
	0.42	s		9	-SiMe$_3$
	0.94	s		9	$-CH_2CMe_3$
	2.71	d	7	1	$-CH_2CMe_3$
	3.21	br s		1	$-CH_2CMe_3$
	6.79 to 7.59				aromatic
	18.48	s	$^1J_{W-H}$ =156	1	W-H
$W(NPh)(\eta^2\text{-}C_2H_4)(PMe_3)_2$-$[(Me_3SiN)_2C_6H_4]$ **46** spectrum taken at -25 °C	0.37	s		9	-SiMe$_3$
	0.65	s		9	-SiMe$_3$
	1.03	s		18	-PMe$_3$
	1.91	m		2	C_2H_4
	2.09	m		2	C_2H_4
	6.61 to 7.42				aromatic
$W(NPh)(\eta^2\text{-}CH_2CHPh)(PMe_3)_2$-$[(Me_3SiN)_2C_6H_4]$ **47**	0.41	s		18	-SiMe$_3$
	0.86	d		3	-PMe$_3$
	2.62	m		1	$-CH_2CHPh$
	2.80	m		1	$-CH_2CHPh$
	3.87	t	8	1	$-CH_2CHPh$

6.41 to 7.24	aromatic

Table A-2. ^{13}C NMR Data

coumpound	δ, ppm	mult.	J_{CH}, Hz	assignmt
1,8-$(Me_3SiNH)_2C_{10}H_6$ **7**	0.80	s		-$SiMe_3$
	116.13	s		aromatic
	121.22	s		
	122.21	s		
	125.99	s		
	138.15	s		
	144.60	s		
1,2-$(^iPrNH)_2C_6H_4$ **9**	23.2	s		-NCHMe_2
	44.6	s		-NCHMe_2
	114.2	s		
	119.8	s		aromatic
	137.7	s		
1,2-[N(H)C(Me)$_2$CH$_2$CH(Me)N(H)]-C_6H_4 **10**	23.9	s		
	26.9	s		
	32.8	s		
	48.1	s		
	51.6	s		
	52.0	s		
	119.6	s		
	120.9	s		
	121.6	s		
	121.8	s		
	138.2	s		
	141.6	s		
1,8-[N(H)C(Me)$_2$N(H)]$C_{10}H_4$ **11**	28.1	s		NC$(Me)_2$N
	63.8	s		NC$(Me)_2$N
	105.6	s		
	111.3	s		
	117.0	s		
	127.1	s		
	135.2	s		
	140.6	s		
$WOCl_2[(Me_3SiN)_2C_6H_4]$ **13**	0.02	s		-$SiMe_3$
	121.09	s		
	129.18	s		
	132.43			
$W(NPh)Cl_2[(Me_3SiN)_2C_6H_4]$ **14**	0.6	s		-$SiMe_3$
	122.0	s		aromatic
	126.1	s		
	128.1	s		
	128.5	s		
	128.6	s		
	130.8	s		

$W(NPh)Cl_2[1,8\text{-}(Me_3SiN)_2C_{10}H_6]$ **18**	3.13	s		-$SiMe_3$
	121.31	s		aromatic
	125.72	s		
	127.31	s		
	127.67	s		
	128.41	s		
	129.32	s		
	138.13	s		
	140.86	s		
$W(NPh)Cl_2[4,5\text{-}Me_2\text{-}1,2\text{-}(Me_3SiN)_2C_6H_4]$ **19**	1.98	s		-$SiMe_3$
	19.87	s		4,5-Ph-Me_2
	122.32	s		aromatic
	124.67	s		
	126.43	s		
	128.76	s		
	133.32	s		
	142.12	s		
	148.98	s		
$W(NPh)Cl_2(PMe_3)[(Me_3SiN)_2C_6H_4]$ **21**	1.99	s		-$SiMe_3$
	11.64	d	$^1J_{C\text{-}P} = 21$	-PMe_3
	120.94	s		aromatic
	122.99	s		
	127.03	s		
	127.29	s		
	128.35	s		
	145.41	s		
$W(NPh)Cl_2(THF)[(Me_3SiN)_2C_6H_4]$ **22**	1.50	s		-$SiMe_3$
	25.05	s		THF
	70.07	s		THF
	120.41	s		aromatic
	124.10	s		
	126.64	s		
	128.25	s		
	128.57	s		
	144.12	s		
	154.09	s		
$W(NPh)Cl_2$(3-Me-Py)-$[(Me_3SiN)_2C_6H_4]$ **23**	1.69	s		-$SiMe_3$
	17.70	s		3-Me-py
	119.92	s		aromatic
	122.61	s		
	123.16	s		
	127.03	s		
	127.91	s		
	128.15	s		
	128.55	s		
	132.81	s		

	137.86	s		
	147.12	s		
	148.83	s		
	152.51	s		
$W(NPh)(CH_2CMe_3)_2[(Me_3SiN)_2C_6H_4]$ **25**	4.4	s		-Si$\underline{Me}_3$
	34.8	s		-C$\underline{Me}_3$
	38.3	s		-$\underline{C}Me_3$
	90.8	s	123	-$\underline{C}H_2CMe_3$
	118.9	s		aromatic
	119.3	s		
	126.0	s		
	128.5	s		
	129.2	s		
	144.2	s		
	155.8	s		
$W(NPh)(CH_2CMe_2Ph)_2$-$[(Me_3SiN)_2C_6H_4]$ **26**	4.1	s		-Si$\underline{Me}_3$
	32.5	s		-C$\underline{Me}_2$Ph
	35.9	s		-C$\underline{Me}_2$Ph
	44.2	s		-$\underline{C}Me_2$Ph
	93.1	s	126	-$\underline{C}H_2CMe_2Ph$
	119.4	s		aromatic
	119.8	s		
	125.5			
	125.6			
	126.1			
	128.2			
	128.4			
	129.2			
	143.8			
	153.4			
	155.2			
$W(NPh)(CH_3)_2[(Me_3SiN)_2C_6H_4]$ **27**	2.3	s		-SiMe$_3$
	41.2	s	123	-$\underline{C}H_3$
	122.4	s		aromatic
	124.8	s		
	125.2	s		
	125.8	s		
	128.7	s		
	129.8	s		
	131.2	s		
$W(NPh)(CH_2CH_3)_2[(Me_3SiN)_2C_6H_4]$ **28**	1.5	s		-SiMe$_3$
	17.4	s		-$CH_2\underline{C}H_3$
	58.4	s	120	-$\underline{C}H_2CH_3$
	122.3			
	123.9			
	125.0			
	125.6			

	128.8			
	135.1			
	156.2			
$W(NPh)(CH_2Ph)_2[(Me_3SiN)_2C_6H_4]$ **29**	2.10	s		-SiMe$_3$
	66.33	s		-CH$_2$Ph
	123.49	s		
	123.78	s		
	125.65	s		
	126.20	s		
	126.51	s		
	127.68	s		
	128.04	s		
	128.42	s		
	128.61	s		
	128.97	s		
	154.20	s		
$W(NPh)Cl(CH_2CMe_3)$-$[(Me_3SiN)_2C_6H_4]$ **33**	1.26	s		-SiMe$_3$
	2.08	s		-SiMe$_3$
	35.13	s		-CH$_2$CMe$_3$
	36.11	s		-CH$_2$CMe$_3$
	80.15	s	121	-CH$_2$CMe$_3$
	121.7	s		
	122.3	s		
	123.6	s		
	126.1	s		
	127.2	s		
	128.6	s		
	132.0	s		
	136.9	s		
	155.9	s		
$W(NPh)(CHCMe_3)(PMe_3)$-$[(Me_3SiN)_2C_6H_4]$ **36**	3.4	s		-SiMe$_3$
	4.1	s		-SiMe$_3$
	16.2	d		-PMe$_3$
	34.9	s		-CMe$_3$
	45.0	s		-CMe$_3$
	117.6	s		aromatic
	119.3	s		
	122.4	s		
	123.6	s		
	124.7	s		
	128.7	s		
	148.1	s		aromatic
	277.4	s	110	-CHCMe$_3$
$W(NPh)[CH(t\text{-}Bu)C(Ph)C(Ph)]$-$[(Me_3SiN)_2C_6H_4]$ **38**	1.33	s		-SiMe$_3$
	2.01	s		-SiMe$_3$
	33.81	s		-CMe$_3$
	38.61	s		-CMe$_3$

	77.10	s		-CH-*t*-Bu
	90.08	s		-CH-*t*-Bu-CPhCPh-
	122.08	s		
	123.09	s		
	123.42	s		
	123.92	s		
	124.68	s		
	124.99	s		
	125.38	s		
	125.91	s		
	126.01	s		
	126.46	s		
	127.00	s		
	128.20	s		
	128.62	s		
	128.78	s		
	128.93	s		
	131.97	s		
	133.15	s		
	133.31	s		
	139.91	s		
	140.03	s		
	147.08	s		
	157.83	s		
$W(NPh)(H)_2(PMe_3)_2$-$[(Me_3SiN)_2C_6H_4]$ **39**				
	4.92	s		-Si<u>Me</u>$_3$
	6.43	s		-Si<u>Me</u>$_3$
	15.99	s		-P<u>Me</u>$_3$
	115.21	s		aromatic
	116.53	s		
	118.17	s		
	119.20	s		
	123.31	s		
	126.71	s		
	128.68	s		
	151.13	s		
$W(NPh)(\eta^2\text{-}C_2H_4)(PMe_3)_2$-$[(Me_3SiN)_2C_6H_4]$ **46**				
	2.67	s		-Si<u>Me</u>$_3$
	6.34	s		-Si<u>Me</u>$_3$
	15.78	s		-P<u>Me</u>$_3$
	38.13	s	156	-<u>C</u>$_2$H$_4$
	122.23	s		
	123.13	s		
	124.28	s		
	125.51	s		
	127.23	s		
	128.91	s		
	129.23	s		
	129.78	s		
	158.23	s		

Table A-3. ^{31}P NMR Data

$W(NPh)Cl_2(PMe_3)[(Me_3SiN)_2C_6H_4]$ **21**	-18.22	br s	
$W(NPh)(CHCMe_3)(PMe_3)[(Me_3SiN)_2C_6H_4]$ **36**	-2.49	s	$J^1_{W\text{-}P}$=128
$W(NPh)(CHCMe_3)(PEt_3)[(Me_3SiN)_2C_6H_4]$ **37**	-11.42	br s	
$W(NPh)(H)_2(PMe_3)_2[(Me_3SiN)_2C_6H_4]$ **39**	-24.46	s	$J^1_{W\text{-}P}$=188
$W(NPh)(H)_2(PMe_2Ph)_2[(Me_3SiN)_2C_6H_4]$ **40**	-17.43	s	$J^1_{W\text{-}P}$=164
$W(NPh)(H)_2(PCy_3)[(Me_3SiN)_2C_6H_4]$ **41**	66.71	s	$J^1_{W\text{-}P}$= 56
$W(NPh)(H)_2$DPPE$[(Me_3SiN)_2C_6H_4]$ **42**	30.43 -12.70	d d	$J^2_{P\text{-}P}$=83 $J^2_{P\text{-}P}$=83
$W(NPh)(\eta^2\text{-}C_2H_4)(PMe_3)_2[(Me_3SiN)_2C_6H_4]$ **46**	-23.30	br s	
spectrum taken in C_7D_8 at -40 °C	-21.61	s	$J^1_{W\text{-}P}$=238

APPENDIX B
TABLES OF CRYSTALLOGRAPHIC DATA

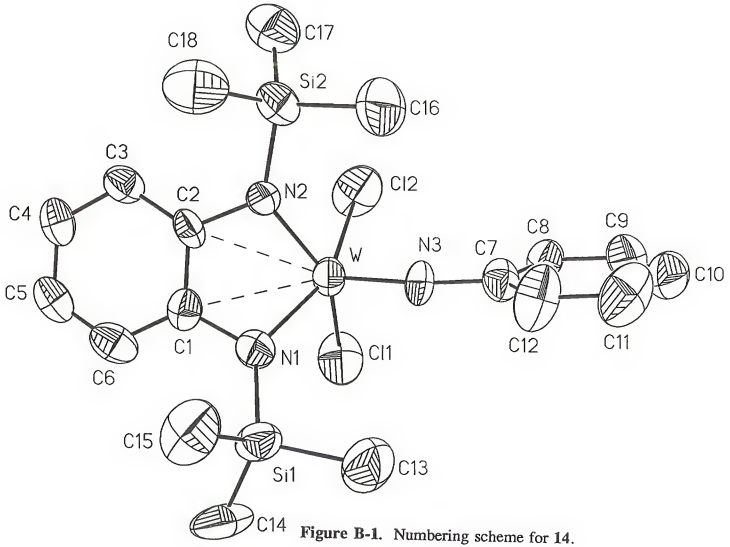

Figure B-1. Numbering scheme for **14**.

Crystallographic Data for $W(NPh)Cl_2[(Me_3SiN)_2C_6H_4]$, **14**

Table B-1. Crystallographic data for **14**.

A. Crystal data (298 K)	**14**
a, Å	10.294(2)
b, Å	17.859(3)
c, Å	13.377(3)
α, deg.	
β, deg.	104.15(2)
γ, deg.	
V, Å^3	2384.6(8)
d_{calc}, g cm^{-3}(298 K)	1.661
Empirical formula	$C_{18}H_{27}N_3Si_2Cl_2W$
Formula wt, g	596.36
Crystal system	Monoclinic
Space group	P 2_1/n
Z	4
F(000), electrons	1168
Crystal size (mm^3)	0.14 x 0.21 x 0.11
B. Data collection (298 K)	
Radiation, λ (Å)	Mo-K_α, 0.71073
Mode	ω-scan
Scan range	Symmetrically over 1.2° about $K_{\alpha 1,2}$ maximum
Background	offset 1.0 and -1.0 in ω from $K_{\alpha 1,2}$ maximum
Scan rate, deg. min.$^{-1}$	3 – 6
2θ range, deg.	3 – 55
Range of *h k l*	$0 \leq h \leq 13$ $0 \leq k \leq 23$ $-17 \leq l \leq 17$
Total reflections measured	5770
Unique reflections	5300
Absorption coeff. μ (Mo-K_α), mm^{-1}	5.18
Min. & Max. Transmission	0.352, 0.153
C. Structure refinement	
S, Goodness-of-fit	1.73
Reflections used, I > 2σ(I)	2985
No. of variables	235
R, wR* (%)	5.83%, 6.12%
$R_{int.}$ (%)	5.63%
Max. shift/esd	0.0003

Table B-1. continued.

min. peak in diff. four. map (e $Å^{-3}$)	-2.45
max. peak in diff. four. map (e $Å^{-3}$)	1.56

* Relevant expressions are as follows, where in the footnote F_o and F_c represent, respectively, the observed and calculated structure-factor amplitudes.

Function minimized was $w(|F_o| - |F_c|)^2$, where $w = (\sigma(F))^{-2}$

$R = \Sigma(||F_o| - |F_c||) / \Sigma|F_o|$

$wR = [\Sigma w(|F_o| - |F_c|)^2 / \Sigma|F_o|^2]^{1/2}$

$S = [\Sigma w(|F_o| - |F_c|)^2 / (m-n)]^{1/2}$

Table B-2: Fractional coordinates and equivalent isotropic[a] thermal parameters (Å2) for the non-H atoms of compound **14**.

Atom	x	y	z	U
W	0.16873(5)	0.21558(3)	0.30838(4)	0.0439(2)
Cl1	0.0285(4)	0.1100(3)	0.2519(3)	0.079(2)
Cl2	0.1131(5)	0.2447(3)	0.1288(3)	0.088(2)
Si1	0.1700(4)	0.1558(2)	0.5550(3)	0.0543(14)
Si2	0.2852(4)	0.3984(3)	0.3248(3)	0.056(2)
N1	0.1191(10)	0.2080(6)	0.4397(7)	0.051(4)
N2	0.1783(10)	0.3226(6)	0.3385(7)	0.045(4)
N3	0.3280(10)	0.1796(6)	0.3214(8)	0.048(4)
C1	0.0275(13)	0.2686(7)	0.4272(8)	0.044(5)
C2	0.0602(11)	0.3307(7)	0.3721(8)	0.041(4)
C3	-0.0280(12)	0.3933(8)	0.3513(9)	0.049(5)
C4	-0.1391(12)	0.3937(9)	0.3912(10)	0.054(5)
C5	-0.1708(13)	0.3330(9)	0.4451(10)	0.057(6)
C6	-0.0916(13)	0.2718(9)	0.4624(9)	0.057(6)
C7	0.4462(12)	0.1497(8)	0.3062(10)	0.051(5)
C8	0.4420(13)	0.1245(8)	0.2079(11)	0.054(5)
C9	0.556(2)	0.0924(9)	0.1887(13)	0.076(7)
C10	0.672(2)	0.0858(10)	0.266(2)	0.082(8)
C11	0.6756(15)	0.1119(10)	0.361(2)	0.089(8)
C12	0.5616(14)	0.1442(9)	0.3827(12)	0.078(7)
C13	0.313(2)	0.0961(10)	0.5456(12)	0.092(8)
C14	0.032(2)	0.0939(9)	0.5689(13)	0.088(8)
C15	0.214(2)	0.2225(10)	0.6625(11)	0.090(7)
C16	0.4484(15)	0.3572(11)	0.3311(14)	0.097(9)
C17	0.216(2)	0.4451(10)	0.1994(11)	0.080(7)
C18	0.298(2)	0.4619(10)	0.4354(11)	0.087(8)

[a]For anisotropic atoms, the U value is U_{eq}, calculated as $U_{eq} = 1/3\ \Sigma_i\Sigma_j\ U_{ij}\ a_i^*\ a_j^*\ A_{ij}$ where A_{ij} is the dot product of the i^{th} and j^{th} direct space unit cell vectors.

Table B-3: Bond Lengths (Å) and Angles (º) for the non-H atoms of compound **14**.

1	2	3	1-2	1-2-3
Cl1	W	Cl2	2.383(4)	82.9(2)
Cl1	W	N1		87.7(3)
Cl1	W	N2		146.8(3)
Cl1	W	N3		102.9(4)
Cl1	W	C1		95.6(3)
Cl2	W	N1	2.387(4)	150.5(3)
Cl2	W	N2		88.9(3)
Cl2	W	N3		99.8(4)
Cl2	W	C1		120.5(3)
Cl2	W	C2		98.2(3)
N1	W	N2	1.951(11)	83.9(4)
N1	W	N3		109.5(5)
N1	W	C1		32.9(4)
N1	W	C2		61.9(4)
N2	W	N3	1.952(11)	110.2(5)
N2	W	C1		61.4(4)
N2	W	C2		32.4(4)
N3	W	C1	1.730(10)	137.4(4)
N3	W	C2		137.6(4)
C1	W	C2	2.582(13)	31.9(4)
C2	W	Cl1	2.582(13)	117.2(3)
N1	Si1	C13	1.768(10)	108.4(7)
N1	Si1	C14		109.4(6)
C13	Si1	C14	1.85(2)	107.8(8)
C13	Si1	C15		112.2(8)
C14	Si1	C15	1.84(2)	111.1(8)
C15	Si1	N1	1.84(2)	107.8(7)
N2	Si2	C16	1.781(12)	106.0(7)
N2	Si2	C17		109.0(6)
C16	Si2	C17	1.82(2)	111.6(8)
C16	Si2	C18		109.2(8)
C17	Si2	C18	1.85(2)	112.7(8)
C18	Si2	N2	1.84(2)	108.0(7)
C1	N1	W	1.42(2)	98.8(7)
C1	N1	Si1		123.5(9)
W	N1	Si1		137.4(7)
C2	N2	W	1.40(2)	99.4(8)
C2	N2	Si2		124.1(9)
W	N2	Si2		136.4(6)
C7	N3	W	1.39(2)	166.2(9)
C2	C1	C6	1.42(2)	118.4(12)
C2	C1	W		74.1(7)
C2	C1	N1		115.0(12)
C6	C1	W	1.42(2)	151.9(9)
C6	C1	N1		126.6(12)
W	C1	N1		48.3(6)

Table B-3. continued.

C3	C2	W	1.42(2)	150.1(8)
C3	C2	N2		125.3(11)
C3	C2	C1		119.7(12)
W	C2	N2		48.2(6)
W	C2	C1		74.1(8)
N2	C2	C1		114.9(11)
C4	C3	C2	1.38(2)	118.6(13)
C5	C4	C3	1.38(2)	121.6(13)
C6	C5	C4	1.35(2)	120.9(14)
C1	C6	C5		120.8(13)
C8	C7	C12	1.38(2)	120.5(13)
C8	C7	N3		116.2(10)
C12	C7	N3	1.37(2)	123.3(13)
C9	C8	C7	1.39(2)	118.7(12)
C10	C9	C8	1.37(2)	121.(2)
C11	C10	C9	1.34(3)	120.(2)
C12	C11	C10	1.40(2)	120.6(14)
C7	C12	C11		119.(2)

Table B-4: Anisotropic thermal parameters[a] for the non-H atoms of compound **14**

Atom	U11	U22	U33	U12	U13	U23
W	0.0429(3)	0.0511(3)	0.0386(3)	0.0116(3)	0.0120(2)	0.0013(3)
Cl1	0.065(2)	0.081(3)	0.091(3)	-0.011(2)	0.018(2)	-0.024(2)
Cl2	0.128(4)	0.089(3)	0.042(2)	0.028(3)	0.012(2)	0.004(2)
Si1	0.068(3)	0.048(3)	0.045(2)	0.007(2)	0.010(2)	0.010(2)
Si2	0.045(2)	0.064(3)	0.060(2)	-0.005(2)	0.019(2)	0.002(2)
N1	0.058(6)	0.054(8)	0.044(6)	0.007(6)	0.019(5)	0.006(5)
N2	0.064(7)	0.038(6)	0.043(5)	0.007(5)	0.029(5)	0.003(5)
N3	0.048(7)	0.046(7)	0.053(6)	0.012(5)	0.020(5)	-0.014(5)
C1	0.044(7)	0.053(10)	0.033(6)	0.010(6)	0.004(5)	-0.005(5)
C2	0.038(6)	0.059(9)	0.031(5)	0.006(6)	0.016(5)	0.002(6)
C3	0.040(7)	0.058(9)	0.049(7)	-0.001(7)	0.013(6)	0.009(7)
C4	0.038(7)	0.075(11)	0.051(7)	0.005(7)	0.014(6)	-0.008(7)
C5	0.042(7)	0.085(12)	0.046(7)	-0.004(8)	0.016(6)	-0.003(8)
C6	0.051(8)	0.077(12)	0.041(7)	-0.010(8)	0.008(6)	0.009(7)
C7	0.040(7)	0.045(9)	0.068(8)	-0.006(6)	0.018(6)	-0.013(7)
C8	0.046(8)	0.049(9)	0.066(8)	0.009(7)	0.014(7)	0.005(7)
C9	0.089(12)	0.070(12)	0.088(11)	0.013(10)	0.056(10)	0.003(9)
C10	0.051(10)	0.065(12)	0.14(2)	0.007(9)	0.033(11)	0.017(12)
C11	0.039(9)	0.079(14)	0.13(2)	0.003(8)	-0.020(10)	-0.009(12)
C12	0.058(9)	0.090(13)	0.071(9)	0.019(9)	-0.014(8)	-0.029(9)
C13	0.113(15)	0.093(15)	0.073(11)	0.038(12)	0.025(10)	0.019(10)
C14	0.099(13)	0.054(11)	0.109(13)	-0.003(10)	0.019(11)	0.038(10)
C15	0.120(14)	0.086(13)	0.053(8)	0.018(12)	-0.003(9)	-0.017(9)
C16	0.064(11)	0.10(2)	0.13(2)	0.025(11)	0.037(10)	0.026(13)
C17	0.075(11)	0.085(14)	0.082(11)	-0.017(10)	0.025(9)	-0.001(10)
C18	0.085(12)	0.084(13)	0.085(12)	-0.021(10)	0.010(9)	0.000(10)

[a] Uij are the mean-square amplitudes of vibration in $Å^2$ from the general temperature factor expression

$$\exp[-2\pi^2(h^2a^{*2}U11 + k^2b^{*2}U22 + l^2c^{*2}U33 + 2hka^*b^*U12 + 2hla^*c^*U13 + 2klb^*c^*U23)]$$

Table B-5: Fractional coordinates and isotropic-thermal parameters (Å2) for the H atoms of compound **14**.

Atom	x	y	z	U
H3	-0.0103(12)	0.4344(8)	0.3102(9)	0.08
H4	-0.1961(12)	0.4370(9)	0.3814(10)	0.08
H5	-0.2502(13)	0.3346(9)	0.4706(10)	0.08
H6	-0.1163(13)	0.2300(9)	0.4988(9)	0.08
H8	0.3616(13)	0.1291(8)	0.1539(11)	0.08
H9	0.555(2)	0.0746(9)	0.1207(13)	0.08
H10	0.750(2)	0.0624(10)	0.252(2)	0.08
H11	0.7571(15)	0.1085(10)	0.414(2)	0.08
H12	0.5645(14)	0.1622(9)	0.4508(12)	0.08
H13a	0.342(2)	0.0673(10)	0.6077(12)	0.08
H13b	0.385(2)	0.1270(10)	0.5363(12)	0.08
H13c	0.286(2)	0.0628(10)	0.4878(12)	0.08
H14a	0.060(2)	0.0656(9)	0.6315(13)	0.08
H14b	0.010(2)	0.0603(9)	0.5112(13)	0.08
H14c	-0.045(2)	0.1236(9)	0.5712(13)	0.08
H15a	0.242(2)	0.1955(10)	0.7262(11)	0.08
H15b	0.138(2)	0.2527(10)	0.6640(11)	0.08
H15c	0.286(2)	0.2541(10)	0.6534(11)	0.08
H16a	0.5103(15)	0.3958(11)	0.3241(14)	0.08
H16b	0.4410(15)	0.3215(11)	0.2764(14)	0.08
H16c	0.4800(15)	0.3324(11)	0.3963(14)	0.08
H17a	0.274(2)	0.4860(10)	0.1915(11)	0.08
H17b	0.128(2)	0.4636(10)	0.1972(11)	0.08
H17c	0.212(2)	0.4097(10)	0.1446(11)	0.08
H18a	0.355(2)	0.5033(10)	0.4297(11)	0.08
H18b	0.335(2)	0.4353(10)	0.4983(11)	0.08
H18c	0.210(2)	0.4803(10)	0.4359(11)	0.08

Table B-6: Bond Lengths (Å) and Angles (º) of the H atoms of compound **14**.

1	2	3	1-2	1-2-3
H3	C3	C4	0.96(2)	121.(2)
H3	C3	C2		120.7(15)
H4	C4	C5	0.96(2)	119.(2)
H4	C4	C3		119.(2)
H5	C5	C6	0.96(2)	120.(2)
H5	C5	C4		120.(2)
H6	C6	C1	0.96(2)	120.(2)
H6	C6	C5		120.(2)
H8	C8	C9	0.96(2)	121.(2)
H8	C8	C7		121.(2)
H9	C9	C10	0.96(3)	120.(2)
H9	C9	C8		120.(2)
H10	C10	C11	0.96(3)	120.(2)
H10	C10	C9		120.(2)
H11	C11	C12	0.96(2)	120.(2)
H11	C11	C10		120.(2)
H12	C12	C7	0.96(2)	120.(2)
H12	C12	C11		120.(2)
H13a	C13	H13b	0.96(2)	109.(2)
H13a	C13	H13c		109.(2)
H13a	C13	Si1		109.(2)
H13b	C13	H13c	0.96(3)	109.(2)
H13b	C13	Si1		109.(2)
H13c	C13	Si1	0.96(2)	109.(2)
H14a	C14	H14b	0.96(2)	109.(2)
H14a	C14	H14c		109.(2)
H14a	C14	Si1		109.5(15)
H14b	C14	H14c	0.96(2)	109.(2)
H14b	C14	Si1		109.(2)
H14c	C14	Si1	0.96(2)	109.(2)
H15a	C15	H15b	0.96(2)	109.(2)
H15a	C15	H15c		109.(2)
H15a	C15	Si1		109.(2)
H15b	C15	H15c	0.96(3)	109.(2)
H15b	C15	Si1		109.5(14)
H15c	C15	Si1	0.96(3)	110.(2)
H16a	C16	H16b	0.96(3)	109.(2)
H16a	C16	H16c		109.(2)
H16a	C16	Si2		109.(2)
H16b	C16	H16c	0.96(3)	109.(2)
H16b	C16	Si2		109.5(14)
H16c	C16	Si2	0.96(3)	109.(2)
H17a	C17	H17b	0.96(2)	109.(2)
H17a	C17	H17c		109.(2)
H17a	C17	Si2		109.5(13)
H17b	C17	H17c	0.96(2)	109.(2)

Table B-6 continued.

H17b	C17	Si2		109.(2)
H17c	C17	Si2	0.96(2)	109.(2)
H18a	C18	H18b	0.96(2)	109.(2)
H18a	C18	H18c		109.(2)
H18a	C18	Si2		109.(2)
H18b	C18	H18c	0.96(2)	109.(2)
H18b	C18	Si2		109.(2)
H18c	C18	Si2	0.96(2)	109.5(14)

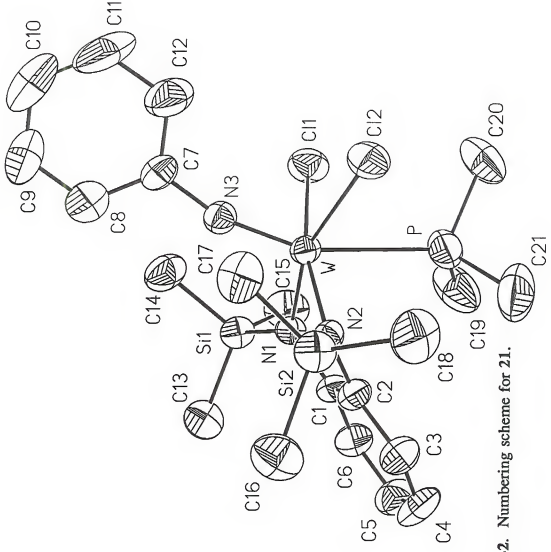

Figure B-2. Numbering scheme for **21.**

Crystallographic Data for $W(NPh)Cl_2(PMe_3)[(Me_3SiN)_2C_6H_4]$, **21**

Table B-7. Crystallographic Data.

A. Crystal data (298 K)	**21**
a, Å	9.562 (1)
b, Å	10.277 (1)
c, Å	14.920 (2)
α, deg.	82.15 (1)
β, deg.	80.18 (1)
γ, deg.	80.41 (1)
V, Å^3	1415.6 (3)
d_{calc}, g cm^{-3}(298 K)	1.578
Empirical formula	$C_{21}H_{36}N_3PCl_2W$
Formula wt, g	672.43
Crystal system	Triclinic
Space group	P-1
Z	2
F(000), electrons	668.0
Crystal size (mm^3)	0.25 x 0.10 x 0.09
B. Data collection (298 K)	
Radiation, λ (Å)	Mo-K_α, 0.71073
Mode	ω-scan
Scan range	Symmetrically over 1.2° about $K_{\alpha 1,2}$ maximum
Background	offset 1.0 and -1.0 in ω from $K_{\alpha 1,2}$ maximum
Scan rate, deg. min.$^{-1}$	3 – 6
2θ range, deg.	3 – 45
Range of *h k l*	$0 \le h \le 11$ $-12 \le k \le 12$ $-17 \le l \le 17$
Total reflections measured	5312
Unique reflections	4981
Absorption coeff. μ (Mo-K_α), cm^{-1}	4.42
Min. & Max. Transmission	0.34906, 0.75350
C. Structure refinement	
S, Goodness-of-fit	1.2810
Reflections used, I > 2σ(I)	4224
No. of variables	271
R, wR* (%)	0.0408, 0.0426
$R_{int.}$ (%)	0.0149
Max. shift/esd	0.0005

Supplementary Table 1 continued.

min. peak in diff. four. map (e $Å^{-3}$)	-1.280
max. peak in diff. four. map (e $Å^{-3}$)	0.823

* Relevant expressions are as follows, where in the footnote F_o and F_c represent, respectively, the observed and calculated structure-factor amplitudes.

Function minimized was $w(|F_o| - |F_c|)^2$, where $w = (\sigma(F))^{-2}$

$R = \sum(||F_o| - |F_c||) / \sum|F_o|$

$wR = [\sum w(|F_o| - |F_c|)^2 / \sum |F_o|^2]^{1/2}$

$S = [\sum w(|F_o| - |F_c|)^2 / (m-n)]^{1/2}$

Table B-8: Fractional coordinates and equivalent isotropic[a] thermal parameters ($Å^2$) for the non-H atoms of compound **21**.

Atom	x	y	z	U
W	0.12434(3)	0.18104(3)	0.23475(2)	0.03253(10)
Cl1	0.3444(2)	0.2738(2)	0.23418(14)	0.0566(8)
Cl2	0.1471(2)	0.2147(2)	0.06792(12)	0.0544(8)
P	0.0480(3)	0.4471(2)	0.1953(2)	0.0531(8)
Si1	0.1579(2)	0.1751(2)	0.46064(14)	0.0414(7)
Si2	-0.1611(2)	0.0550(2)	0.18439(14)	0.0453(8)
N1	0.0590(5)	0.2082(6)	0.3671(3)	0.034(2)
N2	-0.0803(5)	0.1576(6)	0.2443(4)	0.034(2)
N3	0.2226(6)	0.0219(6)	0.2314(4)	0.038(2)
C1	-0.0875(6)	0.2593(7)	0.3790(5)	0.034(2)
C2	-0.1635(7)	0.2302(7)	0.3112(5)	0.038(2)
C3	-0.3100(8)	0.2741(8)	0.3181(5)	0.048(3)
C4	-0.3805(8)	0.3426(9)	0.3898(7)	0.063(4)
C5	-0.3075(8)	0.3702(8)	0.4552(6)	0.056(3)
C6	-0.1616(8)	0.3299(8)	0.4507(5)	0.047(3)
C7	0.3211(7)	-0.0877(8)	0.2074(5)	0.044(3)
C8	0.3295(10)	-0.2036(10)	0.2659(7)	0.073(4)
C9	0.4230(12)	-0.3135(11)	0.2402(10)	0.099(6)
C10	0.5067(11)	-0.3108(13)	0.1580(10)	0.091(6)
C11	0.4990(11)	-0.1985(14)	0.1002(8)	0.096(5)
C12	0.4076(9)	-0.0843(11)	0.1239(6)	0.075(4)
C13	0.0412(9)	0.1159(9)	0.5674(5)	0.058(3)
C14	0.3150(8)	0.0453(9)	0.4378(6)	0.063(4)
C15	0.2179(9)	0.3319(9)	0.4779(6)	0.067(4)
C16	-0.3014(9)	-0.0258(10)	0.2649(6)	0.065(4)
C17	-0.0214(9)	-0.0765(9)	0.1388(6)	0.059(3)
C18	-0.2416(10)	0.1603(10)	0.0909(6)	0.069(4)
C19	0.0354(13)	0.5472(10)	0.2883(7)	0.090(5)
C20	0.1727(11)	0.5247(10)	0.1071(7)	0.081(4)
C21	-0.1202(11)	0.4987(12)	0.1528(9)	0.106(6)

[a]For anisotropic atoms, the U value is U_{eq}, calculated as $U_{eq} = 1/3\ \Sigma_i\Sigma_j\ U_{ij}\ a_i^*\ a_j^*\ A_{ij}$ where A_{ij} is the dot product of the i^{th} and j^{th} direct space unit cell vectors.

Table B-9: Bond Lengths (Å) and Angles (°) for the non-H atoms of compound **21**.

1	2	3	1-2	1-2-3
Cl1	W	Cl2	2.449(2)	92.43(7)
Cl1	W	P		75.86(7)
Cl1	W	N1		91.2(2)
Cl1	W	N2		163.5(2)
Cl1	W	N3		90.4(2)
Cl1	W	C1		111.4(2)
Cl2	W	P	2.443(2)	75.70(7)
Cl2	W	N1		161.0(2)
Cl2	W	N2		90.7(2)
Cl2	W	N3		91.2(2)
Cl2	W	C1		135.07(14)
Cl2	W	C2		109.9(2)
P	W	N1	2.720(2)	87.2(2)
P	W	N2		89.2(2)
P	W	N3		160.3(2)
P	W	C1		74.25(14)
P	W	C2		75.3(2)
N1	W	N2	2.010(5)	80.8(2)
N1	W	N3		107.4(2)
N1	W	C1		28.3(2)
N1	W	C2		56.8(2)
N2	W	N3	1.990(5)	105.8(3)
N2	W	C1		56.5(2)
N2	W	C2		27.9(2)
N3	W	C1	1.747(6)	124.6(2)
N3	W	C2		123.6(2)
C1	W	C2	2.797(6)	29.7(2)
C2	W	Cl1	2.785(6)	137.4(2)
N1	Si1		1.781(6)	
C1	N1	W	1.402(8)	108.8(4)
C1	N1	Si1		121.6(4)
W	N1	Si1		129.6(3)
C2	N2	W	1.387(9)	109.8(5)
C7	N3	W	1.388(9)	164.3(5)
C2	C1	C6	1.430(11)	119.7(6)
C2	C1	W		74.7(4)
C2	C1	N1		114.4(6)
C6	C1	W	1.399(10)	160.3(6)
C6	C1	N1		125.9(7)
W	C1	N1		42.8(3)
C3	C2	W	1.389(9)	159.9(5)
C3	C2	N2		126.3(7)
C3	C2	C1		118.8(6)
W	C2	N2		42.2(3)
W	C2	C1		75.6(3)
N2	C2	C1		114.9(5)

Table B-9 continued.

C4	C3	C2	1.377(12)	120.3(8)
C5	C4	C3	1.376(14)	120.9(7)
C6	C5	C4	1.380(11)	120.9(8)
C1	C6	C5		119.4(8)
C8	C7	C12	1.377(12)	118.9(8)
C8	C7	N3		120.2(7)
C12	C7	N3	1.372(11)	120.8(7)
C9	C8	C7	1.373(14)	120.0(9)
C10	C9	C8	1.35(2)	121.2(11)
C11	C10	C9	1.34(2)	119.4(11)
C12	C11	C10	1.39(2)	121.4(10)
C7	C12	C11		119.1(9)

Table B-10: Anisotropic thermal parameters[a] for the non-H atoms of compound **21.**

Atom	U11	U22	U33	U12	U13	U23
W	0.0293(2)	0.0372(2)	0.0298(2)	-0.00271(10)	-0.00254(10)	-0.00437(11)
Cl1	0.0403(10)	0.0696(15)	0.0610(13)	-0.0191(10)	-0.0036(9)	-0.0024(11)
Cl2	0.0601(12)	0.0670(14)	0.0324(10)	-0.0052(10)	-0.0014(8)	-0.0048(10)
P	0.0638(14)	0.0431(13)	0.0489(12)	-0.0067(10)	-0.0066(10)	0.0026(10)
Si1	0.0376(10)	0.0516(13)	0.0384(11)	-0.0085(9)	-0.0094(8)	-0.0097(10)
Si2	0.0453(12)	0.0555(14)	0.0396(11)	-0.0103(10)	-0.0135(9)	-0.0092(10)
N1	0.030(3)	0.040(3)	0.031(3)	-0.007(2)	-0.003(2)	-0.003(3)
N2	0.033(3)	0.036(3)	0.033(3)	-0.000(2)	-0.009(2)	-0.003(3)
N3	0.038(3)	0.041(4)	0.033(3)	-0.003(3)	-0.004(2)	-0.005(3)
C1	0.025(3)	0.039(4)	0.040(4)	-0.006(3)	-0.002(3)	-0.006(3)
C2	0.030(3)	0.040(4)	0.042(4)	-0.002(3)	-0.003(3)	-0.006(3)
C3	0.037(4)	0.054(5)	0.054(5)	-0.003(4)	-0.011(3)	-0.011(4)
C4	0.032(4)	0.063(6)	0.091(7)	0.011(4)	-0.006(4)	-0.024(5)
C5	0.050(5)	0.052(5)	0.062(5)	0.001(4)	0.003(4)	-0.016(4)
C6	0.042(4)	0.053(5)	0.046(4)	-0.006(4)	-0.002(3)	-0.013(4)
C7	0.029(4)	0.048(5)	0.053(5)	0.001(3)	-0.008(3)	-0.009(4)
C8	0.072(6)	0.063(7)	0.075(7)	0.000(5)	0.009(5)	-0.009(5)
C9	0.087(8)	0.056(7)	0.135(11)	0.022(6)	-0.004(8)	0.000(7)
C10	0.062(7)	0.083(9)	0.128(11)	0.028(6)	-0.025(7)	-0.043(8)
C11	0.066(7)	0.139(12)	0.071(7)	0.029(7)	0.009(5)	-0.045(8)
C12	0.064(6)	0.101(8)	0.044(5)	0.019(5)	0.002(4)	-0.008(5)
C13	0.067(5)	0.067(6)	0.043(5)	-0.013(5)	-0.012(4)	-0.009(4)
C14	0.042(4)	0.083(7)	0.060(5)	0.005(4)	-0.012(4)	-0.009(5)
C15	0.062(5)	0.078(7)	0.074(6)	-0.031(5)	-0.011(5)	-0.026(5)
C16	0.058(5)	0.078(7)	0.069(6)	-0.032(5)	-0.016(4)	-0.007(5)
C17	0.070(6)	0.054(5)	0.059(5)	-0.007(4)	-0.017(4)	-0.022(4)
C18	0.068(6)	0.092(8)	0.051(5)	-0.003(5)	-0.032(4)	-0.004(5)
C19	0.151(11)	0.050(6)	0.063(6)	-0.025(6)	0.014(6)	-0.009(5)
C20	0.107(8)	0.064(7)	0.068(6)	-0.035(6)	-0.003(6)	0.016(5)
C21	0.078(7)	0.086(9)	0.140(11)	0.005(6)	-0.036(7)	0.037(8)

[a] Uij are the mean-square amplitudes of vibration in $Å^2$ from the general temperature factor expressio

$\exp[-2\pi^2(h^2a^{*2}U11 + k^2b^{*2}U22 + l^2c^{*2}U33 + 2hka^*b^*U12 + 2hla^*c^*U13 + 2klb^*c^*U23)]$

Table B-11: Fractional coordinates and isotropic thermal parameters ($Å^2$) for the H atoms of compound **21**.

Atom	x	y	z	U
H3	-0.3623(8)	0.2566(8)	0.2726(5)	1.08
H4	-0.4819(8)	0.3716(9)	0.3941(7)	1.08
H5	-0.3587(8)	0.4179(8)	0.5047(6)	1.08
H6	-0.1115(8)	0.3502(8)	0.4964(5)	1.08
H8	0.2700(10)	-0.2076(10)	0.3247(7)	1.08
H9	0.4288(12)	-0.3936(11)	0.2817(10)	1.08
H10	0.5713(11)	-0.3884(13)	0.1408(10)	1.08
H11	0.5578(11)	-0.1971(14)	0.0412(8)	1.08
H12	0.4051(9)	-0.0041(11)	0.0825(6)	1.08
H13a	0.0954(9)	0.0983(9)	0.6174(5)	1.08
H13b	0.0082(9)	0.0360(9)	0.5586(5)	1.08
H13c	-0.0397(9)	0.1830(9)	0.5809(5)	1.08
H14a	0.3668(8)	0.0288(9)	0.4889(6)	1.08
H14b	0.3767(8)	0.0748(9)	0.3837(6)	1.08
H14c	0.2829(8)	-0.0351(9)	0.4289(6)	1.08
H15a	0.2715(9)	0.3157(9)	0.5282(6)	1.08
H15b	0.1357(9)	0.3978(9)	0.4911(6)	1.08
H15c	0.2775(9)	0.3631(9)	0.4233(6)	1.08
H16a	-0.3437(9)	-0.0800(10)	0.2325(6)	1.08
H16b	-0.3743(9)	0.0413(10)	0.2900(6)	1.08
H16c	-0.2585(9)	-0.0801(10)	0.3135(6)	1.08
H17a	-0.0636(9)	-0.1313(9)	0.1070(6)	1.08
H17b	0.0199(9)	-0.1298(9)	0.1885(6)	1.08
H17c	0.0520(9)	-0.0366(9)	0.0974(6)	1.08
H18a	-0.2849(10)	0.1070(10)	0.0585(6)	1.08
H18b	-0.1685(10)	0.2008(10)	0.0495(6)	1.08
H18c	-0.3134(10)	0.2282(10)	0.1158(6)	1.08
H19a	-0.0291(13)	0.5146(10)	0.3399(7)	1.08
H19b	0.0001(13)	0.6379(10)	0.2688(7)	1.08
H19c	0.1286(13)	0.5422(10)	0.3055(7)	1.08
H20a	0.2676(11)	0.5033(10)	0.1231(7)	1.08
H20b	0.1448(11)	0.6192(10)	0.1018(7)	1.08
H20c	0.1718(11)	0.4926(10)	0.0498(7)	1.08
H21a	-0.1953(11)	0.4626(12)	0.1950(9)	1.08
H21b	-0.1140(11)	0.4673(12)	0.0943(9)	1.08
H21c	-0.1409(11)	0.5939(12)	0.1463(9)	1.08

Table B-12: Bond Lengths (Å) and Angles (°) of the H atoms of compound **21.**

1	2	3	1-2	1-2-3
H3	C3	C4	0.960(12)	119.9(8)
H3	C3	C2		119.8(8)
H4	C4	C5	0.960(11)	119.6(11)
H4	C4	C3		119.6(11)
H5	C5	C6	0.960(12)	119.6(10)
H5	C5	C4		119.5(9)
H6	C6	C1	0.960(12)	120.3(8)
H6	C6	C5		120.3(9)
H8	C8	C9	0.960(13)	120.0(11)
H8	C8	C7		120.0(10)
H9	C9	C10	0.96(2)	119.4(13)
H9	C9	C8		119.4(14)
H10	C10	C11	0.96(2)	120.3(14)
H10	C10	C9		120.3(14)
H11	C11	C12	0.960(15)	119.2(14)
H11	C11	C10		119.3(15)
H12	C12	C7	0.960(14)	120.4(11)
H12	C12	C11		120.5(10)
H13a	C13	H13b	0.960(12)	109.5(11)
H13a	C13	H13c		109.5(11)
H13b	C13	H13c	0.960(14)	109.5(11)
H14a	C14	H14b	0.960(13)	109.5(11)
H14a	C14	H14c		109.5(12)
H14b	C14	H14c	0.960(11)	109.5(12)
H15a	C15	H15b	0.960(14)	109.5(12)
H15a	C15	H15c		109.5(12)
H15b	C15	H15c	0.960(12)	109.5(11)
H16a	C16	H16b	0.960(15)	109.5(11)
H16a	C16	H16c		109.5(12)
H16b	C16	H16c	0.960(12)	109.5(12)
H17a	C17	H17b	0.960(14)	109.5(11)
H17a	C17	H17c		109.5(11)
H17b	C17	H17c	0.960(12)	109.5(11)
H18a	C18	H18b	0.96(2)	109.5(12)
H18a	C18	H18c		109.5(12)
H18b	C18	H18c	0.960(13)	109.5(13)
H19a	C19	H19b	0.960(14)	109.5(13)
H19a	C19	H19c		109.5(13)
H19b	C19	H19c	0.960(13)	109.5(15)
H20a	C20	H20b	0.96(2)	109.5(15)
H20a	C20	H20c		109.5(13)
H20b	C20	H20c	0.960(14)	109.5(12)
H21a	C21	H21b	0.96(2)	109.(2)
H21a	C21	H21c		109.5(14)
H21b	C21	H21c	0.96(2)	109.(2)

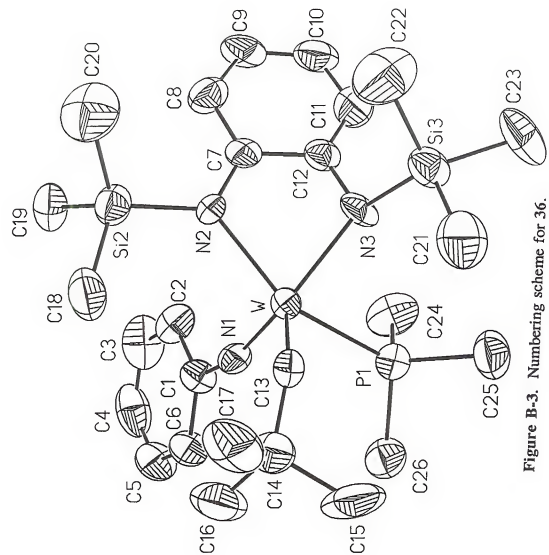

Figure B-3. Numbering scheme for **36**.

Crystallographic data for W(NPh)(CHCMe$_3$)(PMe$_3$)I[(Me$_3$SiN)$_2$C$_6$H$_4$], **36**.

Table B-13: Crystallographic data for **36**.

A. Crystal data (298 K)	**36**
a, Å	16.116(3)
b, Å	11.340(2)
c, Å	17.960(4)
α, deg.	
β, deg.	106.28(2)
γ, deg.	
V, Å^3	3151(1)
d_{calc}, g cm^{-3}(298 K)	1.416
Empirical formula	$C_{26}H_{46}N_3Si_2PW$
Formula wt, g	671.66
Crystal system	Monoclinic
Space group	P 2_1/c
Z	4
F(000), electrons	1360
Crystal size (mm^3)	0.38 x 0.21 x 0.13
B. Data collection (298 K)	
Radiation, λ (Å)	Mo-K$_\alpha$, 0.71073
Mode	ω-scan
Scan range	Symmetrically over 1.2° about K$_{\alpha 1,2}$ maximum
Background	offset 1.0 and -1.0 in ω from K$_{\alpha 1,2}$ maximum
Scan rate, deg. min.$^{-1}$	3 – 6
2θ range, deg.	3 – 50
Range of h k l	$0 \le h \le 19$ $0 \le k \le 12$ $-19 \le l \le 19$
Total reflections measured	6099
Unique reflections	5563
Absorption coeff. μ (Mo-K$_\alpha$), mm^{-1}	3.81
Min. & Max. Transmission	0.486, 0.618
C. Structure refinement	
S, Goodness-of-fit	1.15
Reflections used, I > 2σ(I)	3209
No. of variables	298
R, wR* (%)	5.25%, 5.10%
R$_{int.}$ (%)	4.00%
Max. shift/esd	0.0001

Table B-13 continued.

min. peak in diff. four. map (e $Å^{-3}$)	-1.10
max. peak in diff. four. map (e $Å^{-3}$)	1.40

* Relevant expressions are as follows, where in the footnote F_o and F_c represent, respectively, the observed and calculated structure-factor amplitudes.

Function minimized was $w(|F_o| - |F_c|)^2$, where $w = (\sigma(F))^{-2}$

$R = \sum(||F_o| - |F_c||) / \sum|F_o|$

$wR = [\sum w(|F_o| - |F_c|)^2 / \sum|F_o|^2]^{1/2}$

$S = [\sum w(|F_o| - |F_c|)^2 / (m-n)]^{1/2}$

Table B-14: Fractional coordinates and equivalent isotropic[a] thermal parameters (Å^2) for the non-H atoms of compound 36

Atom	x	y	z	U
W	-0.25717(3)	0.13867(5)	0.03328(3)	0.0334(2)
P1	-0.3548(2)	0.2116(3)	0.1098(2)	0.0443(14)
Si2	-0.1756(3)	0.0067(4)	-0.1059(2)	0.046(2)
Si3	-0.1715(3)	-0.0438(4)	0.1953(2)	0.050(2)
N1	-0.3349(6)	0.2095(9)	-0.0450(6)	0.040(4)
N2	-0.2221(6)	0.0012(8)	-0.0297(5)	0.034(4)
N3	-0.2474(6)	-0.0029(9)	0.1078(6)	0.043(4)
C1	-0.4058(8)	0.2263(12)	-0.1088(7)	0.040(5)
C2	-0.4478(8)	0.1309(14)	-0.1508(8)	0.053(6)
C3	-0.5195(9)	0.149(2)	-0.2139(8)	0.074(7)
C4	-0.5471(10)	0.263(2)	-0.2342(9)	0.073(8)
C5	-0.5086(10)	0.354(2)	-0.1924(8)	0.064(6)
C6	-0.4371(9)	0.3402(12)	-0.1294(8)	0.054(6)
C7	-0.2633(8)	-0.0999(11)	-0.0138(7)	0.037(5)
C8	-0.2879(9)	-0.2024(13)	-0.0601(8)	0.055(6)
C9	-0.3293(9)	-0.2908(12)	-0.0398(9)	0.057(7)
C10	-0.3502(10)	-0.2888(13)	0.0297(9)	0.062(7)
C11	-0.3261(9)	-0.1941(14)	0.0771(9)	0.061(7)
C12	-0.2796(8)	-0.1003(11)	0.0602(7)	0.039(5)
C13	-0.1697(8)	0.2529(11)	0.0663(7)	0.043(5)
C14	-0.1401(8)	0.3780(13)	0.0621(8)	0.052(6)
C15	-0.1472(11)	0.4449(13)	0.1341(9)	0.089(9)
C16	-0.1978(10)	0.4429(13)	-0.0079(9)	0.081(8)
C17	-0.0464(9)	0.3786(14)	0.0597(9)	0.081(8)
C18	-0.1271(9)	0.1518(13)	-0.1067(7)	0.066(6)
C19	-0.2553(8)	-0.0145(13)	-0.2021(7)	0.055(6)
C20	-0.0896(9)	-0.1054(14)	-0.0931(9)	0.089(8)
C21	-0.1049(10)	0.0828(14)	0.2422(8)	0.080(7)
C22	-0.1015(10)	-0.156(2)	0.1742(9)	0.108(9)
C23	-0.2206(9)	-0.1051(14)	0.2697(8)	0.083(8)
C24	-0.4488(8)	0.1170(13)	0.0819(9)	0.072(7)
C25	-0.3214(9)	0.2068(14)	0.2147(7)	0.071(7)
C26	-0.4003(8)	0.3587(12)	0.0893(8)	0.058(6)

[a]For anisotropic atoms, the U value is U_{eq}, calculated as $U_{eq} = 1/3\ \Sigma_i\Sigma_j\ U_{ij}\ a_i^*\ a_j^*\ A_{ij}$ where A_{ij} is the dot product of the i^{th} and j^{th} direct space unit cell vectors.

Table B-15: Bond Lengths (Å) and Angles (º) for the non-H atoms of compound 36.

1	2	3	1-2	1-2-3
P1	W	N1	2.502(4)	82.8(4)
P1	W	N2		148.1(3)
P1	W	N3		81.2(3)
N1	W	N2	1.789(9)	98.4(4)
N1	W	N3		140.1(4)
N1	W	C13		103.6(5)
N2	W	N3	2.095(10)	77.8(4)
N2	W	C13		113.0(5)
N3	W	C13	2.067(10)	114.6(4)
C13	W	P1	1.884(13)	97.5(4)
C24	P1	C25	1.809(13)	104.6(7)
C24	P1	C26		103.2(6)
C24	P1	W		105.0(5)
C25	P1	C26	1.808(13)	102.9(7)
C25	P1	W		120.9(5)
C26	P1	W	1.818(14)	118.2(5)
N2	Si2	C18	1.736(11)	108.6(6)
N2	Si2	C19		113.0(6)
C18	Si2	C19	1.82(2)	107.2(6)
C18	Si2	C20		108.3(7)
C19	Si2	C20	1.856(11)	109.1(7)
C20	Si2	N2	1.85(2)	110.6(6)
N3	Si3	C21	1.761(9)	111.8(6)
N3	Si3	C22		108.4(6)
C21	Si3	C22	1.85(2)	109.0(7)
C21	Si3	C23		105.7(7)
C22	Si3	C23	1.81(2)	107.5(8)
C23	Si3	N3	1.87(2)	114.2(6)
C1	N1	W	1.387(14)	160.8(9)
C7	N2	W	1.39(2)	106.6(8)
C7	N2	Si2		121.8(8)
W	N2	Si2		129.8(5)
C12	N3	W	1.40(2)	105.6(7)
C12	N3	Si3		112.4(8)
W	N3	Si3		133.6(6)
C2	C1	C6	1.38(2)	119.6(11)
C2	C1	N1		120.5(11)
C6	C1	N1	1.40(2)	119.9(11)
C3	C2	C1	1.39(2)	119.9(14)
C4	C3	C2	1.39(3)	119.(2)
C5	C4	C3	1.33(2)	121.1(13)
C6	C5	C4	1.38(2)	122.(2)
C1	C6	C5		118.8(13)
C8	C7	C12	1.42(2)	116.7(12)
C8	C7	N2		128.6(13)
C12	C7	N2	1.43(2)	114.6(11)

Table B-15 continued.

C9	C8	C7	1.31(2)	122.9(15)
C10	C9	C8	1.38(2)	120.7(14)
C11	C10	C9	1.36(2)	118.7(15)
C12	C11	C10	1.38(2)	123.(2)
N3	C12	C7		115.6(12)
N3	C12	C11		127.1(13)
C7	C12	C11		117.3(12)
C14	C13	W	1.50(2)	148.4(9)
C15	C14	C16	1.53(2)	106.5(12)
C15	C14	C17		109.3(11)
C15	C14	C13		109.0(12)
C16	C14	C17	1.53(2)	110.8(13)
C16	C14	C13		111.6(10)
C17	C14	C13	1.52(2)	109.7(12)

Table B-16: Anisotropic thermal parameters[a] for the non-H atoms of compound 36.

Atom	U11	U22	U33	U12	U13	U23
W	0.0377(3)	0.0318(3)	0.0298(3)	0.0030(4)	0.0078(2)	0.0020(4)
P1	0.048(2)	0.045(2)	0.041(2)	0.000(2)	0.015(2)	-0.001(2)
Si2	0.050(2)	0.052(3)	0.038(2)	0.004(2)	0.012(2)	-0.003(2)
Si3	0.050(2)	0.052(3)	0.043(2)	0.005(2)	0.003(2)	0.010(2)
N1	0.043(7)	0.035(7)	0.049(7)	0.010(5)	0.024(6)	0.000(6)
N2	0.046(8)	0.028(6)	0.028(5)	0.002(5)	0.012(6)	-0.006(5)
N3	0.046(7)	0.038(7)	0.035(6)	0.003(6)	-0.007(5)	0.016(6)
C1	0.036(8)	0.039(8)	0.042(8)	-0.007(7)	0.003(6)	0.001(7)
C2	0.041(8)	0.056(10)	0.064(9)	-0.009(8)	0.021(7)	-0.016(9)
C3	0.039(9)	0.11(2)	0.060(10)	-0.027(12)	-0.000(7)	-0.011(13)
C4	0.051(11)	0.12(2)	0.050(10)	0.011(12)	0.012(8)	0.025(12)
C5	0.070(11)	0.060(10)	0.050(9)	0.022(10)	-0.001(8)	0.018(9)
C6	0.062(10)	0.049(11)	0.045(8)	0.022(8)	0.005(7)	0.014(7)
C7	0.032(8)	0.036(9)	0.037(8)	0.017(6)	-0.001(6)	0.006(6)
C8	0.065(10)	0.048(10)	0.044(9)	0.011(9)	0.005(8)	-0.010(8)
C9	0.073(11)	0.024(8)	0.066(11)	-0.018(8)	0.005(9)	-0.002(8)
C10	0.077(12)	0.034(9)	0.071(11)	0.001(8)	0.014(9)	0.006(9)
C11	0.068(11)	0.057(11)	0.056(10)	-0.003(9)	0.016(9)	-0.003(9)
C12	0.040(8)	0.034(9)	0.038(8)	0.003(6)	0.001(6)	0.004(6)
C13	0.057(9)	0.044(9)	0.035(8)	0.005(7)	0.022(7)	0.001(7)
C14	0.049(8)	0.045(10)	0.068(9)	0.002(8)	0.024(7)	0.003(9)
C15	0.115(15)	0.032(10)	0.12(2)	-0.010(10)	0.040(13)	-0.022(10)
C16	0.107(14)	0.042(10)	0.086(13)	0.004(10)	0.016(11)	0.015(10)
C17	0.080(12)	0.065(12)	0.101(13)	-0.035(11)	0.031(10)	0.008(11)
C18	0.082(11)	0.076(12)	0.045(8)	-0.004(11)	0.026(8)	0.006(9)
C19	0.056(9)	0.070(11)	0.041(8)	-0.017(8)	0.018(7)	-0.007(8)
C20	0.054(10)	0.11(2)	0.105(14)	0.018(11)	0.026(9)	0.001(12)
C21	0.081(12)	0.090(13)	0.055(10)	0.000(11)	-0.001(9)	-0.000(10)
C22	0.094(14)	0.12(2)	0.084(13)	0.050(13)	-0.023(11)	-0.019(12)
C23	0.084(12)	0.10(2)	0.051(9)	-0.006(11)	-0.007(8)	0.036(10)
C24	0.043(9)	0.071(13)	0.100(12)	0.007(8)	0.017(8)	-0.012(10)
C25	0.088(12)	0.085(12)	0.042(9)	0.027(10)	0.019(8)	0.011(9)
C26	0.056(9)	0.058(9)	0.062(9)	0.011(9)	0.021(7)	-0.001(9)

[a] Uij are the mean-square amplitudes of vibration in Å^2 from the general temperature factor expression

$$\exp[-2\pi^2(h^2a^{*2}U11 + k^2b^{*2}U22 + l^2c^{*2}U33 + 2hka^*b^*U12 + 2hla^*c^*U13 + 2klb^*c^*U23)]$$

Table B-17: Fractional coordinates and isotropic-thermal parameters (Å2) for the H atoms of compound **36**.

Atom	x	y	z	U
H2	-0.42722	0.05235	-0.13645	0.08
H3	-0.54983	0.08306	-0.24286	0.08
H4	-0.59452	0.27668	-0.2795	0.08
H5	-0.53144	0.43207	-0.20612	0.08
H6	-0.40926	0.40742	-0.10044	0.08
H8	-0.27357	-0.20739	-0.10841	0.08
H9	-0.34533	-0.35766	-0.07361	0.08
H10	-0.38132	-0.35296	0.04413	0.08
H11	-0.34192	-0.19235	0.12477	0.08
H13	-0.12276	0.21359	0.10272	0.08
H15a	-0.127290	0.52443	0.13252	0.08
H15b	-0.11236	0.40633	0.17977	0.08
H15c	-0.2064	0.44583	0.13525	0.08
H16a	-0.19522	0.4038	-0.0546	0.08
H16b	-0.17822	0.52277	-0.00837	0.08
H16c	-0.25625	0.44263	-0.00474	0.08
H17a	-0.02728	0.45839	0.05759	0.08
H17b	-0.04195	0.33658	0.01462	0.08
H17c	-0.01102	0.34089	0.10548	0.08
H18a	-0.10114	0.15618	-0.1486	0.08
H18b	-0.08369	0.1644	-0.05838	0.08
H18c	-0.17096	0.21134	-0.11335	0.08
H19a	-0.28215	-0.09034	-0.2038	0.08
H19b	-0.22622	-0.01003	-0.24194	0.08
H19c	-0.29855	0.04603	-0.21029	0.08
H20a	-0.064660	-0.10107	-0.13569	0.08
H20b	-0.11369	-0.18242	-0.09148	0.08
H20c	-0.04566	-0.09078	-0.04542	0.08
H21a	-0.07776	0.11823	0.20648	0.08
H21b	-0.06128	0.0559	0.28723	0.08
H21c	-0.14092	0.13996	0.25745	0.08
H22a	-0.05966	-0.17966	0.22133	0.08
H22b	-0.07223	-0.12558	0.13858	0.08
H22c	-0.13551	-0.22349	0.15141	0.08
H23a	-0.2563	-0.17154	0.24851	0.08
H23b	-0.25518	-0.04549	0.28462	0.08
H23c	-0.17553	-0.129550	0.3144	0.08
H24a	-0.43103	0.03618	0.09071	0.08
H24b	-0.47791	0.1284	0.02796	0.08
H24c	-0.48724	0.13625	0.11238	0.08
H25a	-0.29616	0.13132	0.23158	0.08
H25b	-0.37078	0.21877	0.23374	0.08
H25c	-0.2796	0.26768	0.23438	0.08
H26a	-0.42015	0.37045	0.03424	0.08
H26b	-0.35672	0.41621	0.11183	0.08
H26c	-0.4479	0.3673	0.11118	0.08

Table B-17: Bond Lengths (Å) and Angles (º) of the H atoms of compound 36.

1	2	3	1-2	1-2-3
H2	C2	C3	0.960(15)	120.1(14)
H2	C2	C1		120.0(11)
H3	C3	C4	0.96(2)	120.5(13)
H3	C3	C2		121.(2)
H4	C4	C5	0.960(14)	119.(2)
H4	C4	C3		120.(2)
H5	C5	C6	0.96(2)	119.3(15)
H5	C5	C4		119.1(14)
H6	C6	C1	0.960(13)	120.7(11)
H6	C6	C5		120.5(14)
H8	C8	C9	0.96(2)	118.5(14)
H8	C8	C7		118.6(14)
H9	C9	C10	0.960(14)	119.6(15)
H9	C9	C8		120.(2)
H10	C10	C11	0.96(2)	121.(2)
H10	C10	C9		120.6(15)
H11	C11	C12	0.96(2)	118.4(14)
H11	C11	C10		118.(2)
H13	C13	C14	0.960(11)	105.8(11)
H13	C13	W		105.8(10)
H15a	C15	H15b	0.960(15)	109.5(14)
H15a	C15	H15c		109.(2)
H15a	C15	C14		110.(2)
H15b	C15	H15c	0.960(15)	109.(2)
H15b	C15	C14		109.3(14)
H15c	C15	C14	0.96(2)	109.5(13)
H16a	C16	H16b	0.96(2)	109.(2)
H16a	C16	H16c		109.5(14)
H16a	C16	C14		109.4(14)
H16b	C16	H16c	0.96(2)	109.(2)
H16b	C16	C14		109.7(12)
H16c	C16	C14	0.96(2)	109.3(14)
H17a	C17	H17b	0.96(2)	109.(2)
H17a	C17	H17c		109.5(13)
H17a	C17	C14		109.8(14)
H17b	C17	H17c	0.96(2)	109.(2)
H17b	C17	C14		109.3(12)
H17c	C17	C14	0.960(14)	109.3(15)
H18a	C18	H18b	0.960(15)	109.5(14)
H18a	C18	H18c		109.5(13)
H18a	C18	Si2		109.5(11)
H18b	C18	H18c	0.960(11)	109.5(14)
H18b	C18	Si2		109.4(11)
H18c	C18	Si2	0.960(14)	109.5(11)

Table B-17 continued.

H19a	C19	H19b	0.960(14)	109.5(13)
H19a	C19	H19c		109.5(13)
H19a	C19	Si2		109.5(9)
H19b	C19	H19c	0.960(14)	109.5(13)
H19b	C19	Si2		109.4(9)
H19c	C19	Si2	0.960(14)	109.5(10)
H20a	C20	H20b	0.96(2)	109.(2)
H20a	C20	H20c		109.5(14)
H20a	C20	Si2		109.4(12)
H20b	C20	H20c	0.96(2)	109.(2)
H20b	C20	Si2		109.5(11)
H20c	C20	Si2	0.960(14)	109.4(13)
H21a	C21	H21b	0.96(2)	109.5(15)
H21a	C21	H21c		109.5(15)
H21a	C21	Si3		109.6(11)
H21b	C21	H21c	0.960(13)	109.5(14)
H21b	C21	Si3		109.4(12)
H21c	C21	Si3	0.96(2)	109.5(11)
H22a	C22	H22b	0.960(14)	109.(2)
H22a	C22	H22c		109.(2)
H22a	C22	Si3		109.5(14)
H22b	C22	H22c	0.96(2)	109.(2)
H22b	C22	Si3		109.5(13)
H22c	C22	Si3	0.96(2)	109.4(13)
H23a	C23	H23b	0.960(15)	109.5(15)
H23a	C23	H23c		109.5(15)
H23a	C23	Si3		109.5(11)
H23b	C23	H23c	0.96(2)	109.5(14)
H23b	C23	Si3		109.4(12)
H23c	C23	Si3	0.960(12)	109.4(12)
H24a	C24	H24b	0.960(14)	109.5(14)
H24a	C24	H24c		109.(2)
H24a	C24	P1		109.5(9)
H24b	C24	H24c	0.960(14)	109.5(12)
H24b	C24	P1		109.6(12)
H24c	C24	P1	0.96(2)	109.4(11)
H25a	C25	H25b	0.96(2)	109.(2)
H25a	C25	H25c		109.5(13)
H25a	C25	P1		109.4(11)
H25b	C25	H25c	0.96(2)	109.5(15)
H25b	C25	P1		109.4(9)
H25c	C25	P1	0.960(15)	109.6(12)
H26a	C26	H26b	0.960(13)	109.5(14)
H26a	C26	H26c		109.5(11)
H26a	C26	P1		109.6(11)
H26b	C26	H26c	0.960(13)	109.5(14)
H26b	C26	P1		109.4(9)
H26c	C26	P1	0.960(15)	109.5(11)

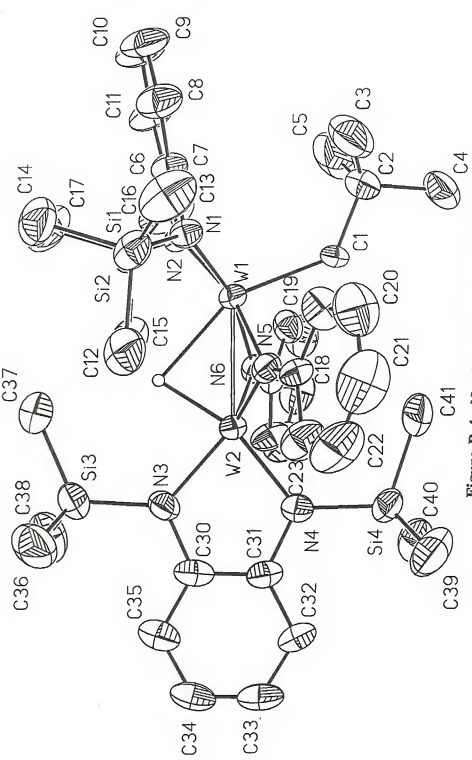

Figure B-4. Numbering scheme for **45**.

Crystallographic data for $\{[(Me_3SiN)_2C_6H_4]WH_2\}(\mu\text{-}H)(\mu\text{-}NPh)_2\{[(Me_3SiN)_2C_6H_4]W(CH_2CMe_3)\}$, **45**

Table B-18: Crystallographic data for **45**.

A. Crystal data (298 K)	**45**
a, Å	11.430 (1)
b, Å	11.640 (1)
c, Å	19.012 (2)
α, deg.	96.52 (1)
β, deg.	92.39 (1)
γ, deg.	104.44 (1)
V, Å^3	2427.2 (4)
d_{calc}, g cm^{-3}(298 K)	1.532
Empirical formula	$C_{41}H_{68}N_6Si_4W_2$
Formula wt, g	1125.07
Crystal system	Triclinic
Space group	P-1
Z	2
F(000), electrons	1120
Crystal size (mm^3)	0.34 x 0.30 x 0.25
B. Data collection (298 K)	
Radiation, λ (Å)	Mo-K_α, 0.71073
Mode	ω-scan
Scan range	Symmetrically over 1.2° about $K_{\alpha 1,2}$ maximum
Background	offset 1.0 and -1.0 in ω from $K_{\alpha 1,2}$ maximum
Scan rate, deg. min.$^{-1}$	3 – 6
2θ range, deg.	3 – 45
Range of *h k l*	$0 \leq h \leq 12$ $-12 \leq k \leq 12$ $-20 \leq l \leq 20$
Total reflections measured	7033
Unique reflections	6235
Absorption coeff. μ (Mo-K_α), cm^{-1}	4.84
Min. & Max. Transmission	0.365, 0.537
C. Structure refinement	
S, Goodness-of-fit	1.11
Reflections used, $I > 2\sigma(I)$	4878
No. of variables	482
R, wR* (%)	0.0293, 0.0328

Table B-18: Crystallographic data for **45**, continued

$R_{int.}$ (%)	0.0119
Max. shift/esd	0.0006
min. peak in diff. four. map (e $Å^{-3}$)	-0.993
max. peak in diff. four. map (e $Å^{-3}$)	1.631

* Relevant expressions are as follows, where in the footnote F_o and F_c represent, respectively, the observed and calculated structure-factor amplitudes.

Function minimized was $w(|F_o| - |F_c|)^2$, where $w = (\sigma(F))^{-2}$

$R = \sum(||F_o| - |F_c||) / \sum|F_o|$

$wR = [\sum w(|F_o| - |F_c|)^2 / \sum |F_o|^2]^{1/2}$

$S = [\sum w(|F_o| - |F_c|)^2 / (m-n)]^{1/2}$

Table B-19: Fractional coordinates and equivalent isotropic[a] thermal parameters ($Å^2$) for the non-H atoms of compound **45**.

Atom	x	y	z	U
W1	0.23216(3)	0.11989(2)	0.276090(10)	0.02849(12)
W2	0.31577(3)	0.28833(3)	0.20326(2)	0.03111(13)
Si1	0.2917(2)	0.2682(2)	0.44958(12)	0.0485(9)
Si2	0.4317(3)	-0.0668(3)	0.26414(13)	0.0583(11)
Si3	0.6162(2)	0.4336(2)	0.24674(14)	0.0563(10)
Si4	0.1192(2)	0.3415(3)	0.07887(13)	0.0547(10)
N1	0.2352(5)	0.1410(5)	0.3831(3)	0.035(2)
N2	0.3082(6)	-0.0138(5)	0.2968(3)	0.036(2)
N3	0.4762(6)	0.4110(6)	0.1965(3)	0.041(2)
N4	0.2633(6)	0.3718(6)	0.1238(3)	0.041(3)
N5	0.2759(5)	0.1199(5)	0.1713(3)	0.032(2)
N6	0.1935(5)	0.2825(5)	0.2693(3)	0.035(2)
C1	0.0445(6)	0.0298(7)	0.2408(4)	0.039(3)
C2	-0.0453(8)	-0.0796(8)	0.2632(5)	0.051(3)
C3	-0.0743(9)	-0.0540(11)	0.3389(5)	0.099(6)
C4	-0.1649(8)	-0.1021(8)	0.2160(5)	0.066(4)
C5	-0.0001(10)	-0.1893(9)	0.2519(8)	0.110(6)
C6	0.2320(7)	0.0299(7)	0.4101(4)	0.040(3)
C7	0.2721(7)	-0.0532(7)	0.3643(4)	0.040(3)
C8	0.2721(9)	-0.1637(8)	0.3854(5)	0.061(4)
C9	0.2320(10)	-0.1926(9)	0.4503(5)	0.073(5)
C10	0.1907(10)	-0.1117(9)	0.4940(5)	0.072(5)
C11	0.1911(9)	-0.0001(8)	0.4745(4)	0.059(4)
C12	0.5130(9)	0.0165(10)	0.1956(5)	0.075(5)
C13	0.3790(12)	-0.2252(9)	0.2240(6)	0.098(6)
C14	0.5455(10)	-0.0475(11)	0.3405(6)	0.100(6)
C15	0.3523(9)	0.4132(7)	0.4146(5)	0.066(4)
C16	0.1730(10)	0.2897(9)	0.5101(5)	0.081(5)
C17	0.4230(9)	0.2387(9)	0.4989(5)	0.077(4)
C18	0.1238(7)	0.3553(6)	0.2998(4)	0.035(3)
C19	0.0357(7)	0.3128(8)	0.3446(4)	0.049(3)
C20	-0.0338(9)	0.3842(9)	0.3763(5)	0.070(4)
C21	-0.0141(11)	0.5007(10)	0.3617(6)	0.085(6)
C22	0.0702(11)	0.5429(9)	0.3164(6)	0.079(5)
C23	0.1406(9)	0.4723(8)	0.2865(5)	0.060(4)
C24	0.2816(7)	0.0485(7)	0.1068(4)	0.035(3)
C25	0.2324(7)	-0.0735(7)	0.1008(4)	0.047(3)
C26	0.2420(9)	-0.1460(9)	0.0380(5)	0.070(4)
C27	0.3013(9)	-0.0945(10)	-0.0164(5)	0.071(5)
C28	0.3475(9)	0.0266(10)	-0.0109(5)	0.069(5)
C29	0.3375(8)	0.0980(8)	0.0506(4)	0.051(4)
C30	0.4707(8)	0.4899(7)	0.1442(4)	0.043(3)
C31	0.3588(7)	0.4683(7)	0.1047(4)	0.041(3)
C32	0.3462(8)	0.5419(7)	0.0537(4)	0.051(4)
C33	0.4433(10)	0.6314(8)	0.0403(5)	0.062(4)
C34	0.5504(9)	0.6531(8)	0.0781(5)	0.060(4)
C35	0.5655(8)	0.5835(7)	0.1294(5)	0.055(4)

Table B-19: continued.

C36	0.7328(9)	0.4112(11)	0.1852(6)	0.099(6)
C37	0.6209(9)	0.3282(10)	0.3131(6)	0.093(5)
C38	0.6523(10)	0.5835(9)	0.2994(5)	0.088(5)
C39	0.0529(9)	0.4724(10)	0.0954(5)	0.087(5)
C40	0.1251(9)	0.2961(9)	-0.0178(5)	0.076(5)
C41	0.0148(8)	0.2151(10)	0.1134(6)	0.093(5)

[a]For anisotropic atoms, the U value is U_{eq}, calculated as $U_{eq} = 1/3 \Sigma_i \Sigma_j U_{ij} a_i^* a_j^* A_{ij}$ where A_{ij} is the dot product of the i^{th} and j^{th} direct space unit cell vectors.

Table B-20: Bond Lengths (Å) and Angles (º) for the non-H atoms of compound 45.

1	2	3	1-2	1-2-3
W2	W1	H1	2.5430(5)	42.3(15)
W2	W1	N1		124.0(2)
W2	W1	N2		127.1(2)
W2	W1	N5		47.8(2)
W2	W1	N6		47.6(2)
H1	W1	N1	2.19(5)	95.5(13)
H1	W1	N2		96.(2)
H1	W1	N5		70.5(13)
H1	W1	N6		72.(2)
H1	W1	C1		153.4(15)
N1	W1	N2	2.019(6)	80.4(2)
N1	W1	N5		165.3(2)
N1	W1	N6		92.7(2)
N1	W1	C1		104.7(3)
N2	W1	N5	2.029(7)	96.0(2)
N2	W1	N6		165.6(2)
N2	W1	C1		104.6(3)
N5	W1	N6	2.075(6)	87.4(2)
N5	W1	C1		90.0(2)
N6	W1	C1	2.064(6)	89.4(3)
C1	W1	W2	2.179(6)	111.0(2)
H1	W2	N3	1.74(6)	80.(2)
H1	W2	N4		161.(2)
H1	W2	N5		84.(2)
H1	W2	N6		87.(2)
H1	W2	W1		58.(2)
N3	W2	N4	2.043(6)	81.4(2)
N3	W2	N5		127.5(3)
N3	W2	N6		131.8(2)
N3	W2	W1		137.9(2)
N4	W2	N5	2.034(7)	108.0(2)
N4	W2	N6		105.0(3)
N4	W2	W1		140.7(2)
N5	W2	N6	1.919(5)	96.6(2)
N5	W2	W1		53.2(2)
N6	W2	W1	1.912(6)	52.9(2)
N1	Si1	C15	1.799(6)	115.2(3)
N1	Si1	C16		111.4(4)
C15	Si1	C16	1.865(9)	107.2(5)
C15	Si1	C17		105.5(4)
C16	Si1	C17	1.860(11)	111.2(5)
C17	Si1	N1	1.861(11)	106.2(4)
N2	Si2	C12	1.783(7)	115.0(4)
N2	Si2	C13		110.6(5)
C12	Si2	C13	1.854(10)	106.4(5)
C12	Si2	C14		105.8(5)
C13	Si2	C14	1.853(10)	111.6(6)
C14	Si2	N2	1.863(11)	107.2(4)

Table B-20: continued.

N3	Si3	C36	1.773(7)	108.6(4)
N3	Si3	C37		116.2(4)
C36	Si3	C37	1.857(12)	104.5(6)
C36	Si3	C38		114.1(5)
C37	Si3	C38	1.865(12)	104.9(5)
C38	Si3	N3	1.850(10)	108.7(4)
N4	Si4	C39	1.758(7)	110.7(4)
N4	Si4	C40		111.2(4)
C39	Si4	C40	1.866(13)	111.6(5)
C39	Si4	C41		106.5(5)
C40	Si4	C41	1.862(9)	106.9(4)
C41	Si4	N4	1.852(11)	109.7(4)
W1	H1	W2		80.(2)
C6	N1		1.437(10)	
C7	N2	Si2	1.453(10)	113.3(5)
C30	N3		1.438(11)	
C31	N4	Si4	1.448(9)	118.6(6)
C24	N5		1.414(9)	
C18	N6		1.398(10)	
C3	C2	C4	1.504(13)	107.3(8)
C4	C2	C5	1.551(12)	107.9(7)
C5	C2	C3	1.489(15)	111.6(10)
C7	C6	C11	1.403(12)	119.6(8)
C7	C6	N1		114.7(7)
C11	C6	N1	1.380(12)	125.6(8)
C8	C7	N2	1.389(13)	126.0(7)
C8	C7	C6		119.2(7)
N2	C7	C6		114.8(7)
C9	C8	C7	1.382(14)	120.8(9)
C10	C9	C8	1.37(2)	119.5(10)
C11	C10	C9	1.390(15)	120.9(9)
C6	C11	C10		120.0(9)
C19	C18	C23	1.380(11)	117.5(8)
C19	C18	N6		121.1(7)
C23	C18	N6	1.380(12)	121.4(7)
C20	C19	C18	1.393(15)	122.0(8)
C21	C20	C19	1.38(2)	118.6(9)
C22	C21	C20	1.36(2)	120.0(12)
C23	C22	C21	1.38(2)	120.9(10)
C18	C23	C22		120.8(9)
C25	C24	C29	1.380(11)	119.4(7)
C25	C24	N5		119.3(7)
C29	C24	N5	1.377(11)	121.2(6)
C26	C25	C24	1.406(13)	119.8(8)
C27	C26	C25	1.373(14)	119.5(9)
C28	C27	C26	1.37(2)	120.6(9)
C29	C28	C27	1.382(13)	119.9(9)
C24	C29	C28		120.7(8)
C31	C30	C35	1.408(12)	118.3(8)
C31	C30	N3		115.8(6)
C35	C30	N3	1.394(11)	126.0(8)
C32	C31	N4	1.390(12)	125.3(7)

Table B-20: continued.

C32	C31	C30		119.1(7)
N4	C31	C30		115.5(7)
C33	C32	C31	1.375(12)	120.2(8)
C34	C33	C32	1.345(14)	121.0(9)
C35	C34	C33	1.369(14)	120.2(8)
C30	C35	C34		121.1(8)

Table B-21: Anisotropic thermal parameters[a] for the non-H atoms of compound **45**.

Atom	U11	U22	U33	U12	U13	U23
W1	0.0342(2)	0.0276(2)	0.0243(2)	0.0076(2)	0.0029(2)	0.00628(14
W2	0.0329(2)	0.0308(2)	0.0292(2)	0.0049(2)	0.0017(2)	0.0094(2)
Si1	0.067(2)	0.0446(14)	0.0317(13)	0.0152(13)	-0.0072(12)	-0.0039(11)
Si2	0.069(2)	0.078(2)	0.0453(15)	0.047(2)	0.0119(13)	0.0162(13)
Si3	0.0396(14)	0.063(2)	0.058(2)	-0.0024(12)	-0.0028(12)	0.0127(13)
Si4	0.0430(14)	0.079(2)	0.0471(15)	0.0159(13)	-0.0014(12)	0.0320(14)
N1	0.043(4)	0.032(4)	0.030(3)	0.011(3)	0.005(3)	0.004(3)
N2	0.046(4)	0.038(4)	0.029(3)	0.018(3)	0.005(3)	0.009(3)
N3	0.036(4)	0.042(4)	0.040(4)	-0.000(3)	0.006(3)	0.009(3)
N4	0.041(4)	0.043(4)	0.039(4)	0.007(3)	0.008(3)	0.014(3)
N5	0.032(3)	0.031(3)	0.034(4)	0.010(3)	-0.002(3)	0.004(3)
N6	0.040(4)	0.030(3)	0.035(4)	0.008(3)	-0.005(3)	0.005(3)
C1	0.032(4)	0.043(5)	0.037(5)	-0.004(4)	0.002(4)	0.021(4)
C2	0.044(5)	0.047(5)	0.061(6)	0.002(4)	0.007(4)	0.018(4)
C3	0.062(7)	0.149(12)	0.060(7)	-0.026(7)	0.007(6)	0.026(7)
C4	0.045(6)	0.064(6)	0.073(7)	-0.014(5)	-0.003(5)	0.009(5)
C5	0.067(8)	0.056(7)	0.197(15)	-0.013(6)	-0.014(9)	0.042(8)
C6	0.055(5)	0.040(5)	0.028(4)	0.013(4)	0.009(4)	0.007(4)
C7	0.045(5)	0.047(5)	0.032(4)	0.011(4)	-0.007(4)	0.019(4)
C8	0.096(8)	0.049(6)	0.050(6)	0.036(5)	0.011(5)	0.021(5)
C9	0.118(9)	0.047(6)	0.063(7)	0.028(6)	0.008(6)	0.031(5)
C10	0.100(8)	0.075(7)	0.044(6)	0.017(6)	0.015(6)	0.032(6)
C11	0.088(7)	0.051(6)	0.036(5)	0.014(5)	0.010(5)	0.008(4)
C12	0.069(7)	0.114(9)	0.060(6)	0.054(7)	0.017(5)	0.020(6)
C13	0.169(13)	0.073(8)	0.080(8)	0.078(8)	0.026(8)	0.015(6)
C14	0.087(8)	0.160(12)	0.079(8)	0.066(8)	0.009(7)	0.050(8)
C15	0.082(7)	0.052(6)	0.053(6)	0.006(5)	-0.020(5)	-0.009(5)
C16	0.127(10)	0.075(7)	0.049(6)	0.047(7)	0.008(6)	-0.001(5)
C17	0.084(8)	0.071(7)	0.064(7)	0.006(6)	-0.032(6)	0.004(5)
C18	0.043(5)	0.030(4)	0.036(5)	0.013(4)	0.004(4)	0.011(4)
C19	0.050(5)	0.046(5)	0.053(5)	0.018(4)	0.012(5)	-0.005(4)
C20	0.058(6)	0.080(8)	0.073(7)	0.025(6)	0.013(5)	-0.002(6)
C21	0.093(9)	0.087(9)	0.093(9)	0.065(8)	0.010(7)	-0.009(7)
C22	0.109(10)	0.055(7)	0.089(8)	0.051(7)	-0.002(7)	0.008(6)
C23	0.081(7)	0.045(6)	0.060(6)	0.026(5)	-0.002(5)	0.007(5)
C24	0.036(4)	0.036(5)	0.035(5)	0.013(4)	-0.001(4)	-0.003(4)
C25	0.042(5)	0.055(6)	0.040(5)	0.006(4)	0.003(4)	0.001(4)
C26	0.072(7)	0.057(6)	0.070(7)	0.012(5)	-0.012(6)	-0.014(6)
C27	0.084(8)	0.093(9)	0.037(6)	0.034(7)	-0.001(5)	-0.012(6)
C28	0.090(8)	0.091(8)	0.039(6)	0.047(7)	0.022(5)	0.004(5)
C29	0.073(6)	0.061(6)	0.029(5)	0.029(5)	0.022(4)	0.018(4)
C30	0.053(6)	0.032(5)	0.051(5)	0.015(4)	0.025(5)	0.013(4)
C31	0.050(5)	0.039(5)	0.042(5)	0.019(4)	0.016(4)	0.016(4)
C32	0.068(6)	0.045(5)	0.047(5)	0.021(5)	0.003(5)	0.021(4)
C33	0.085(8)	0.051(6)	0.054(6)	0.012(6)	0.021(6)	0.029(5)
C34	0.067(7)	0.051(6)	0.061(6)	0.001(5)	0.029(6)	0.022(5)
C35	0.060(6)	0.043(5)	0.058(6)	0.000(5)	0.017(5)	0.010(5)
C36	0.052(7)	0.123(10)	0.121(11)	0.020(7)	0.005(7)	0.021(8)

Table B-21: continued.

C37	0.060(7)	0.111(9)	0.106(9)	0.003(6)	-0.025(6)	0.053(8)
C38	0.092(8)	0.079(8)	0.068(7)	-0.022(6)	-0.012(6)	0.005(6)
C39	0.079(8)	0.137(10)	0.070(7)	0.058(7)	0.012(6)	0.048(7)
C40	0.069(7)	0.095(8)	0.061(7)	0.018(6)	-0.017(5)	0.013(6)
C41	0.051(6)	0.138(11)	0.084(8)	-0.001(6)	-0.025(6)	0.054(8)

[a] Uij are the mean-square amplitudes of vibration in $Å^2$ from the general temperature factor expressic

$exp[-2\pi^2(h^2a^{*2}U11 + k^2b^{*2}U22 + l^2c^{*2}U33 + 2hka^*b^*U12 + 2hla^*c^*U13 + 2klb^*c^*U23)]$

Table B-22: Fractional coordinates and isotropic-thermal parameters ($Å^2$) for the H atoms of compound **45**.

Atom	x	y	z	U
H1	0.404(5)	0.253(5)	0.270(3)	0.011(14)
H1a	0.04745	0.00848	0.1907	0.08
H1b	0.00337	0.0922	0.24846	0.08
H3a	-0.00196	-0.03966	0.36964	0.08
H3b	-0.1336	-0.12142	0.35135	0.08
H3c	-0.10576	0.01536	0.34398	0.08
H4a	-0.19577	-0.032390	0.22229	0.08
H4b	-0.22332	-0.16926	0.22938	0.08
H4c	-0.14943	-0.11847	0.16711	0.08
H5a	0.07397	-0.17747	0.28063	0.08
H5b	0.01432	-0.20514	0.20278	0.08
H5c	-0.05958	-0.25592	0.26504	0.08
H8	0.30009	-0.22066	0.35439	0.08
H9	0.23332	-0.26875	0.46464	0.08
H10	0.16127	-0.13233	0.53861	0.08
H11	0.16265	0.05609	0.50585	0.08
H12a	0.4583	0.00964	0.15475	0.08
H12b	0.57922	-0.01627	0.18224	0.08
H12c	0.54353	0.09928	0.21444	0.08
H13a	0.33616	-0.27209	0.25773	0.08
H13b	0.44759	-0.25452	0.21104	0.08
H13c	0.3261	-0.23108	0.18246	0.08
H14a	0.61348	-0.07528	0.32471	0.08
H14b	0.50937	-0.09287	0.3767	0.08
H14c	0.57217	0.03559	0.35928	0.08
H15a	0.28831	0.43343	0.38841	0.08
H15b	0.4154	0.40581	0.38393	0.08
H15c	0.38447	0.47481	0.45347	0.08
H16a	0.1397	0.21655	0.52911	0.08
H16b	0.10986	0.31189	0.48418	0.08
H16c	0.20825	0.35188	0.54816	0.08
H17a	0.45662	0.30448	0.53524	0.08
H17b	0.48355	0.2299	0.46668	0.08
H17c	0.39661	0.16662	0.520260	0.08
H19	0.02177	0.23153	0.3543	0.08
H20	-0.09417	0.35316	0.40767	0.08
H21	-0.06001	0.55191	0.38354	0.08
H22	0.0811	0.62294	0.30494	0.08
H23	0.20209	0.50492	0.256180	0.08
H25	0.19178	-0.10875	0.13925	0.08
H26	0.20735	-0.23083	0.03316	0.08
H27	0.31052	-0.14399	-0.05873	0.08
H28	0.38671	0.06209	-0.04978	0.08
H29	0.37004	0.18302	0.05424	0.08
H32	0.26931	0.53024	0.02782	0.08
H33	0.43462	0.67914	0.00339	0.08
H34	0.61651	0.7177	0.06909	0.08

Table B-22: continued.

H35	0.64259	0.59926	0.15572	0.08
H36a	0.73586	0.46294	0.14901	0.08
H36b	0.71233	0.32944	0.16349	0.08
H36c	0.81035	0.4295	0.21114	0.08
H37a	0.70114	0.34614	0.33573	0.08
H37b	0.59956	0.24763	0.28949	0.08
H37c	0.56448	0.33664	0.34809	0.08
H38a	0.65146	0.6428	0.26831	0.08
H38b	0.7312	0.59958	0.32359	0.08
H38c	0.59311	0.58575	0.33351	0.08
H39a	0.10425	0.5405	0.07826	0.08
H39b	0.04634	0.49015	0.14539	0.08
H39c	-0.02609	0.45386	0.07097	0.08
H40a	0.17851	0.35955	-0.03775	0.08
H40b	0.04535	0.27976	-0.04094	0.08
H40c	0.15442	0.22545	-0.02445	0.08
H41b	-0.063710	0.19883	0.08873	0.08
H41c	0.00847	0.23537	0.16321	0.08
H41D	0.04561	0.14539	0.10611	0.08

Table B-23: Bond Lengths (Å) and Angles (º) of the H atoms of compound **45**.

1	2	3	1-2	1-2-3
H1a	C1	H1b	0.960(7)	109.5(8)
H3a	C3	H3b	0.960(10)	109.5(11)
H3a	C3	H3c		109.5(10)
H3a	C3	C2		109.5(9)
H3b	C3	H3c	0.960(11)	109.5(11)
H3b	C3	C2		109.5(9)
H3c	C3	C2	0.960(13)	109.4(10)
H4a	C4	H4b	0.960(10)	109.5(9)
H4a	C4	H4c		109.5(10)
H4a	C4	C2		109.5(7)
H4b	C4	H4c	0.960(8)	109.5(8)
H4b	C4	C2		109.5(9)
H4c	C4	C2	0.960(9)	109.4(8)
H5a	C5	H5b	0.960(12)	109.5(12)
H5a	C5	H5c		109.5(13)
H5a	C5	C2		109.4(9)
H5b	C5	H5c	0.960(14)	109.5(10)
H5b	C5	C2		109.6(11)
H5c	C5	C2	0.960(10)	109.4(10)
H8	C8	C9	0.960(10)	119.6(9)
H8	C8	C7		119.6(9)
H9	C9	C10	0.960(11)	120.3(10)
H9	C9	C8		120.2(10)
H10	C10	C11	0.960(10)	119.5(10)
H10	C10	C9		119.6(11)
H11	C11	C6	0.960(9)	120.0(9)
H11	C11	C10		120.0(9)
H12a	C12	H12b	0.960(10)	109.5(9)
H12a	C12	H12c		109.5(11)
H12a	C12	Si2		109.5(7)
H12b	C12	H12c	0.960(11)	109.5(9)
H12b	C12	Si2		109.4(9)
H12c	C12	Si2	0.960(10)	109.5(7)
H13a	C13	H13b	0.960(11)	109.5(12)
H13a	C13	H13c		109.5(11)
H13a	C13	Si2		109.4(8)
H13b	C13	H13c	0.960(14)	109.5(11)
H13b	C13	Si2		109.5(8)
H13c	C13	Si2	0.960(12)	109.5(9)
H14a	C14	H14b	0.960(13)	109.5(13)
H14a	C14	H14c		109.5(10)
H14a	C14	Si2		109.4(8)
H14b	C14	H14c	0.960(11)	109.5(10)
H14b	C14	Si2		109.5(8)
H14c	C14	Si2	0.960(12)	109.5(10)
H15a	C15	H15b	0.960(10)	109.5(9)
H15a	C15	H15c		109.5(9)
H15b	C15	H15c	0.960(10)	109.5(9)

Table B-23: continued.

H16a	C16	H16b	0.960(10)	109.5(10)
H16a	C16	H16c		109.5(9)
H16b	C16	H16c	0.960(12)	109.5(11)
H17a	C17	H17b	0.960(9)	109.5(9)
H17a	C17	H17c		109.5(9)
H17b	C17	H17c	0.960(10)	109.5(11)
H19	C19	C20	0.960(9)	119.0(8)
H19	C19	C18		119.0(9)
H20	C20	C21	0.960(10)	120.6(11)
H20	C20	C19		120.7(10)
H21	C21	C22	0.960(13)	119.9(12)
H21	C21	C20		120.0(11)
H22	C22	C23	0.960(11)	119.5(11)
H22	C22	C21		119.6(13)
H23	C23	C18	0.960(9)	119.6(10)
H23	C23	C22		119.6(9)
H25	C25	C26	0.960(8)	120.1(8)
H25	C25	C24		120.1(8)
H26	C26	C27	0.960(10)	120.3(10)
H26	C26	C25		120.3(10)
H27	C27	C28	0.960(10)	119.7(10)
H27	C27	C26		119.7(10)
H28	C28	C29	0.960(10)	120.1(10)
H28	C28	C27		120.0(10)
H29	C29	C24	0.960(9)	119.7(8)
H29	C29	C28		119.6(8)
H32	C32	C33	0.960(9)	119.9(9)
H32	C32	C31		119.9(8)
H33	C33	C34	0.960(10)	119.5(9)
H33	C33	C32		119.5(10)
H34	C34	C35	0.960(9)	119.9(10)
H34	C34	C33		119.9(10)
H35	C35	C30	0.960(9)	119.4(9)
H35	C35	C34		119.5(8)
H36a	C36	H36b	0.960(13)	109.5(11)
H36a	C36	H36c		109.5(10)
H36b	C36	H36c	0.960(12)	109.5(13)
H37a	C37	H37b	0.960(10)	109.5(12)
H37a	C37	H37c		109.5(11)
H37b	C37	H37c	0.960(11)	109.5(10)
H38a	C38	H38b	0.960(11)	109.5(9)
H38a	C38	H38c		109.5(12)
H38b	C38	H38c	0.960(11)	109.5(10)
H39a	C39	H39b	0.960(11)	109.5(10)
H39a	C39	H39c		109.5(12)
H39a	C39	Si4		109.5(9)
H39b	C39	H39c	0.960(10)	109.5(11)
H39b	C39	Si4		109.5(9)
H39c	C39	Si4	0.960(10)	109.5(8)

Table B-23: continued.

H40a	C40	H40b	0.960(10)	109.5(10)
H40a	C40	H40c		109.5(10)
H40a	C40	Si4		109.5(7)
H40b	C40	H40c	0.960(10)	109.5(9)
H40b	C40	Si4		109.5(8)
H40c	C40	Si4	0.960(12)	109.5(8)
H41b	C41	H41c	0.960(10)	109.5(10)
H41b	C41	H41D		109.5(10)
H41b	C41	Si4		109.5(9)
H41c	C41	H41D	0.960(11)	109.5(12)
H41c	C41	Si4		109.5(7)
H41D	C41	Si4	0.960(12)	109.4(8)

REFERENCES

1. a) Nugent, W. A.; Mayer, J. M. *Metal-Ligand Multiple Bonds*; John Wiley & Sons: New York, 1988. b) Wigley, D. E. *Prog. Inorg. Chem.* **1994**, *42*, 239.

2. a) Collman, J. P.; Hegadus, L. S.; Norton, J. R.; Finke, R. G. *Principles and Applications of Organotransition Metal Chemistry*; 2 ed.; University Science Books: Mill Valley, LA. 1987. b) Yamamoto, A. *Organotransition Metal Chemitry*; John Wiley & Sons: New York, 1986.

3. Kress, J.; Wesolek, M.; Le Ny, J. P.; Osborn, J. A. *J. Chem. Soc., Chem. Commun.* **1981**, 1039.

4. Herrmann, W. A.; Felixberger, J. K.; Herdweck, E.; Schafer. A.; Okuda, J. *Angew. Chem., Int. Ed. Engl.* **1987**, *26*, 466.

5. a) Herrmann, W. A. *J. Organomet. Chem.* **1986**, *300*, 111. b) Bokiy, N. G.; Gatilov, Yu. V.; Struchov, Yu. T.; Ustynyuk, N. A. *J. Organomet. Chem.* **1973**, *54*, 213.

6. a) Chatt, J.; Rowe, G. A. *J. Chem. Soc.* **1962**, 4019. b) Nugent, W. A.; Dilworth, B. L. *Coord. Chem. Rev.* **1980**, *31*, 123. c) Hursthouse, M. B.; Motevalli, M.; Sullivan, A. C.; Wilkinson, G. *J. Chem. Soc., Chem. Commun.* **1986**, 1398.

7. a) Chatt, J.; Garforth, J. D.; Rowe, G. A. *Chem. Ind.* **1963**, 332. b) Griffith, W. P.; *Coord. Chem. Rev.* **1972**, *8*, 369. c) Chatt, J.; Garforth, J. D.; Rowe, G. A. *J. Chem. Soc., A* **1966**, 1834.

8. a) Schrock, R. R. *Reactions of Coordinated Ligands*; P. S. Braterman, Ed., Plenum, New York, 1986. b) Feldman, J.; Schrock, R. R. *Prog. Inorg. Chem.* **1991**, *39*, 1.

9. a) Carter, E.; Goddard III, W. A. *J. Am. Chem. Soc.* **1986**, *108*, 4746. b) Cundari, T. R.; Gordon, M. S. *J. Am. Chem. Soc.* **1991**, *113*, 5231. c) Fox, H. F.; Schrock, R. R. *Organometallics* **1994**, *33*, 2804. d) Gibson, V. C. *Angewandte Chem., Int. Ed. Engl.* **1994**, *33*, 1565.

10. Ivin, K. J. *Olefin Metathesis*; Academic Press: New York, 1982.

11. a) Dragutan, V.; Balaban, A. T.; Dimonie, M. *Olefin Metathesis and Ring-Opening Polymerizations of Cyclo-Olefins*; 2 ed.; Wiley-Interscience: Bucharest, 1985. b) Odian, G. G. *Principles of Polymerizations*; John Wiley & Sons: New York, 1981.

12. Herrison, J. L.; Chauvin, Y. *Makromol. Chem.* **1970**, *141*, 161.

13. Schrock, R. R. *J. Am. Chem. Soc.* **1974**, *96*, 6796.

14. a) Schrock, R. R.; DePue, R. T.; Feldman, J.; Yap, K. B.; Yang, D. C.; Davis, W. M.; Park, L.; DiMare, M.; Schofield, M.; Anhaus, J.; Walborsky, E.; Evitt, E.; Kruger, C.; Betz, P. *Organometallics* **1990**, *9*, 2262.

15. a) Freudenberger, J. H.; Schrock, R. R. *Organometallics* **1985**, *4*, 1937. b) Aguero, A.; Kress, J.; Osborn, J. A. *J. Chem. Soc., Chem. Commun.* **1985**, 793. c) Kress, J.; Osborn, J. A. *J. Am. Chem. Soc.* **1987**, *109*, 3953.

16. a) Legzdins, P.; Rettig, J. J.; Sanchez, L. *Organometallics* **1985**, *4*, 1471. b) Legzdins, P.; Phillips, E.; Sanchez, L. *Organometallics* **1989**, *8*, 940. c) Bryan, J. C.; Mayer, J. M. *J. Am. Chem. Soc.* **1987**, *109*, 7213. d) Bryan, J. C.; Mayer, J. M. *J. Am. Chem. Soc.* **1990**, *112*, 2298.

17. a) Schrock, R. R.; Krouse, S. A.; Knoll, K.; Feldman, J.; Murdzek, J. S.; Yang, D. C. *J. Mol. Cat.* **1988**, *46*, 243. b) Oskam, J. H.; Schrock, R. R. *J. Am. Chem. Soc.* **1993**, *115*, 11831. c) Schrock, R. R.; Murdzek, J. S.; Bazan, G. C.; Robbins, J.; DiMare, M.; O'Regan, M. *J. Am. Chem. Soc.* **1990**, *112*, 3875. d) Bazan, G. C.; Oskam, J. H.; Cho, H. N.; Park, L. Y.; Schrock, R. R. *J. Am. Chem. Soc.* **1991**, *113*, 6899. e) Wallace, K. C.; Schrock, R. R. *Macromolecules* **1987**, *20*, 450. f) Schrock, R. R.; Feldman, J.; Cannizzo, L. F.; Grubbs, R. H. *Macromolecules* **1987**, *20*, 1172. g) Nguyen, S. T.; Johnson, L. K.; Grubbs, R. H. *J. Am. Chem. Soc.* **1992**, *114*, 3974.

18. a) Wagener, K. B.; Boncella, J. M.; Nel, J. G. *Macromolecules* **1991**, *24*, 2649. b) Wagener, K. B.; Brzezinska, K. *Macromolecules* **1991**, *24*, 5273. c) Wagener, K. B.; Brzezinska, K.; Bauch, C. G. *Makromol. Chem., Rapid Commun.* **1992**, *13*, 75. d) Brzezinska, K.; Wagener, K. B. *Macromolecules* **1992**, *25*, 2049. e) O'Gara, J. E.; Portmess, J. D.; Wagener, K. B. *Macromolecules* **1993**, *26*, 2837. f) Patton, J. T.; Boncella, J. M.; Wagener, K. B. *Macromolecules* **1992**, *25*, 3862. g) Smith, D. W., Jr.; Wagener, K. B. *Macromolecules* **1993**, *26*, 1633.

19. a) Viswanathan, T.; Gomez, F.; Wagener, K. B. *Polym. Prep. (Am. Chem. Soc., Div. Polm. Chem.)* **1993**, *34(1)*, 465. b) Wagener, K. B.; Puts, R. D.; Smith, D. W., Jr.; *Makromol. Chem., Rapid Commun.* **1991**, *12*, 419.

20. Blosch, L. L. Ph.D. dissertation, University of Florida, 1993.

21. McConville, D. H.; Wolf, J. R.; Schrock, R. R. *J. Am. Chem. Soc.* **1993**, *115*, 4413.

22. Johnson, L. K.; Virgil, S. C.; Grubbs, R. H. *J. Am. Chem. Soc.* **1990**, *112*, 5384.

23. a) van der Schaaf, P. A.; Abbenhuis, R. A. T. M.; van der Noort, W. P. A.; deGraf, R.; Grove, D. M.; Smeets, W. J. J.; Spek, A. J.; van koten, G. *Organometallics* **1994**, *13*, 1433. b) van der Schaaf, P. A.; Grove, D. M.; Smeets, W. J. J.; Spek, A. J.; van koten, G. *Organometallics* **1993**, *12*, 3955. c) van der Schaaf, P. A.; Smeets, W. J. J.; Spek, A. J.; van Koten, G. *J. Chem. Soc., Chem. Commun.* **1992**, 717.

24. a) Blosch, L. L.; Abboud, K. A.; Boncella, J. M. *J. Am. Chem. Soc.* **1991**, *113*, 7076. b) Gamble, A. S.; Boncella, J. M.; *Organometallics* **1993**, *12*, 2814. c)

Blosch, L. L.; Gamble, A. S.; Abboud, K. A.; Boncella, J. M. *Organometallics* **1992**, *11*, 2342. d) Blosch, L. L.; Gamble, A. S.; Boncella, J. M. *J. Mol. Cat.* **1992**, *76*, 229. e) Vaughan, W. M.; Abboud, K. A.; Boncella, J. M. *J. Organomet. Chem.* in press. f) Vaughan, W. M.; Abboud, K. A.; Boncella, J. M. *Organometallics* submitted.

25. a) Cummins, C. C.; Schrock, R. R.; Davis, W. M. *Organometallics* **1992**, *11*, 1452. b) Cummins, C. C.; Lee, J.; Schrock, R. R.; Davis, W. M. *Angew. Chem., Int. Ed. Engl.* **1992**, *31*, 1501.

26. Cummins, C. C.; Schrock, R. R.; Davis, W. M. *Angew. Chem., Int. Ed. Engl.* **1993**, *32*, 756.

27. Verkade, J. G. *Acc. Chem. Res.* **1993**, *26*, 483.

28. a) Gade, L. H.; Mahr, N *J. Chem. Soc., Dalton Trans.* **1993**, 489. (b) Friedrich, S.; Gade, L. H.; Edwards, A. J.; McPartlin, M. *Chem. Ber.* **1993**, *126*, 1797.

29. a) Redshaw, C.; Wilkinson, G.; Hussain-Bates, B.; Hursthouse, M. B. *J. Chem. Soc., Dalton Trans.* **1992**, 555. b) Redshaw, C.; Wilkinson, G.; Sweet, T. K. N.; Hursthouse, M. B. *Polyhedron* **1993**, *12*, 2013. c) Redshaw, C.; Wilkinson, G.; Sweet, T. K. N.; Hursthouse, M. B. *Polyhedron* **1993**, *12*, 2417.

30. a) VanderLende, D. D.; Abboud, K. A.; Boncella, J. M. *Organometallics* **1994**, *13*, 3378. b) VanderLende, D. D.; Boncella, J. M. *Polym. Prep. (Am. Chem. Soc., Div. Polm. Chem.)* **1994**, 35(1), 691.

31. Cheeseman, G. W. H. *J. Chem. Soc.* **1955**, 3308.

32. Cheng, P.; Cheng, H.; Lin, C.; Peng, S. *Inorg. Chim. Acta* **1990**, *169*, 19.

33. Birkofer, L.; Kuhlthau, H. P.; Ritter, A. *Chem. Ber.* **1960**, *93*, 2810.

34. Stewart, H. F.; Koepsell, D. G.; West, R. *J. Am. Chem. Soc.* **1970**, *92*, 846.

35. Duff, A. W.; Hitchcock, P. B.; Lappert, M. F.; Taylor, R. G.; Segal, J. A. *J. Organomet. Chem.* **1985**, *293*, 271.

36. Liang, M.; Maatta, E. A. *Inorg. Chem.* **1992**, *31*, 953.

37. a) Redshaw, C.; Wilkinson, G.; Hussain-Bates, B.; Hursthouse, M. B. *J. Chem. Soc., Dalton Trans.* **1992**, 1803. b) Danopoulos, A. A.; Wong, A. C. C.; Wilkinson, G.; Hursthouse, M. B.; Hussain, B. . *Chem. Soc., Dalton Trans.* **1990**, 315.

38. Anillo, A; Obeso-Rosete, R.; Lafranchi, M.; Tiripicchio, A. *J. Organomet. Chem.* **1993**, *453*, 71.

39. Berg, F. J.; Peterson, J. L. *Organometallics* **1991**, *11*, 1599.

40. a) Chamberlain, L. R.; Durfee, L. D.; Fanwick, P. E.; Kobriger, L. M.; Latesky, S. L.; McMullen, A. K.; Steffey, B. D.; Rothwell, I. P.; Folting, K.; Huffman, J. C. *J. Am. Chem. Soc.* **1987**, *109*, 6068. b) McMullen, A. K.; Rothwell, I. P.; Huffman, J. C. *J. Am. Chem. Soc.* **1985**, *107*, 1072. c) Latesky, S. L.;

McMullen, A. K.; Niccolai, G. P.; Rothwell, I. P.; Huffman, J. C. *Organometallics* **1985**, *4*, 1986.

41. Bristow, G. S.; Lappert, M. F.; Martin, T. R.; Atwood, J. L.; Hunter, W. F. *J. Chem. Soc., Dalton Trans.* **1984**, 399.

42. a) Schrock, R. R.; Parshall, G. W. *Chem. Rev.* **1976**, *76*, 243. b) Davidson, P. J.; Lappert, M. F.; Pearce, R. *Chem. Rev.* **1976**, *76*, 219.

43. a) Kress, J.; Wesolek, M.; LeNy, J.; Osborn, J. A. *J. Chem. Soc., Chem. Commun.* **1981**, 1039. b) Bradley, D. C.; Hursthouse, M. B.; Malik, K. M. A.; Nielson, A. J. *J. Chem. Soc., Chem. Commun.* **1981**, 103. c) Chiu, K. W.; Jones, R. A.; Wilkinson, G.; Galas, A. M. R.; Hursthouse, M. B. *J. Am. Chem. Soc.* **1980**, *102*, 7978. d) Nugent, W. A.; Harlow, R. L. *J. Am. Chem. Soc.* **1980**, *102*, 1759. e) Glassman, T. E.; Vale, M. G.; Schrock, R. R. *Organometallics* **1991**, *10*, 4046.

44. Pederson, S. F.; Schrock, R. R. *J. Am. Chem. Soc.* **1982**, *104*, 7483.

45. Zhang, C.; Schlemper, E. O.; Schrauzer, G. N. *Organometallics* **1990**, *9*, 1016.

46. a) Bryan, J. C.; Mayer, J. M. *J. Am. Chem. Soc.* **1990**, *112*, 2298. b) Gagne, M. R.; Grubbs, R. H.; Feldman, J.; Ziller, J. W. *Organometallics* **1992**, *11*, 3933. c) van Asselt, A.; Burger, B. J.; Gibson, V. C.; Bercaw, J. E. *J. Am. Chem. Soc.* **1986**, *108*, 5347.

47. Brookhart, M.; Green, M. L. H. *J. Organomet. Chem.* **1983**, *230*, 395.

48. a) Schrock, R. R.; DePue, R. T.; Feldman, J.; Schaverien, C. J.; Dewn, J. C.; Liu, A. H. *J. Am. Chem. Soc.* **1988**, *110*, 1423. b) Feldman, J.; Schrock, R. R.; *Organometallics* **1989**, *8*, 2266.

49. a) Bruno, J. W.; Smith, G. M.; Marks, T. J.; Fair, C. K.; Schultz, A. J.; Williams, J. M. *J. Am. Chem. Soc.* **1986**, *108*, 40. b) Fendrick, C. M.; Marks, T. J. *J. Am. Chem. Soc.* **1986**, *108*, 425.

50. a) Latesky, S. L.; McMullen, A. K.; Rothwell, I. P.; Huffman, J. C. *J. Am. Chem. Soc.* **1985**, *107*, 5981. b) Chamberlain, L.; Rothwell, I. P.; Huffman, J. C. *J. Am. Chem. Soc.* **1982**, *104*, 7338. c) Chamberlain, L.; Rothwell, I. P. *J. Am. Chem. Soc.* **1982**, *104*, 7338.

51. Parshall, G. W. *Acc. Chem. Res.* **1970**, *3*, 139.

52. Schrock, R. R.; Crowe, W. E.; Bazan, G. C.; Dimare, M.; O'Regan, M. B.; Schofield, M. H. *Organometallics* **1991**, *10*, 1832.

53. Johnson, L. K.; Grubbs, R. H.; Ziller, J. W. *J. Am. Chem. Soc.* **1993**, *115*, 8130.

54. Schrock, R. R. *J. Organomet. Chem.* **1976**, *122*, 209.

55. a) Wood, C. D.; McLain, S. J.; Schrock, R. R. *J. Am. Chem. Soc.* **1979**, *101*, 3210. b) Mayr, A.; Lee, K. S.; Kjelsberg, M. A.; Van Engen, D. *J. Am. Chem. Soc.* **1986**, *108*, 6079. c) Strutz, H.; Dewan, J. C.; Scrock, R. R. *J. Am. Chem.*

Soc. **1985**, *107*, 5999. d) Pederson, S. F.; Schrock, R. R.; Churchill, M. R.; Wasserman, H. J. *J. Am. Chem. Soc.* **1982**, *104*, 6808.

56. Wu, Z.; Wheeler, D. R.; Grubbs, R. H. **J. Am. Chem. Soc. 1992**, *114*, 146.

57. Gold, L. *J. Chem. Phys.* **1958**, *28*, 91.

58. Bazan, G. C.; Khosravi, E.; Schrock, R. R.; Feast, W. J.; Gibson, V. C.; O'Regan, M. B.; Thomas, J. K.; Davis, W. M. *J. Am. Chem. Soc.* **1990**, *112*, 8378.

59. Feldman, J.; Davis, W. M.; Thomas, J. K.; Schrock, R. R.; *Organometallics* **1990**, *9*, 2535.

60. a) Marmo, J. C.; Wagener, K. B. *Macromolecules* **1993**, *26*, 2137. b) Marmo, J. C.; Wagener, K. B. *Macromolecules* in press.

61. a) Crabtree, R. H. *Comprehensive Coordination Chemistry*, Wilkinson, G.; Gillard, R.; McCleverty, J. A. Eds.; Pergamon Press: New York, 1987; Chapter 19, Vol. 2. b) Hlatky, G. C.; Crabtree, R. H. *Coord. Chem. Rev.* **1985**, *65*,1. c) Pearson, R. G. *Chem. Rev.* **1985**, *85*, 41. d) Moore, D. S.; Robinson, S. D. *Chem. Soc. Rev.* **1983**, 415.

62. Conner, K. A.; Walton, R. A. *Comprehensive Coordination Chemistry*, Wilkinson, G.; Gillard, R.; McCleverty, J. A. Eds.; Pergamon Press: New York, 1987; Chapter 43, Vol. 4.

63. a) *Transition Metal Hydrides;* Muetterties, E. L., Ed.; Marcel Dekker: New York, 1971. b) Kaesz, H. D.; Saillant, R. B. *Chem. Rev.* **1972**, *72*, 231.

64. a) Muetterties, E. L.; Bleeke, J. R. *Acc. Chem. Res.* **1979**, *12*, 324. b) Stobart, S. R.; Zawrotko, M. J. *J. Chem. Soc., Chem. Commun.* **1985**, 1700. c) Linn, D. E.; Halpern, J. *J. Am. Chem. Soc.* **1987**, *109*, 2969.

65. a) Ankianiec, B. C.; Fanwick, P. E.; Rothwell, I. P. *J. Am. Chem. Soc.* **1991**, *113*, 4710. b) Chestnut, R. W.; Steffey, B. D.; Rothwell, I. P. Polyhedron, **1989**, *8*, 1607.

66. a) LaPointe, R. E.; Wolczanski, P. T.; VanDuyne, G. D. *Organometallics* **1985**, *4*, 1810. b) LaPointe, R. E.; Wolczanski, P. T. *J. Am. Chem. Soc.* **1986**, *108*, 3535.

67. Clark, J. R.; Fanwick, P. E.; Rothwell, I. P. *J. Chem. Soc., Chem. Commun.* **1993**, 1233.

68. Visciglio, V. M.; Fanwick, P. E.; Rothwell, I. P. *J. Chem. Soc., Chem. Commun.* **1992**, 1505.

69. Chen, H.; Cotton, F. A.; Yao, Z. *Inorg. Chem.* **1994**, *33*, 4255.

70. a) Luetkens, M. L., Jr.; Elcesser, J. C.; Huffman, J. C.; Sattelberger, A. P. *Inorg. Chem.* **1984**, *23*, 1718. b) Mayer, J. M.; Wolczanski, P. T.; Santarsiero, B. D.; Olson, W. A.; Bercaw, J. E. *Inorg. Chem.* **1983**, *22*, 1151. c) Holmes, S. J.; Schrock, R. R. *Organometallics* **1983**, *2*, 1463.

71. Robbins, J.; Bazan, G. C.; Murdzek, J. S.; O'Regan, M. B.; Schrock, R. R. *Organometallics*, **1991**, *10*, 2902.

72. Rocklage, S. M.; Schrock, R. R. *J. Am. Chem. Soc.* **1982**, *104*, 3077.

73. a) Clark, G. R.; Nielson, A. J.; Rickard, C. E. F.; Ware, D. C. *J. Chem. Soc., Dalton Trans.* **1990**, 1173. b) Clark, G. R.; Nielson, A. J.; Rickard, C. E. F.; Ware, D. C. *J. Chem. Soc., Chem Commun.* **1989**, 343.

74. a) McLain, S. J.; Wood, C. D.; Schrock, R. R. *J. Am. Chem. Soc.* **1979**, *101*, 4558. b) Grubbs, R. H.; Miyashita, A. *J. Am. Chem. Soc.* **1978**, *100*, 7416.

75. McLain, S. J.; Sancho, J.; Schrock, R. R. *J. Am. Chem. Soc.* **1980**, *102*, 5610.

BIOGRAPHICAL SKETCH

Daniel David VanderLende became enamored with chemistry while testing pool water samples for *Acme Pool Service* in the summer of 1984. The challenge presented to him by the excellent teaching of Donald Hopwood at Creston High School inspired Dan to continue his chemical education at the College of Wooster. Dr. Ted Williams took the time to provoke, inspire, tolerate, and nurture Dan as both a chemist and a person. Dr. Paul Gaus introduced Dan to synthetic organometallic chemistry in 1989 and instilled in him the pride and perseverance to make air-sensitive materials. Paul also explained to Dan that graduate school wasn't for just the 'A' student. Graduate school, according to Dr. Gaus, was for the person who wanted to give what it took to get the job done. He proved to be correct.

After considering offers from numerous professional sports teams, Dan realized that his graduate education was more important. After spending the summer of 1990 in Wooster as a PRF Researcher, Dan's love of synthesis drove him to the University of Florida. Once Dan recovered from a debilitating bicycle/auto accident, he began to create new molecules in the laboratory of his mentor, Dr. Jim Boncella.

Over four years, Dan made strides in group(10) amide chemistry as well as high oxidation state tungsten chemistry. Although few people understand what drives Dan to spend long hours trying to prepare new compounds, the reason is simple. Dan will never hold the world record in the 100 yard dash, hit 716 home runs, or be the first man on the moon. But the feeling might be the same as standing there holding a Schlenk tube containing crystals of $W(NPh)Cl_2(Me_3SiN)_2C_6H_4$.

I certify that I have read this study and that in my opinion it conforms to acceptable standards of scholarly presentation and is fully adequate, in scope and quality, as a thesis for the degree of Doctor of Philosophy.

James M. Boncella, Chair
Associate Professor of Chemistry

I certify that I have read this study and that in my opinion it conforms to acceptable standards of scholarly presentation and is fully adequate, in scope and quality, as a thesis for the degree of Doctor of Philosophy.

David E. Richardson
Professor of Chemistry

I certify that I have read this study and that in my opinion it conforms to acceptable standards of scholarly presentation and is fully adequate, in scope and quality, as a thesis for the degree of Doctor of Philosophy.

William M. Jones
Disinguished Service Professor of Chemistry

I certify that I have read this study and that in my opinion it conforms to acceptable standards of scholarly presentation and is fully adequate, in scope and quality, as a thesis for the degree of Doctor of Philosophy.

Kenneth B. Wagener
Professor of Chemistry

I certify that I have read this study and that in my opinion it conforms to acceptable standards of scholarly presentation and is fully adequate, in scope and quality, as a thesis for the degree of Doctor of Philosophy.

Anthony B. Brennan
Assistant Professor of Materials Science and Engineering

This thesis was submitted to the Graduate Faculty of the of the Department of Chemistry in the College of Liberal Arts and Sciences and to the Graduate School and was accepted as partial fulfillment of the requirements for the degree of Doctor of Philosophy.

December, 1994

Dean, Graduate School